A CELLULAR AUTOMATON BASED ELECTROMECHANICAL MODEL OF THE HEART

A THESIS SUBMITTED TO
THE GRADUATE SCHOOL OF NATURAL AND APPLIED SCIENCES
OF
MIDDLE EAST TECHNICAL UNIVERSITY

BY

CEREN BORA

IN PARTIAL FULFILLMENT OF THE REQUIREMENTS
FOR
THE DEGREE OF MASTER OF SCIENCE
IN
BIOMEDICAL ENGINEERING

SEPTEMBER 2010

Approval of the thesis:

A CELLULAR AUTOMATON BASED ELECTROMECHANICAL MODEL OF THE HEART

submitted by **CEREN BORA** in partial fulfillment of the requirements for the degree of **Master of Science in Biomedical Engineering Department, Middle East Technical University** by,

Prof. Dr. Canan Özgen _____
Dean, Graduate School of **Natural and Applied Sciences**

Prof. Dr. M. Zülfü Aşık _____
Head of Department, **Biomedical Engineering**

Asst. Prof. Dr. Yeşim Serinağaoğlu Doğrusöz _____
Supervisor, **Electrical and Electronics Engineering Dept., METU**

Asst. Prof. Dr. Ergin Tönük _____
Co-Supervisor, **Mechanical Engineering Dept., METU**

Examining Committee Members:

Prof. Dr. Nevzat Güneri Gençer _____
Electrical and Electronics Engineering Dept., METU

Asst. Prof. Dr. Yeşim Serinağaoğlu Doğrusöz _____
Electrical and Electronics Engineering Dept., METU

Asst. Prof. Dr. Ergin Tönük _____
Mechanical Engineering Dept., METU

Assoc.Prof. Dr. Hakan Işık Tarman _____
Engineering Sciences Dept., METU

Assist. Prof. Dr. Hakan Öktem _____
Institute of Applied Mathematics, METU

Date: 16.09.2010

I hereby declare that all information in this document has been obtained and presented in accordance with academic rules and ethical conduct. I also declare that, as required by these rules and conduct, I have fully cited and referenced all material and results that are not original to this work.

Name, Last name : Ceren Bora

Signature :

ABSTRACT

A CELLULAR AUTOMATON BASED ELECTROMECHANICAL MODEL OF THE HEART

Bora, Ceren

M.Sc., Department of Biomedical Engineering
Supervisor: Asst. Prof. Dr. Yeşim Serinağaoğlu Doğrusöz
Co-Supervisor: Asst. Prof. Dr. Ergin Tönük

September 2010, 119 pages

The heart is a muscular organ which acts as a biomechanical pump. Electrical impulses are generated in specialized cells and flow through the heart myocardium by the ion changes on the cell membrane which is the beginning of both the electrical and the mechanical activity. Both the electrical and the mechanical states of the organ will directly affect the pumping activity. The main motivation of this thesis is to better understand physiological and pathological properties of the heart muscle via studying the electro-mechanics of the heart. This model could be used to gain better solutions of the ill-posed inverse problem of ECG and Body Surface Potential Maps (BSPM) or to estimate the electrical propagation and mechanical response on patient specific heart geometry models which can be obtained by using MRI technique. Cellular automaton technique will be used to simulate the physiological function of the left ventricle to estimate the cardiac functions. To model the heart tissue firstly the anatomical knowledge of the heart will be used such as properties of the myocardium, fiber orientations, etc. to simulate the three dimensional electrical propagation. Then the mechanical activity consisting of contraction and relaxation will be simulated according to the material properties of the heart. Using this simulation, the effects of the cardiac arrhythmias such as reentry will be generated.

In this study, electrical and mechanical properties of the heart tissue are modeled for normal heart beat and heart beat in case of ischemic heart tissue. Contraction of the tissue via electrical activation has also been considered in terms of time synchronization. “Cellular automaton” method is used for modeling the electromechanical interactions in the heart tissue. A simplified left ventricle model is used to observe the electrical and the mechanical behavior. Using this method, both the normal heart beat’s electrical activation and the arrhythmia excitation could be taken on, without using complex differential equations. To consider the anisotropy of the heart tissue, fiber orientations have also been added to the model. In this thesis work, electro-mechanic models at cellular, macroscopic and heart left ventricle level are presented. The electro-mechanical adaptation is performed by cellular electrophysiology and cellular force development due to intercellular excitation propagation. Varying densities of transmembrane proteins, changes on concentration of calcium, metabolic and hormonal effects are neglected. Also in simplified ventricular model the fluid mechanics and mechanoelectrical feed-back is not taken into-account.

Keywords: heart tissue, electromechanical model, cellular automaton, heart modeling

ÖZ

HÜCRESEL OTOMATON YÖNTEMİ İLE KALBİN ELEKTROMEKANİK MODELLENMESİ

Bora, Ceren

Yüksek Lisans, Biyomedikal Mühendisliği Anabilim Dalı
Tez Yöneticisi: Yrd. Doç. Dr. Yeşim Serinağaoğlu Doğrusöz
Ortak Tez Yöneticisi: Yrd. Doç. Dr. Ergin Tönük

Eylül 2010, 119 sayfa

Kalp biyomekanik pompa görevi gören kas yapısında bir organdır. Elektriksel uyarılar bu iş için özelleşmiş hücrelerce oluşturulur ve iyon değişimleri sayesinde tüm miyokardiyum yüzeyi boyunca akarak hem elektriksel hem de mekanik aktivitenin oluşumunu sağlar. Hem elektriksel hem de mekanik aktiviteyi etkileyen durumlar kalbin pompa görevini doğrudan etkileyecektir. Bu çalışmanın ana amacı, kalp kasının fizyolojik ve patolojik özelliklerini elektromekanik olarak inceleyerek, kalp hastalıklarının teşhisinde kullanılan yöntemlere ek çözümler geliştirmektir. Bu model vücut yüzeyi potansiyeli ölçümlerinden kalp üzerindeki kaynağın bulunması amacıyla veya MR görüntüleriyle oluşturulabilecek hastaya özel kalp geometrilerinde elektriksel iletim ve buna bağlı olarak mekanik tepkinin etkilerinin kestirilmesinde kullanılabilecektir. Hücresel otomaton yöntemi kullanılarak sol ventrikül fizyolojisi modeli üzerinde kardiyak fonksiyonların tespiti mümkün olacaktır. Modelleme esnasında anatomik bilgiler göz önünde bulundurularak (kas yapısı özellikleri, fiber dağılımı… vb.) öncelikle üç boyutlu akım dağılımı modellenecektir. Daha sonra da malzeme yapısına bağlı kalınarak kasılma ve gevşeme özellikleri belirlenecek ve mekanik aktivite simule edilecektir. Simulasyon reentry gibi aritmi yaratacak durumlar için denenerek klinik verilerle ilişki kurulmaya çalışılacaktır.

Bu çalışmada kalbin normal atım durumunda elektriksel ve mekanik özelliklerinin modellenmesi ile ilgili çalışmalarımız yer almaktadır. Ayrıca kalp elektriksel aktivasyonu dolayısıyla gerçekleşen kasılmanın zamansal senkronizasyonu belirlenerek kalbin elektromekanik doku modeli üzerinde çalışmalar yapılmıştır. 2 boyutlu kalp doku modellemesi ve elektromekanik ilişkilendirme için hücresel otomaton yöntemi kullanılmıştır. Bu yöntemle kalpteki elektriksel yayılım ve mekanik kasılma başlangıcı hem normal atım hem de kalp doku bozulmaları kaynaklı aritmiye sebep olacak uyarıların yayılımını karmaşık diferansiyel denklemlerden bağımsız olarak çözümlenmesine olanak sağlamaktadır. Kalp dokusunun anizotropik yapısı da göz önünde bulunarak fiber yönelimleri doğrultusunca gerçekleşecek aktivasyon gözlemlenmiştir.

Tez çalışmasında elektromekanik model; makroskopik, düzlemsel ve basitleştirilmiş sol ventrikül düzeyinde ele alınmıştır. Her hücredeki elektriksel ve mekanik davranışlar, hücrenin uyarı yayılımına bağlı olarak hesaplanmıştır. Zamana bağlı fizyolojik durum değişimleri ile ifade edilen iyon potansiyel eğrisi ile kuvvet değişimi eğrisi ilişkilendirilmiş ve mekanik tepki de durum değişimi olarak elastik özellikte modellenmiştir. Hücre zar proteinlerinin yoğunluğunun, kalsiyum iyon konsantrasyonunun, metabolik ve hormonal değişimlerin kalp kası üzerindeki etkileri dikkate alınmamıştır. Ayrıca akışkanlar mekaniği, mekaniğin elektriksel aktiviteye etkisi gibi kasılmayı etkileyecek özellikler ihmal edilmiştir.

Anahtar Sözcükler: kalp dokusu, elektromekanik model, hücresel otomaton, kalp modeli

To My Family,

ACKNOWLEDGMENTS

I would like to express my sincere gratitude to my supervisor Asst. Prof. Dr. Yeşim Serinağaoğlu Doğrusöz and co-supervisor Asst. Prof. Dr. Ergin Tönük for their guidance, advice, encouragements and support throughout the research.

As a national Master of Science student, I was supported by Turkish Scientific and Technological Research Council (TUBITAK), I also want to thank them for their support.

I would like to thank my laboratory mates and friends Ümit Aydın, Alireza Mazloumi, Uğur Cunedioğlu, Ersin Karcı, Murat Önal, Ali Ersöz, Tankut Topal, Kerim Kara, İlhan Soner Keçeli, Evren Değirmenci, Volkan Emre Arpınar, Alper Çevik, Feza Carlak, Balkar Erdoğan, Berna Akıncı and Reyhan Zengin for their friendship and support throughout my study.

I also would like to express my appreciation to my colleagues in Graduate School of Natural and Applied Sciences, for the enthusiastic support throughout the development of this thesis.

I also wish to thank to my friends: Gökben Aykanat, Günsu Gökhan, Kaan Ekemen, Ömer Aydın, Gizem Altay, Gülden Eroğlu, Fulya Karahan and Hatice Ceylan for all valuable memories and for their encouragements during my studies.

Special thanks to Arda Orçun, for his endless support, patience and love from the moment we met. He always believes in me more than I do.

More than all, I would like to express very special thanks to my dear parents for their endless support and love throughout my education. I would not be able to finish my Master studies without their full support. Their support, confidence, and love make everything easier. I would especially like to thank to my brother Can Bora. No matter how far away he lives, he was only a call away, and he always supported me with his advices, help and guidance.

TABLE OF CONTENTS

LIST OF TABLES

TABLES

LIST OF FIGURES

FIGURES

CHAPTER 1

INTRODUCTION

Most of the countries face high and increasing rates of cardiovascular disease. Each year, heart disease kills more people in our county and in all over the world. Results of the 2004 report of World Health Organization (WHO) show that approximately 54 percent of all death in Turkey is caused by cardiovascular diseases, which is the highest per cent in all disease categories both in communicable and incommunicable diseases that lead to death [1]. Most commonly seen death cause *sudden cardiac death (SCD)* can be describe as "unexpected natural death from a cardiac cause within a short time period" [1]. While 50% of the mortality caused by cardiovascular disease in developed countries, in less-developed countries the percentage is lower, because sudden cardiac death and ischemic heart disease rates parallel. Several population-based studies show that SCD from coronary heart disease have decreased since the early 1980s; however, SCD is still a major health issue [2].

Because of the unexpectable nature of the SCD and because 40% of sudden deaths are indeterminate, classifications based on clinical circumstances can be misleading and often impossible. Only recording the electrical activity by an ECG recorder or a ventricular electrogram data taken via an implanted device at the time of death can give the exact information about an arrhythmia. On the other hand, many people do not know that he/she suffers from cardiac disease or they think that they have low risk for SCD. Although symptomatic of the onset of cardiac diseases is often nonspecific, to be able to decrease the mortality caused by SCD, cardiologist and electrophysiologist should work together and try to define new methods that can be used as clinical diagnosis, prognosis, and therapy to prevent SCD [2, 3].

Normal and failing heart show significant differences in electromechanical behavior, which can be detected via many different devices: i.e. electrocardiography (ECG), catheter based electrograph, angiograph, phonocardiogram (PCG), cardiac computerized tomography (cardiac CT), magnetic resonance imaging (MRI), echocardiography using ultrasound, nuclear imaging etc. Heart sounds and measurable electrical potentials are used for detection of the cardiovascular diseases. The phonocardiogram (PCG) is a vibration or sound signal related to the heart contraction and blood flow activity. The heart sound signal is perhaps the most traditional biomedical signal. It can be detected even with naked ear; however, stethoscope is commonly used for monitoring heart sounds. Cardiovascular diseases and defects cause changes or additional sounds and murmurs that could be used in their diagnosis [4]. The electrocardiograph (ECG) is one of the earliest equipment which measure and manifest the cardiac activity. The first human ECG is published in 1887 by Augustus D. Waller [5]. Contractile activity can be recorded easily with surface electrodes on the limbs or chest. Through the wave shape of the recorded ECG, cardiovascular diseases and many abnormalities can be altered. Although ECG and PCG are standard diagnostic tools and most commonly used diagnostic methods for cardiac diseases, they are not enough to determine the reasons of SCD, since 12-lead ECG technique suffers from its low resolution and its being easily affected from in homogeneities and smoothing effects of organs within the thorax [4, 6]. For the estimation of arrhythmia sources, enhanced techniques are needed. To detect the disorders non-invasive techniques like cardiac CT suffer from the movement of the organ. Not just the electrical behavior record but also the mechanical behavior is important for having information of the disease. Only seeing the mechanical disorders in the heart muscle could also yield information about disorders in electrical behavior.

Besides clinical research and animal experimentation to understand the behavior and pathology of the heart, computer modeling and simulations have great role in clinical diagnosis and therapy to prevent sudden cardiac death [7, 8]. Computer simulations are potentially effective approaches to define the heart rhythm disorders. Anatomically realistic computer models of the heart not only help to characterize dynamic mechanism for arrhythmia development but also will help to choose the right therapy in clinics [6, 7].

Even though the most direct method to study the cardiac disorders is trough biological studies like animal experiments, certain drawbacks make the computer simulations more preferable to biological studies: biological studies are expensive both in terms of time and money, damaging to the tissue, have limited control, have limited access to certain variables and their interactions, and only a limited number of measurements can be obtained in experiments. Also using animals has problems on its own, because of the need of animal models to study specific features, and ethical issues in using the methods to measure the data. On the other hand computer simulations are less limited, cost-effective and complex systems and interaction of variables are possible [9]. Although computer simulations also have disadvantages: e.g. simplification during mathematical modeling, because of its advantages comparing to biological studies, computer models may take the place of experiments, which can freely simulate heart in various pathological conditions [10].

To be able to understand physiological and pathophysiological behavior of an organ, one should have the knowledge of the interplay of anatomical structure and physical phenomena. Using data achieved via new measurement methods, mathematical description of the properties and behavior of cardiac tissue can be applied to simulate the tissue behavior. In recent years, with the great improvement in computing capability simulations has simplified and speeded up significantly. Complex phenomena can be studied using approximate/simplified models that are used to predict unknown behaviors of the tissue.

An ordered contraction of the heart is maintained by the propagation of the electrical impulses through the heart muscle, along with the conduction of impulses from cell to cell. The spread of the electrical activation on the myocardium controls the heart muscle contraction. Thus, any loss of the order or rhythm of the electrical process can lead to disorders in mechanical contraction and can also lead a decreased cardiac output, in other words, a decreased amount of blood pumped out of the heart. Arrhythmias, disorders in electrical activity of the heart, can be caused by numerous conditions and can in some cases lead to death, which makes them clinically important. To be able to understand and diagnose the arrhythmias, and to be able to develop methods for “detection, treatment and management” of cardiac diseases, researchers and clinicians

has been working on different equipments to be able to measure the physiological changes and also trying to model the organ in order to understand all the behavior of the normally working and diseased cardiac system.

Models of interactions between structure and function of the cardiac tissue can be divided into four main headings; molecular, cellular, tissue and organ level modeling [6]. The cardiac tissue models attempt to explain the myocardial electrical activation or the myocardial mechanics individually or the myocardial electro-mechanical activation including both the activation and contraction properties of the tissue in terms of its cellular and tissue components [11, 12].

Large-scale models of the heart are used to describe the cellular level electrical activity of the tissue. First model of an excitable cell was published by Hodgkin and Huxley in 1952 [6]. This model includes a mathematical description of the behavior of ion channels, and correctly predicts the shape of the action potential, the membrane potential changes, and the conduction velocity using experimental results of the squid giant axon. Hodgkin and Huxley achieved the Nobel Prize for Physiology or Medicine for their study [6, 13, 87].

Since then, a number of different cell models have been published as more information has been available about the different functions of the cell. Models of the heart have been developed since 1960, starting with the discovery and modeling of potassium channels. The first models of calcium balance were made in the 1980s and have now reached a high degree of physiological detail. During the 1990s, these cell models were incorporated into anatomically detailed tissue and organ models [8, 14].

Some of the better-known cellular level models are called; the Purkinje fiber cell model by DiFrancesco-Noble [15], ventricular cell model by Beeler-Reuter, mammalian ventricular cell models by Luo-Rudy and the pig ventricular cell model by Noble. The currents, pumps, and action potential generated from these models are getting more complex, through the change of the number of currents included in just a single cardiac cell [8, 16].

Cardiac cells are organized by gap junctions to have rapid activation of the myocardium. It also affects the level of ejection fraction for the ventricles. This tissue structure has been modeled mechanically and electrically to bridge the gap between cell-level and tissue-level models [14]. Computing the propagation of an activation wavefront through a tissue block can also be used in the whole heart models, to be evaluated in different regions of the myocardium [14]. Modeling electrical activity from cell to organ and than from organ to body can also be performed, which would be clinically important since the initial clinical assessment of cardiac electrophysiology is at the body surface [6, 13, 16].

From cell to tissue level, reaction-diffusion equation systems and cellular automaton models are used as models. One of the most commonly used tissue models is the FitzHugh–Nagumo (FHN) equations, because of its simplified computational cost, which is used as the excitability component in some models of action potential propagation using an excitation variable *u* and a recovery variable *v,* which is called reaction-diffusion equations [6, 13, 17]. The dynamic propagation can be represented by displaying an iso-surface of the transmembrane potential value. The complete propagation can be shown with the isochrones, where colors represent the different depolarization times [18, 19]. To model the macroscopic characteristics of the cardiac tissue Aliev-Panfilov modification to the FitzHugh-Nagumo model is also a reaction-diffusion based model, which provides a more realistic shape of the cardiac action potential using spatial temporal and fiber orientation parameters [20].

Computational models are a potentially powerful tool for investigating the complex interaction between abnormal structure and function that causes cardiac arrhythmias. There are many different types of arrhythmia from ectopic beats to lethal ventricular fibrillation [21]. These are Na^+ overload and Ca^{2+} overload causes metabolic changes within the cell result in spontaneous release of intracellular Ca^{2+} that initiates the abnormal depolarization. One of the most serious disorders of cardiac action potential conduction is *re-entry*, which lead to cardiac arrhythmias of tachycardia and fibrillation. During re-entry an action potential circulates, continuously exciting tissue that is refractory. For re-entry to occur, a closed pathway with a length greater than the product of action potential duration and conduction velocity must exist within the tissue.

Re-entry has been widely investigated in 2D computational models, and to a limited extent in 3D [11].

Cellular automata approach, which was chosen as the modeling method in this thesis, is the simplest approximation of cardiac tissue, where the excitation propagation through the heart is described macroscopically. Nodes that include many cardiac cells are arranged in a grid and have a number of discrete states, and the state of a particular cell is determined by a set of rules. In cellular automata, the complex ionic phenomena are represented in terms of changes in state of each model unit. Each state is assigned a physiological significance and specific rules govern the state transitions and propagation of the activation from one element to its neigbors. An anatomically accurate cellular automaton model incorparating anisotropy of propagation based on recorded fiber orientations can be quantitatively shown to achive the activation and propagation phenomena comperable to those in normal heart [9]. The main advantage of this model is computational time required to run simulations. This approach can also be used to study fibrillation and other arrhythmias [6, 9, 13, 22].

The cellular automaton based cardiac model is able to simulate various cardiac diseases. For example, different bundle branch blocks can be introduced by slight changes in the conduction system. Decreasing the action potential amplitude and excitation propagation velocity in some regions of the myocardium represents an ischemia or an infraction [22].

Fiber orientation in cardiac tissue is one of the basic parameters in modeling, because both electrical and mechanical tissue properties are strongly dependent on fiber directions. Patient specific models require in vivo fiber orientation measurements, which is not applicable for human being in invasive manner. Non-invasively, the fiber orientation can be analyzed from a Diffusion Tensor Magnetic Resonance Imaging (DTMRI) measurement of a human heart [10, 17, 22, 23]. Using MRI images or using animal experiment results and cadaver tissue studies, fiber directions can be determined [24, 25]. Those studies show that the fiber directions in the left and right ventricular free wall, typically varies from -60^{o} at the epicardium to $+90^{o}$ at the endocardium, whereas in the septal wall the fiber angle ranges from approximately -90^{o}

at the right ventricular endocardium to around +80 ^{o} at the left ventricular endocardium [26].

The orientation of the muscle fibers was included in the underlying anatomical model allowing the incorporation of anisotropic electrical and mechanical properties. In the ventricular wall models, at any node it is possible to define three structurally based axes: (*a*) axes in the fiber direction, (*b*) axes in the perpendicular to the fiber direction within a muscle layer, and (*c*) axes in the normal to the muscle layer [8, 9].

Mechanical models are highly affected by the fibrous structure of the heart both in cellular and macroscopic in other words tissue level, since the movement of contraction occurs in only one direction which is the fiber direction. Muscle cells control the development of force in the myofilaments via the intracellular calcium concentration and stretch of sacromere. Calcium concentration, sacromere length, excitation duration and excitation current are needed for many models as major input parameters [27-30].

Experimental studies show that the mechanical properties of myocardium are found to be; nonlinear, anisotropic and viscoelastic [7, 31-33]. A first study on mechanical properties of myocardium was done to model the relationship between stain and stress by parameter fitting to experimentally recorded data by Demiray in 1972. Since than, strain energy density functions, viscoelastic properties of the myocardium, diastole and end-systole material descriptions, anisotropy of the material were added to models for tissue properties [7, 18]. Different parameterizations were determined depending on the fiber directions and residual stress in the ventricular wall. To describe the cellular level behavior of the tissue, sarcomere the unit contractile elements is modeled. Constitutive relationships are tried to be established and constitutive law based on the Hill-Maxwell rheological law are used to simulate the relationship between force and displacement of the tissue [34, 35]. Sliding filament theory defines the basic movement of the contractile proteins in activation. Also Hill's three-element model is one of the most commonly used mathematical models to explain the contraction of the cardiac cells [36, 37].

Calculating the ventricular wall deformation, computerizing the whole organ, finite element models and finite difference models (i.e. continuum approach) are more

preferable methods comparing to computing each sarcomere individually [10, 32, 38]. In the heart motion, there is a twist during contraction; using biomechanical volumetric models could help recover this tangential displacement [17, 39, 40].

The myocardium contraction is modeled through a constitutive law including an electromechanical coupling. The myocardium's constitutive law is complex and must include an active element for contraction, controlled by the transmembrane potential and a passive element representing the mechanical elasticity [19]. The recent tension development model consists of 14 state variables incorporated with the three components troponin, tropomyosin, and actin-myosin interaction [22].

As a whole heart modelling approach, electrical and mechanical models are taken as a whole and in the constructed electromechanical model. The propagation of electrical excitation was simulated using an electrical heart model, and the resulting active forces were used to calculate ventricular wall motion. During the period of systole, the right ventricular free wall moves towards the septum, and at the same time, the base and middle of the free wall move towards the apex, which reduces the volume of the right ventricle and the heart does its main function: pumps the blood to the body.

1.1. Motivation of the Thesis

The main motivation of this thesis is to better understand physiological and pathological properties of the heart via studying the electro-mechanics of the heart as any asynchrony of electrical activation and disorder of the mechanical properties can lead to abnormalities in heart function.

As a key idea, the aim was to build a "Beating Heart Model", which contracts under electrical excitation. The modeling includes the areas of anatomy, electrophysiology, excitation propagation, mechanics and force development as well as the coupling of these areas.

A trade-off between biological accuracy and computational efficiency still exist; however, to simulate the lethal tissue, computation time is more preferable for the

clinical applications, to improve diagnostics of infarction and arrhythmia and to enable quantitative therapy planning. It can also be used as a regularization tool to gain better solutions of the ill-posed inverse problem of ECG and Body Surface Potential Maps (BSPM) and MRI, leading to a new non-invasive medical imaging technique.

1.2. Scope of the Thesis

This thesis work includes studies done for model of cardiac tissue at macroscopic level in normal, and some pathological conditions. The simulations represent a cardiac cycle including electrical depolarization and repolarization as well as mechanical contraction and relaxation.

Cellular automaton model was chosen to study electrical propagation in a single fiber, two-dimensional sheet simulation and a simplified left ventricle model. The model can be used to better understand physiology and pathophysiology of the heart, without using complex differential equations.

Truncated ellipsoid is used as simplified left ventricle geometry. The ventricle geometry, fiber directions and size of this ellipsoid were chosen so that it is similar to an adult left ventricle, the simplified model generated by layered structure. The fiber orientation is set using knowledge from anatomical studies with approximately 140 degrees change from epicardium to endocardium: first four layer simplified model is generated in which the fiber orientation is varied from -45^{o} at the epicardium to 90^{o} at the endocardium, and then a more realistic tissue was simulated by varying the fiber angles and number of layers.

1.3. Organization

This thesis is organized as follows: After the 1^{st} Chapter, introduction of the thesis, Chapter 2 describes the anatomical and physiological basis of the heart and myocardium, which is the reference parameter information of all the simulations.

In Chapter 3, method of the simulation is described. Chosen model parameters, simulation algorithm and implementation is explained in details.

In the next chapter, in Chapter 4, results of the simulation are presented. For one dimensional, and two dimensional myocardium simulation results were presented for both electrical and mechanical model. Anisotropy of the cardiac tissue and simulation results were also presented in this part. The results normally propagated electrical wave and re-entry simulations in 2D and 3D models are illustrated and compared. Representations of electromechanical behavior of the tissue are shown in 2D and 3D models, and a simplified left ventricle model can be found in this section.

Chapter 5 describes the overall conclusion from the research and the individual studies described in Chapter 4 and potential future directions of this study.

CHAPTER 2

BACKGROUND INFORMATION

2.1. The Heart

The heart is one of the major components of circulation system, which is composed of cardiovascular and lymphatic systems. The main function of the circulation system can be listed as transportation, regulation and protection. Every cell in our body needs oxygen as respiratory gases, nutritive, and hormones, and the metabolic wastes should be removed. The blood serves the transportation function and carries all those necessary materials pumped out of the heart to each body cell through vessels. The cardiovascular system also helps the body to regulate the body temperature. Another important regulation factor is hormones, which are needed for variety of functions. One other role of circulation system is to protect body from microbes, toxins and help to prevent blood loss [41].

Loss of any of those functions would make many different types of arrhythmia ranging from benign ectopic beats to lethal ventricular fibrillation. All those functions make the heart vital and make the computer simulations useful for investigating the complex interaction between abnormal structure and function that underlies the development of cardiac arrhythmias.

2.1.1. Cardiac Anatomy

The heart is an electromechanical pump, which has four chambers: two atria and two ventricles. Atria receive the blood returned back to the heart, and ventricles eject blood into arteries. As well as atria and ventricles the heart also divided into two as pumps:

right and left pumps. The muscular wall, which separates those pumps, is called the septum. In a normal adult heart the septum prevents mixture of the blood in the right and left of the heart [41].

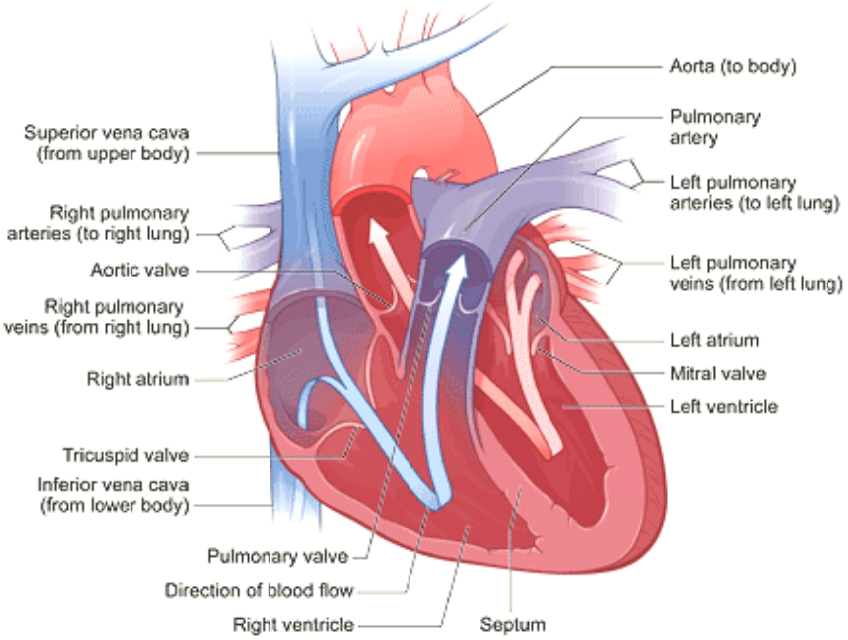

Figure 2.1 The human heart diagram: illustrations of atria and ventricles [42]

Champers, arteries and veins are separated from other cavities via gates called *valves*. The valves allow blood to flow only in a certain direction in the heart. They normally prevent the backflow of the blood. Valves also maintain the pressure change in cavities, which leads to blood exceed from ventricles to arteries. They are named according to their flap numbers and shape: tricuspid valve, bicuspid valve (mitral valve), semilunar valves; and according to the cavity names they separate some of them called: atrioventricular valves, aortic semilunar valve, pulmonary semilunar valve [41]. The position of valves presented in Figure 2.1 and Figure 2.2 presents the superior view of the valves.

Illustrations of the main components of the human heart are given in Figure 2.1. The heart is mainly composed of four cavities surrounded by muscles that are constructed of cells called myocytes. The heart wall has a three-layered structure: *epicardium,*

myocardium and *endocardium*. Epicardium is the thin layer on the outside of the heart, which produces the fluid that protects the heart while its movement when it beats. The innermost layer is called endocardium, which consist of epithelium cells. The actual muscle tissue in between those two layers is myocardium. Its thickness varies over the surface of the heart, which can also be seen in Figure 2.1. The wall of left ventricle (LV) is the thickest wall in the heart and right ventricle (RV) and atria walls follows each other. While LV wall thickness is approximately 8-10 mm, RV thickness is only 2-3 mm [41, 43].

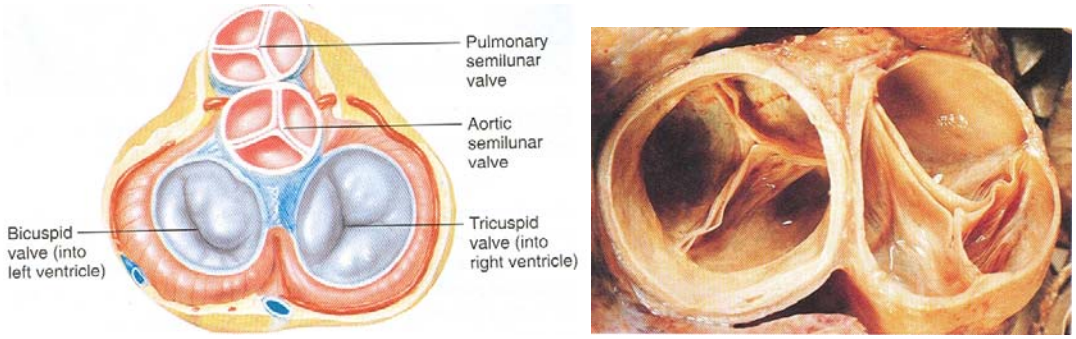

Figure 2.2 The heart valves: (a) a superior view of the heart valves, (b) a closed position photograph of aortic and pulmonary semilunar valves [41]

Total heart size is approximately the size of a fist and its weight is around 300 grams. Heart beats approximately 100.000 times a day and pumps around 7200 liters per day. For an adult, at rest nearly 5 liters of blood is pumped out of the heart per minute and it takes about 1 minute for blood to pump out of the heart to body and to come back through superior or inferior vena cava to the heart again. This pumping action is provided by muscular activity, which is necessary to generate the required pressure to push blood to whole body [41].

Like any other organ in the body, the heart also needs to feed itself. Myocardial oxygen supply is provided by coronary arteries. The blood flow to the myocardium is supplied by the two coronary arteries that arise from the aortic root. In Figure 2.3 the main coronary arteries of the heart were shown. The right coronary artery usually supplies the greater portion of the right ventricle, while the left coronary artery supplies the left

ventricle. The contribution of both arteries to blood flow in the septum and posterior wall of the left ventricle varies. The situations like *hypertension*, the myocardium requires more O_2 than usual to perform the same amount of work and an increased O_2 demand quickly has to lead to vasodilatation, in other words widening of blood vessels [44]. Oxygen supply deficiency causes ischemic heart diseases which leads the most commonly seen mortal disease, sudden cardiac death [41].

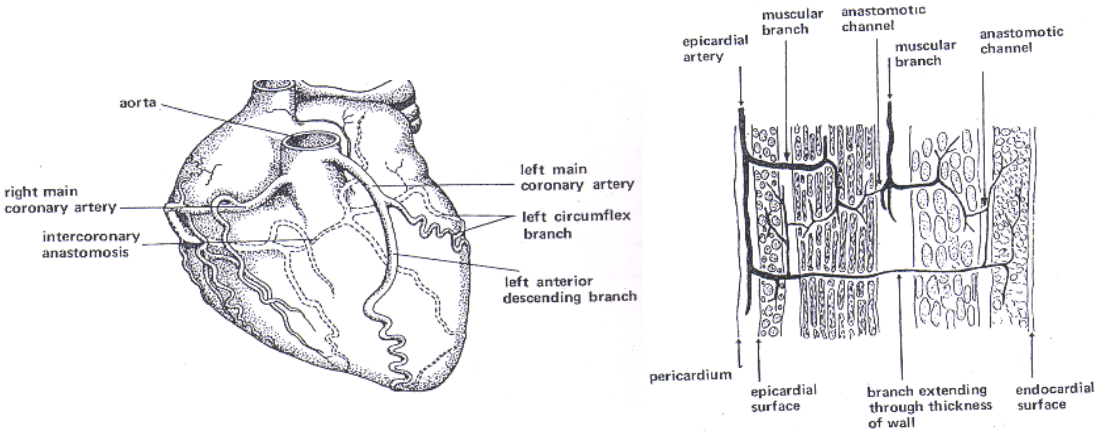

Figure 2.3 Coronary arteries: (a) main coronary arteries, (b) cardiac vessels from epicardium to endocardium [45]

The heart is the first organ form in the fetal body. Before taking its specialized structure, heart is in tubular form. The heart begins to looping and bending on itself and finally becomes fully developed shape in an only 8-day old human embryo. 22-day old heart begins to contract rhythmically and will continue up till the end of the human's lifetime [43].

The morphology of the cardiac muscles can be examine by comparing the structure and function with other type of muscles. The muscle types are divided into 3 main groups: smooth muscles, cardiac muscles and skeletal muscles. Cardiac muscles have striated form and Z lines and also contain actin, tropomyosin and troponin proteins that are similar to those in skeletal muscle [46]. Unlike skeletal muscles, the cardiac muscle cells have branched fibers. It has more mitochondria in the cells comparing to other striated muscle cells but it has only one nucleus for each cell. The end of one muscle

fiber lies adjacent to another fiber; those are connected to each other via gap junctions, which provide low-resistance bridges for the excitation propagation [47]. In Table 2.1, other properties of cardiac muscle are presented and compared to other muscle types.

Table 2.1 Comparison of structure and functions of muscle types [44]

Structure and Function	**Smooth muscle**	**Cardiac muscle (striated)**	**Skeletal muscle (striated)**
Motor end-plates	None	None	Yes
Fibers	Fusiform, short (–< 0.2 mm)	Branched	Cylindrical, long (–<15cm)
Mitochondria	Few	Many	Few (depending on muscle type)
Nucleus per fiber	1	1	Multiple
Sarcomeres	None	Yes, length –< 2.6 µm	Yes, length –< 3.65µm
Electr. Coupling	Some (single-unit type)	Yes (functional syncytium)	No
Sarcoplasmic Reticulum	Little developed	Moderately developed	Highly developed
Ca^{2+} "switch"	Calmodulin/caldesmon	Troponin	Troponin
Pacemaker	Some spontaneous rhythmic activity ($1s^{-1}$–$1h^{-1}$)	Yes (sinus nodes ca.$1s^{-1}$)	No (requires nerve stimulus)
Response to stimulus	Change in tone or rhythm frequency	All or none	Graded
Tetanizable	Yes	No	Yes
Work range	Length-force curve is variable	In rising length-force curve	At peak of length-force curve

Not only the muscle types but also the cardiac tissues themselves vary according to the function and spatial location of the cells. Some of the different cell types in the heart are presented in Figure 2.4.

The gap junction orientation and density differ depending on the tissue. For example, the density of the gap junctions in the SA and AV node is less than the density in the ventricular myocardium [45]. Also in the same tissue it differs in longitudinal orientation and transversal orientation. It can be said that density is larger in longitudinal direction. The average *length* of longitudinal gap junctions is smaller than the length of transversal gap junctions. Both circumstances lead to a macroscopic anisotropic, electrical intracellular conductivity [7]. Due to anisotropy of the tissue speed of the electrical propagation, response of the tissue to excitation also changes in those different cardiac cells; SA node, AV node, Purkinje fibers, and myocardial cells.

The main cardiac muscle consists of myocardial cells. Those striated muscle cells also show anatomically and physiologically differences due to anisotropy. In Figure 2.5, longitudinal and cross-section electron microscopy figures are shown.

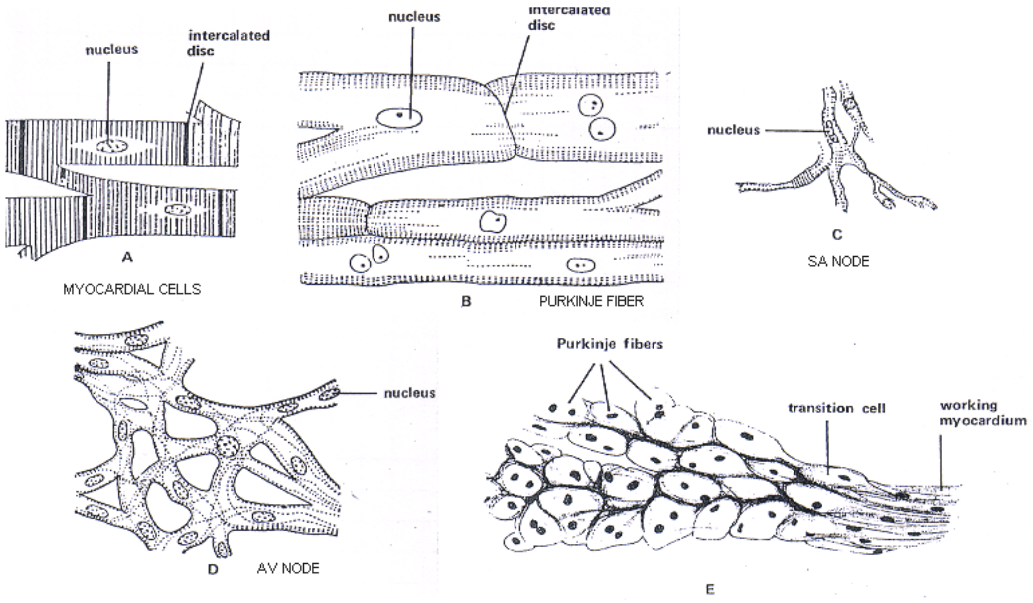

Figure 2.4 illustrations of cardiac cells; (a) myocardial cells, (b) purkinje fibers, (c) SA node, (d) AV node, (e) transition cell [45]

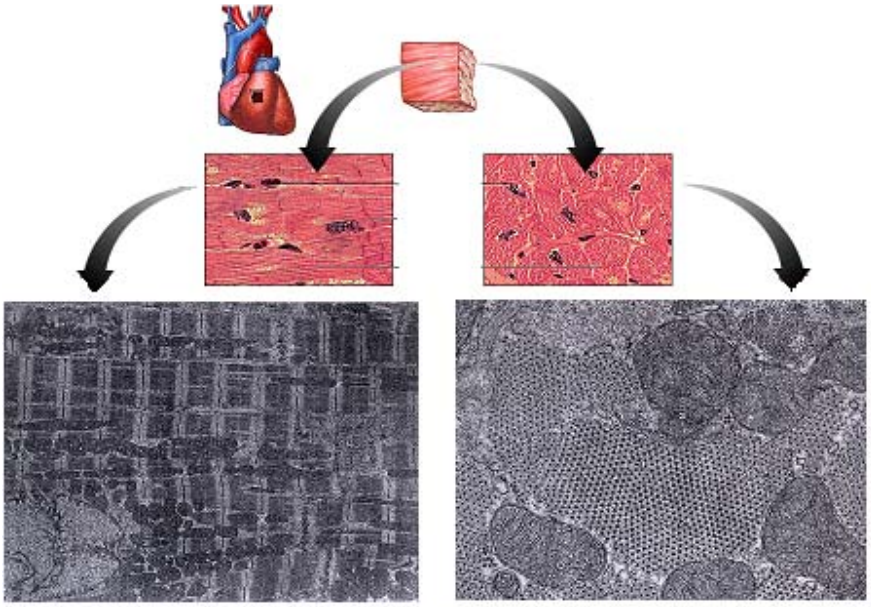

Figure 2.5 Human cardiac muscle in longitudinal section (left) and cross section (right). Electron microphotograpy of myocardial cells [33, 48]

Those longitudinal and cross-section images in Figure 2.5 represent cardiac muscle *sheets*. However, the anisotropy of the heart tissue not only changes due to longitudinal and cross-sectional orientation of the cells. The anisotropy complexity begins with the embryonic heart tissue formation, when the heart begins to looping and bending on itself [43]. If the heart is unwrapped, the anisotropy of the tissue becomes more visible, which can be seen in Figure 2.6.

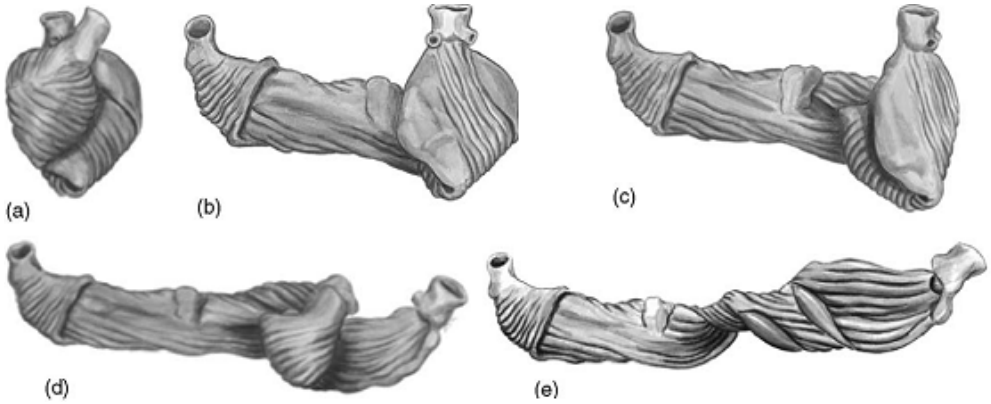

Figure 2.6 Unwrapping the heart [49]

The fibers in the wall are not uniformly oriented throughout the wall. Instead their orientation varies continuously so that stress and strain workload of the muscle fibers yields homogeneously. Some studies report that a total fiber angle varies of 140^{o} degrees from the outermost layer to innermost layer of the heart [43].

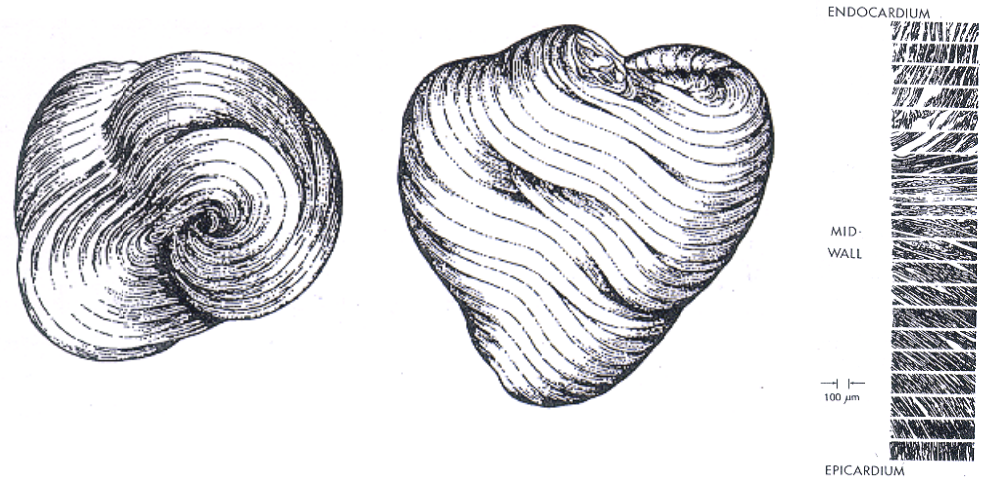

Figure 2.7 Fiber orientation distribution of the heart. View from apex, view from side and angular distribution from endocardium to epicardium [45]

The fiber orientation of the total heart tissue shows angular variation from endocardium to epicardium [13, 50, 51]. Figure 2.7 illustrates the fiber direction change in 100 μm width tissue for twenty separate sheets.

Furthermore, fiber orientation, distribution of gap junctions and pathologies influence the activity of the heart, which leads inhomogeneity in electromechanical properties of the heart.

2.1.2. Cardiac Physiology

The heart is subdivided into two halves by walls: *interatrial* and *interventicular* septa. Each of the septum controls one part of circulatory system [43]. Basic diagram of the circulatory system is illustrated in Figure 2.8. Two atria fill with blood and then contract simultaneously. This is followed by simultaneous contraction of both ventricles, which sends blood out of the heart to the body and organs.

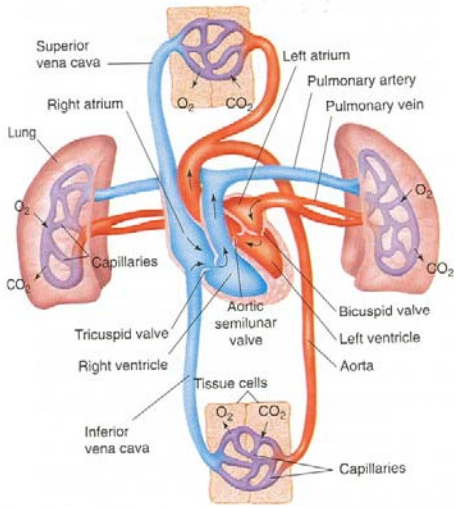

Figure 2.8 Circulation system diagram [41]

Blood is pumped from the left ventricle of the heart to capillaries in the periphery via the arterial vessels of the *systemic circulation* and returns via the veins to the right heart. It is then expelled from the right ventricle to the lungs via the *pulmonary circulation* and returns to the left heart [41].

Source of the pulmonary circulation is right ventricle. The blood, which has low O_2 concentration, is pumped out of the right ventricle through pulmonary arteries and reaches to lungs where will be oxygenized. Oxygen diffuses from the air to the capillary blood, while carbon dioxide diffuses in the opposite direction. After this gas exchange oxygen–rich blood reaches back to the left atrium of the heart through pulmonary veins [41].

Source of the systemic circulation is left ventricle. The blood, which has oxygenized in the lungs, is pumped out of the left ventricle through the aorta, which is the largest and most elastic artery in the body and reaches to each living cell in the body. Oxygen, nitrites and hormones diffuse from the capillary blood to cells, and metabolic wastes are collected from cells to blood. After this exchange, as a result of cellular respiration, the oxygen concentration of the blood decreases and carbon dioxide concentration increases in the blood. Through *superior* and *inferior venae cavaes* the blood coming from organs will return to the right atrium of the heart [41].

The resting heart rate is 60–80 beats per minute. A *cardiac cycle*, therefore takes roughly 1 s. It can be divided into four distinct phases:

(I)	contraction phase and	
(II)	ejection phase,	both occurring in *systole*;
(III)	relaxation phase and	
(IV)	filling phase	both occurring in *diastole*.

The atria contract at the end of phase IV. Electrical excitation of the atria and ventricles come before their contraction. The cardiac valves determine the direction of blood flow within the heart, e.g., from the atria to the ventricles or from the ventricles to the aorta or pulmonary artery. All cardiac valves are closed during phases I and III. Opening and closing of the valves is controlled by the pressures exerted on the two sides of the valves [44].

Near the end of ventricular diastole, the sinoatrial (SA) node emits an electrical impulse. This results in *atrial contraction* and is followed by *ventricular excitation*. The ventricular pressure then starts to rise until it exceeds the atrial pressure, causing the atrioventricular valves (mitral and tricuspid valves) to close. This marks the *end of diastole*.

The mean *end-diastolic volume* (EDV) in the ventricle is now about 120 mL or, more precisely, 70 mL/m^2 body surface area. In the isovolumetric contraction phase with all valves are closed, the ventricles now contract, producing the first heart sound, and the ventricular pressure increases rapidly. The semilunar valves (aortic and pulmonary valves) now open because the pressure in the left ventricle exceeds that in the aorta at about 80 mmHg, and the pressure in the right ventricle exceeds that in the pulmonary artery at about 10 mmHg [44].

During ejection period, the pressure in the left ventricle and aorta reaches a maximum systolic pressure (120 mmHg). In the early phase of ejection, a large portion of the stroke volume (SV) is rapidly ejected and the blood flow rate reaches a maximum. Myocardial excitation subsequently decreases and ventricular pressure decreases until

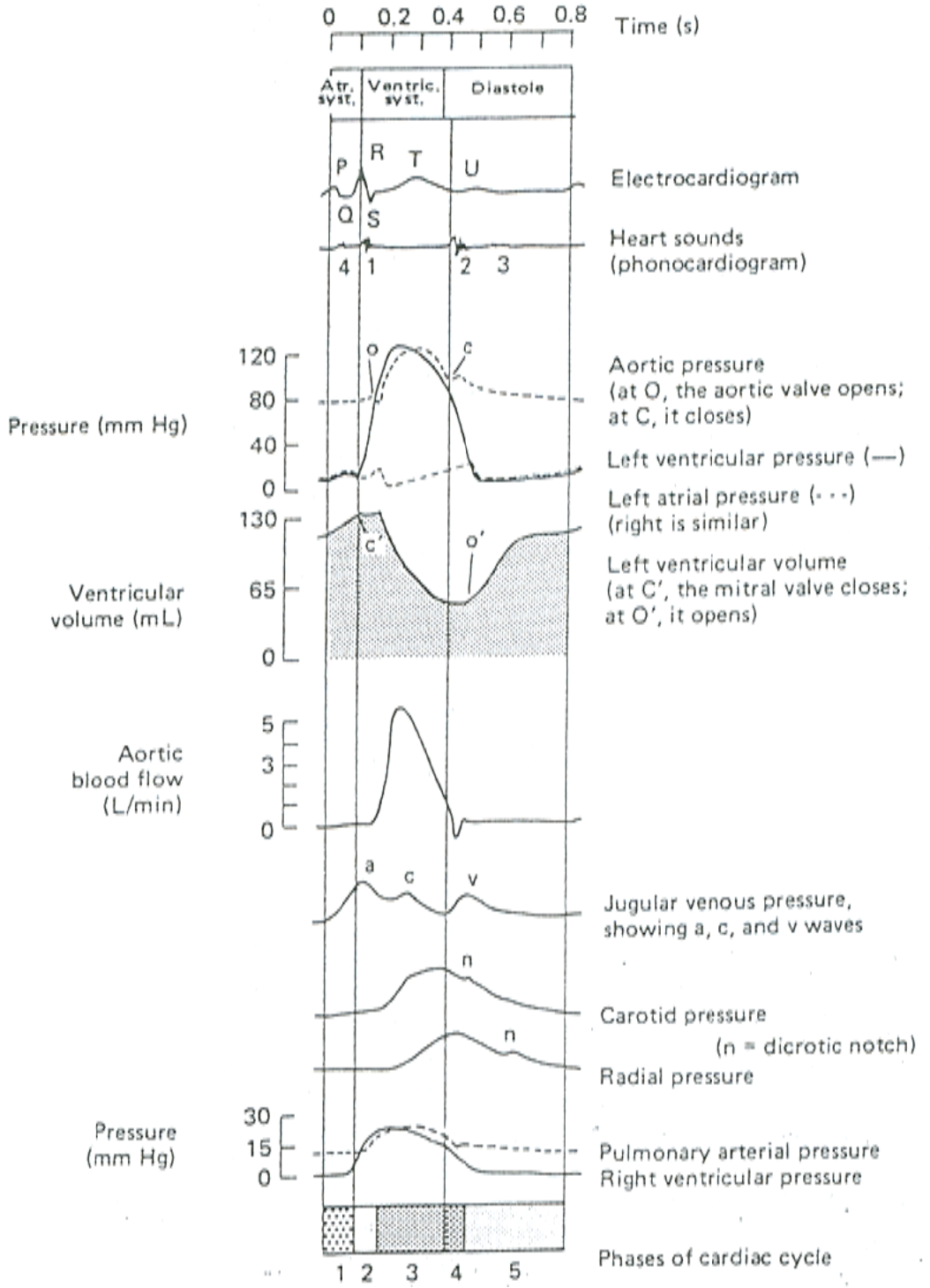

Figure 2.9 Cardiac cycle (1) atrial systole, (2) isovolumetric ventricular contruction, (3) ventricular ejection, (4) isovolumetric ventricular relaxation, (5) ventricular filling [47]

it falls below that of the aorta or pulmonary artery, respectively. This leads to closing of the semilunar valves, producing the second heart sound.

In the first phase of ventricular diastole (isovolumetric relaxation), the atria have meanwhile refilled, mainly due to the suction effect created by the lowering of the valve plane during ejection. As a result, the central venous pressure decreases. The ventricular pressure now drops rapidly, causing the atrioventricular valves to open again when it falls short of atrial pressure.

The blood passes rapidly from the atria into the ventricles, resulting in a drop in central venous pressure at the filling phase. At a normal heart rate, the atrial contraction contributes about 15% to ventricular filling. When the heart rate increases, the duration of the cardiac cycle decreases mainly at the expense of diastole, and the contribution of atrial contraction to ventricular filling increases.

Pressure, volume and blood flow changes during the cardiac cycle can be followed from Figure 2.9. Duration of each cardiac cycle changes due to heart rate. The graphs were illustrated in Figure 2.9 shows the normal heart rate value which is taken as 75 beats per minute.

The amount of blood pumped out of each ventricle beat, is called *stroke volume*, and is about 80 mL in a resting man. The output of the heart in unit time is called *cardiac output*, which is approximately equal to 5.5 L/min in a resting man. Cardiac output can be affected by various conditions, which affect either the heart rate or the stroke volume, like excitement, exercise, drugs, and also arrhythmias, and heart disease [47].

2.2. Cardiac Electrophysiology

The electrophysiology of the heart is necessary for the understanding of many aspects of the physiological and pathophysiological cardiac behavior. The origin of the electrical activity of the heart is the myocytes, which behave like nerve cells an electrical excitability. The electrical excitation of a myocyte is tightly coupled with its mechanical contraction. The electrical excitation propagation from a myocyte to its neighboring myocytes is primarily achieved by ion transportaion via the gap junctions. Additionally,

extracellular voltage changes resulting from the ion changes across the cell membrane from an external current flow and any applied external current can modulate the propagation and initiate an excitation [7].

The heart muscle cells generate the impulse within the heart automatically, conduct and response to electrical impulses. The frequency and regularity of pacemaking activity brings the heart rhythm. Myocardial tissue comprises a *functional syncytium* because the cells are connected by *gap junctions*. This also includes the atrioventricular junction. Thus, an impulse arising in any part of the heart leads to complete contraction of both ventricles and atria [44].

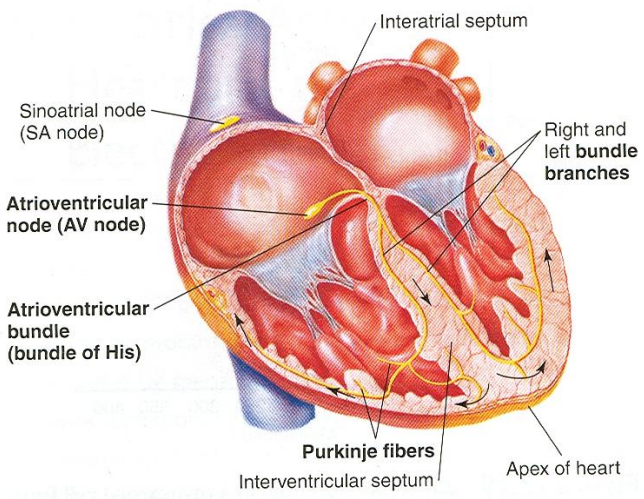

Figure 2.10 The conduction system of the heart [41]

Cardiac contraction is normally started from the sinoatrial node (SA node), which is therefore called the *primary pacemaker*. The impulses are conducted through the atria to the *atrioventricular node* (AV node). The *bundle of His* is the beginning of the specialized conduction system, including also the left and right *bundle branches* and the *Purkinje fibers*, which further transmit the impulses to the ventricular myocardium [44]. Conduction system and specialized myocardial cells are presented in Figure 2.10. Electrical activation propagation and contraction due to the activation of the mussels

were illustrated in Figure 2.11. The cell potential in the SA node is a *pacemaker potential*. These cells do not have a constant resting potential. Instead, they slowly depolarize immediately after each repolarization, the most negative value of which is the *maximum diastolic potential.* The membrane potential begins at -60 mV and gradually depolarize to -40 mV, which is the threshold for produce and action potential (AP). Thus each beat triggers another AP [44].

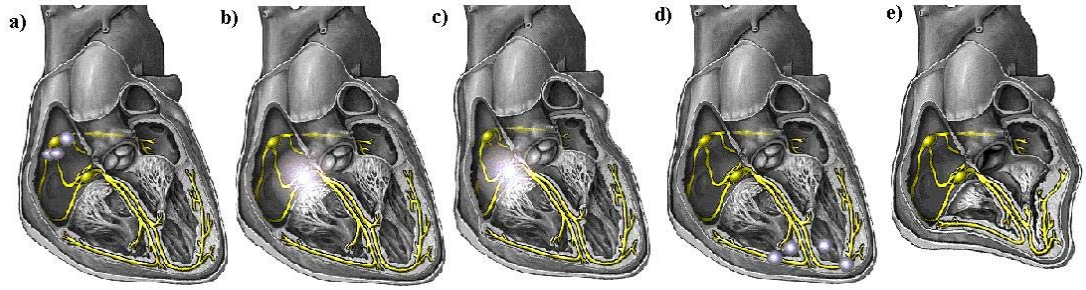

Figure 2.11 Normal spread of electrical activity. Electrical impulse (a) at SA node, pacemaker potential generation, (b) at AV node, atrial activation, (c) atrial contraction, (d) activation of ventricular myocardium, (e) ventricular contraction [48]

The pacemaker potential in SA node is formed by ion conductance and ionic flow through the cell membrane. In response to hyperpolarization a type of channel opens and due to its permeability Na^+ ions enter in the cell and produces depolarization. Cardiac pacemaker channels are also called HCN channels: hyperpolarization cyclic nucleotide channels. After the threshold voltage is passed, activation begins and the upward phase of the AP is reached by the inward diffusion of Ca^{2+} ions. Repolarization is produced by the opening of voltage-gated K^+ channels and the outward diffusion of K^+ ions [41].

Once neighboring myocardial cells have been simulated by AP, the cell also produces its own APs. According to the type and location of the cardiac cells the AP also changes. Different APs can be seen in Figure 2.12. Total electrical activity produces a few mV potential differences on body surface, which can be measured non-invasively and recorded as electrocardiogram (ECG) wave. ECG provides information on heart position, relative chamber size, heart rhythm, impulse origin, propagation and rhythm and conduction disturbances, extent and location of myocardial ischemia, changes in

electrolyte concentrations, and drug effects on the heart. However, it does *not* provide data on cardiac contraction or pumping function. [44]

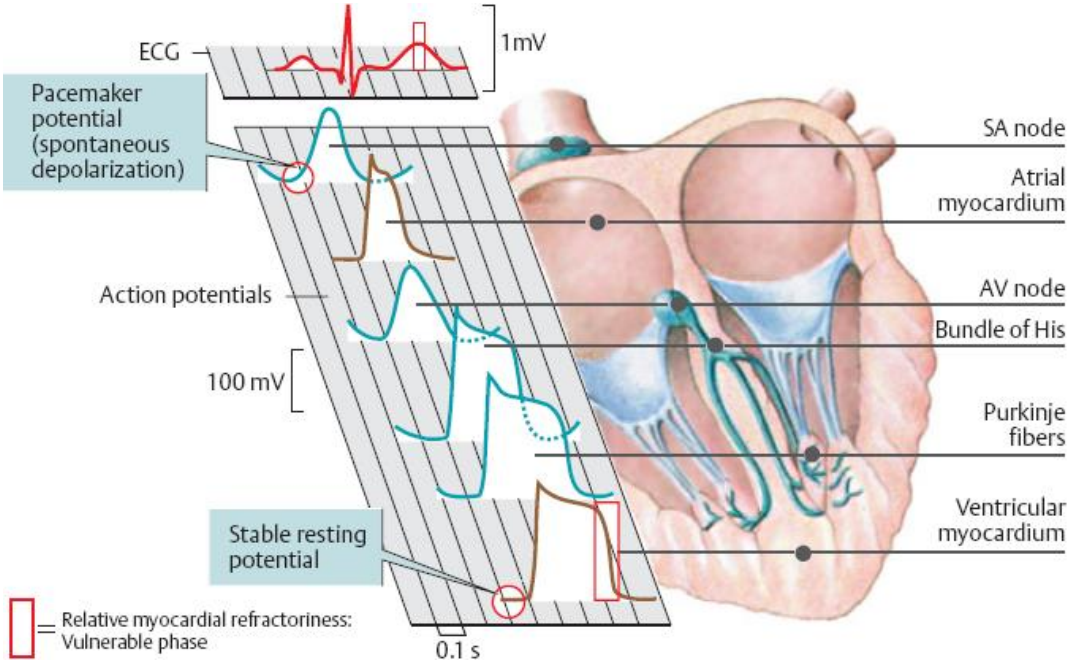

Figure 2.12 Cardiac excitation, action potentials of different myocardial cells [44]

Conduction timing, speed of propagation of myocardial cells on different locations in the heart is presented in Table 2.2. Also ECG waves caused by activated points are given. The highest velocity of excitation propagation is in Purkinje fibers, which provides the simultaneous contraction of ventricles. It can also be seen that right side of the heart is excited earlier than the left side of the heart both in atria and the ventricles. While SA node conduction has the highest rate (60-100 per minute), no rate is seen in ventricular myocardium.

In a classical electrocardiography (ECG), which measures the summation of cardiac action potentials, three main peaks are observed;

- P represents the atrial depolarization
- QRS interval represents the ventricular depolarization (also atrial repolarization occur at this interval but it is surpassed by ventricular depolarization)
- T represents the ventricular repolarization

Measurements of tissue from different regions show electrophysiological differences. These variations are due to different ion channel expression influencing mainly the plateau and repolarization phase of AP and the development of tension. The excitation velocity in ventricular myocardium is given as 1 m/s. However, this value is only valid in fiber direction. Electrical activation propagates also in other directions with a decrease in velocity; for perpendicular direction to the fiber angle the velocity is 1/3 of normal and propagation on other sheets decreases even more to 1/5 of normal [9].

Table 2.2 Cardiac impulse conduction [44]

Normal activation sequence		**Time (ms)**	**ECG**	**Velocity ($m \cdot s^{-1}$)**	**Conduction Intrinsic Rate (min^{-1})**
SA node	Impulse generation	**0**	P	0.05	60-100
Right atrium	Arrival of impulse in distal parts of atrium	**50**		0.8–1.0 in atrium	
Left atrium	Arrival of impulse in distal parts of atrium	**85**			
AV node	Arrival of impulse	**50**	P-Q	0.05	40-45
AV node	Relaying of impulse	**125**		0.05	
His bundle	Activated	**130**	QRS	1.0–1.5	25-40
End of bundle branches	Activated	**145**		1.0–1.5	
Purkinje fibers	Activated	**150**		3.0–3.5	
Inner myocardium	Right ventricle	**175**		1.0 in myocardium	None
Inner myocardium	Left ventricle	**190**			
Outer myocardium	Right ventricle	**205**			
Outer myocardium	Left ventricle	**225**			

Figure 2.13 shows the intra- and extracellular and ion changes and potential changes. The change can be divided into five separate phases: [52]

Phase 0 — The quick Na^+ channels open and sodium inflow begins. Then depolarization occur and membrane potential rises up to +20 mV.

Phase 1 — Slower K^+ channels open and the outward flow of K^+ stops the rising potential due to Na^+.

Phase 2 — Na^+ channels close while K^+ channels are still open.

Phase 3 — Slow Ca^{++} channels open and stay opened for approximately 20 sec which causes the plateau in membrane potential due to the inward flow of Ca^{++}.

Phase 4 — Ca^{++} channels close and repolarization occur and membrane voltage returns its resting value -90 mV.

Ion changes in all those phases have effects on both electrical and mechanical basis of the cardiac tissue response to excitation.

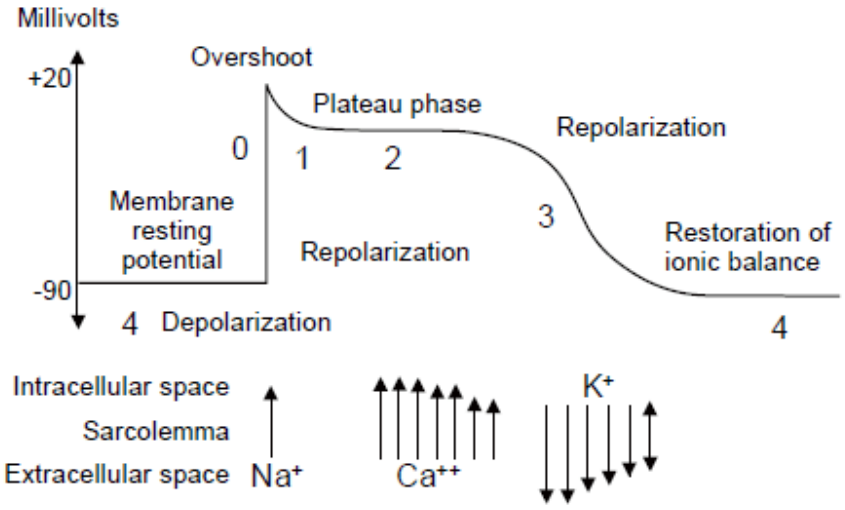

Figure 2.13 Membrane ion changes that causes action potential and an action potential in a myocardial cell from the ventricles [52]

2.3. Cardiac Mechanics

The primary mechanical event in the heart, the development of contractile force, is triggered by an electrical event, the cardiac action potential, through the process of excitation-contraction coupling. The electrical excitation of cardiac cells causes mechanical contraction controlled by intracellular calcium. The activity depends on tissue type and distribution, geometry of the heart, and heart rate.

The contractile response of cardiac muscle begins just after the start of depolarization and lasts about 1.5 times as long as the action potential. The timing and shape of electrical-mechanical coupling is shown in Figure 2.14. In electrical wave, absolute refractory period and relative refractory periods can be seen. In absolute refractory period, no matter how big the excitation potential is, the cell cannot be stimulated; on the other hand, in relative refractory period cell can be stimulated if the exciting potential is big enough.

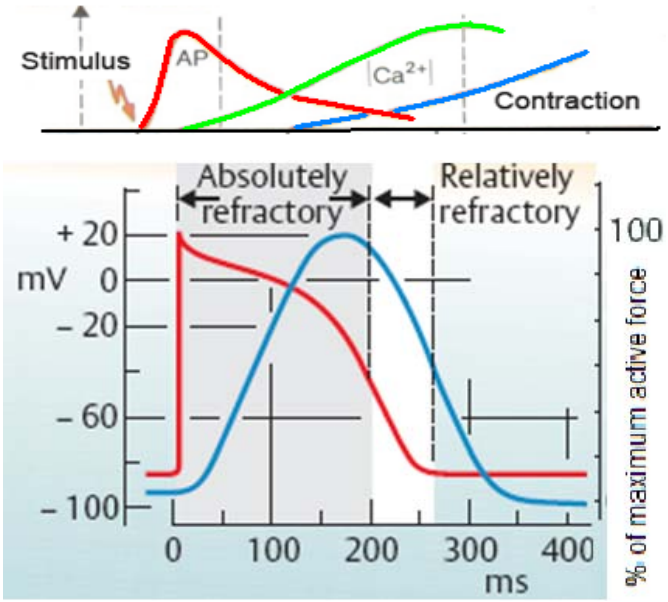

Figure 2.14 Action potential and contractile response of myocardium [41]

Response characters of the muscle are “all or none”, which means muscle fiber contract fully if they respond to the excitation. Since cardiac muscle is absolutely

refractory during most of the action potential, the contractile response is more than half over by the time a second response can be initiated [47]. Therefore, the tetanus of the skeletal muscles cannot be seen in cardiac tissues. It can be said that, this property of the cardiac muscle is a safety feature, because for any length of the time it would have lethal consequences. Ventricle muscle is said to be vulnerable period just at the end of an AP, because stimulation at this time will sometimes initiate ventricular fibrillation.

Myocardial muscle consists of contractile units called sarcomeres. Each sarcomere has characteristic proteins called actin, myosin, troponin, tropoyosin, whose lay out in the muscle fiber gives a striated appearance to myocardium [46]. Figure 2.15 represents the three dimensional structure of the sarcomere. Repeating units can be seen on the longitudinally oriented myofibrils.

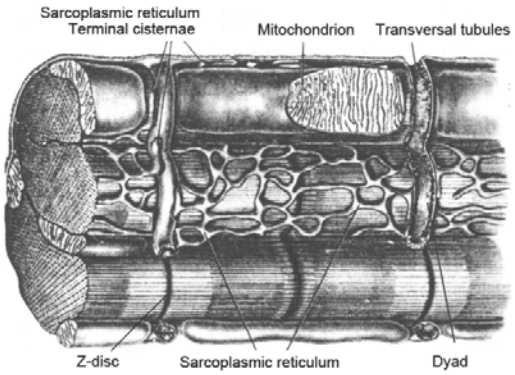

Figure 2.15 A myocardial cell or fiber reconstructed from electron micrographs [33]

The role of Ca^{2+} in excitation-contraction coupling is similar to its role in skeletal muscle, except that Ca^{2+} entering from the extracellular fluid (ECF) as well as Ca^{2+} from the sarcoplasmic reticulum contributes to contraction [47]. The longitudinal section images taken with the electron microscopy and corresponding illustrations of sarcomere is given in Figure 2.16, for relaxation and contraction phases of the tissue.

In the illustrations (Figure 2.16) the contractile mechanism of a sarcomere can be seen. In the schematic diagram, Figure 2.16 (a) is showing the thin actin-containing (orange) and thick myosin-containing (purple) filaments. Names of different colored sections are;

Z lines: separates sarcomeres from each other, which can be seen as dark lines.

I band: lightly straining parts locating outer ends

A band: denser staining locating in the I bands.

H zone: located in the center of the A band.

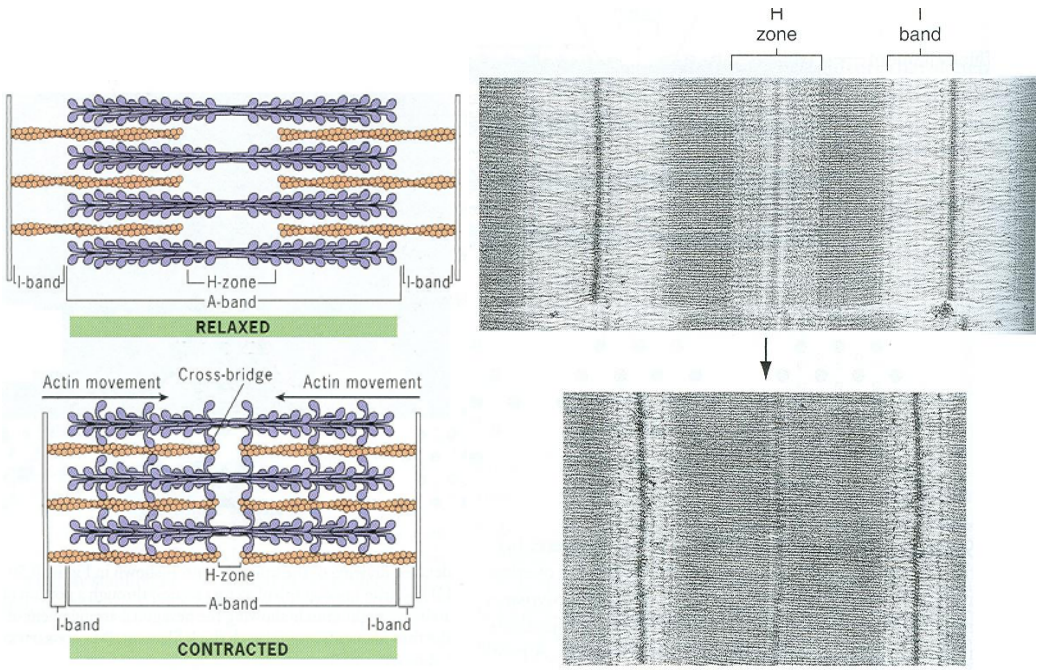

Figure 2.16 Muscle contraction: shortening of the sarcomere, (a)schematic diagram, (b)electron micrographs of longitudinal sections [46]

When the contraction happens: muscle fiber shorten, length of a band stands constant, while H and I bands decreased in width and then disappeared together. As shortening progressed, the Z line of both ends of the sarcomere moved inward until they connected the outer end of the A band. [46]

The molecular basis of the contractile activity of the muscle is highly affected by the Ca^{2+} concentration. The incoming AP opens *voltage gated* Ca^{2+} *channels,* associated with *dihydropyridine receptors*, on the sarcolemma of myocardial cells, starting an influx of Ca^{2+} from the extracellular fluid (ECF). This produces a local increase in cytosolic Ca^{2+} which, in turn, triggers the opening of *ligand-gated*, *ryanodine- sensitive* Ca^{2+} *channels* in the sarcoplasmic reticulum, where the Ca^{2+} is stored. The influx of Ca^{2+} into the cytosol results in electromechanical coupling and myocardial contraction.

The cytosolic Ca^{2+} is also determined by active transport of Ca^{2+} ions back into the Ca^{2+} stores via a Ca^{2+}-ATPase, which is stimulated by *phospholamban*, and to the ECF. This is achieved with the aid of a Ca^{2+}*-ATPase* and a *3Na* $^{+}$/ Ca^{2+} *exchange* carrier that is driven by the electrochemical Na+ gradient established by Na+-K+-ATPase. Contraction activity diagram is given in Figure 2.17 in details.

Although the heart beats autonomously, efferent cardiac nerves are mainly responsible for modulating heart action according to changing needs. The *autonomic nervous system* (and epinephrine in plasma) can alter the following aspects of heart action:

(a) *rate of impulse generation* by the pacemaker and, thus, the heart rate
(b) *velocity of impulse conduction*, especially in the AV node
(c) *contractility* of the heart, i.e., the force of cardiac muscle contraction at a given initial fiber length.

These changes in heart action are induced by acetylcholine released by parasympathetic fibers of the vagus nerve. The firing frequency of the SA node is increased by norepinephrine (NE) and epinephrine (E) and decreased by acetylcholine (ACh). ACh (left branch of vagus nerve) decreases the velocity of impulse conduction in the AV node, whereas NE and E increase it due to their negative and positive dromotropic effects, respectively. This is mainly achieved through changes in the amplitude and slope of the upstroke of the AP, g_K and g_{Ca}.

In positive inotropism, NE and E have a direct effect on the working myocardium. The resulting increase in contractility is based on an increased influx of Ca^{2+} ions from the ECF triggered by adrenoceptors, resulting in an increased cytosolic Ca^{2+}. This Ca^{2+} influx can be inhibited by administering Ca^{2+} channel blockers (Ca^{2+} antagonists). Other factors that increase cardiac contractility are an increase in AP duration, resulting in a longer duration of Ca^{2+} influx, and inhibition of Na+-K+-ATPase [44].

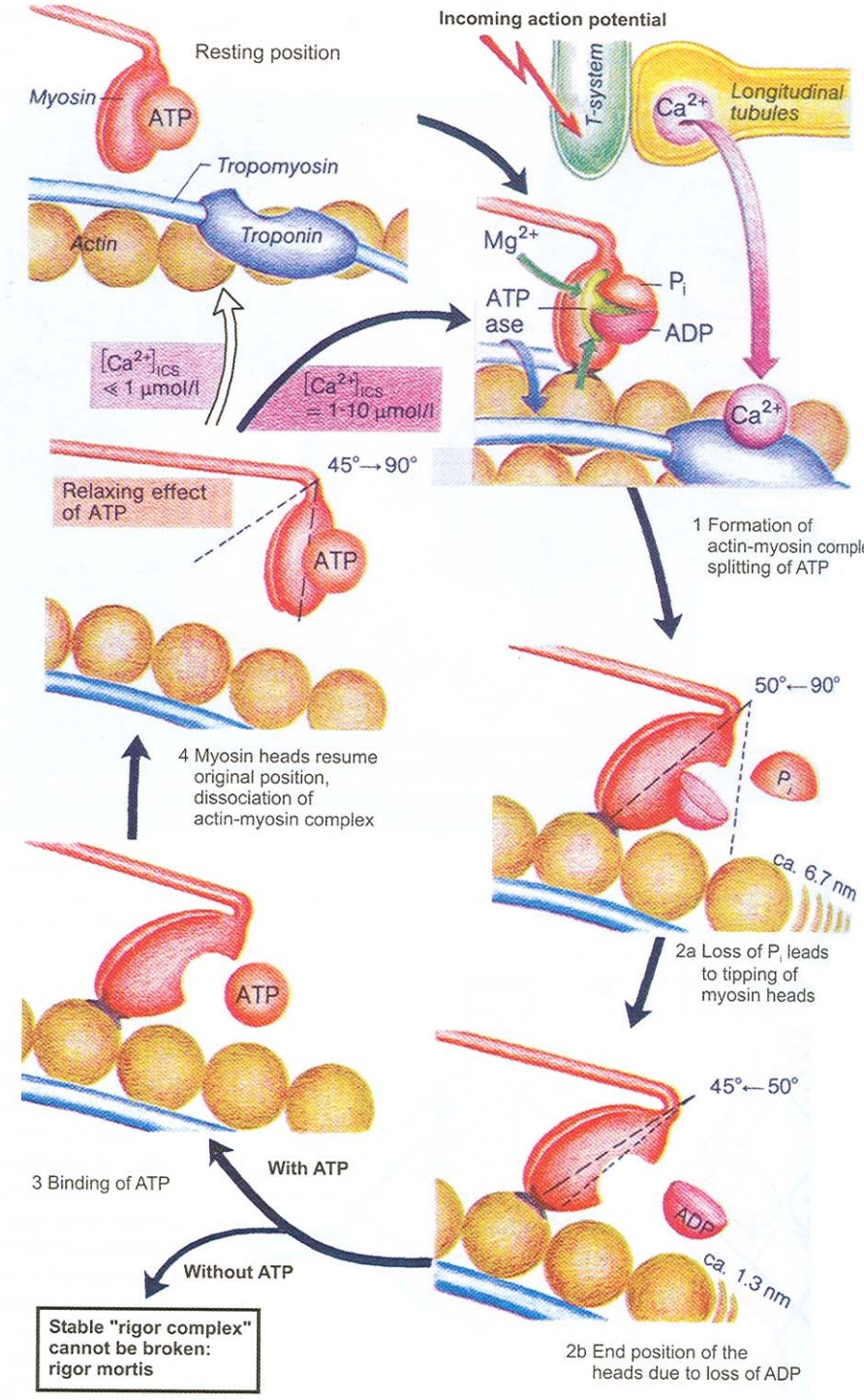

Figure 2.17 Work cycle of sliding filaments [44]

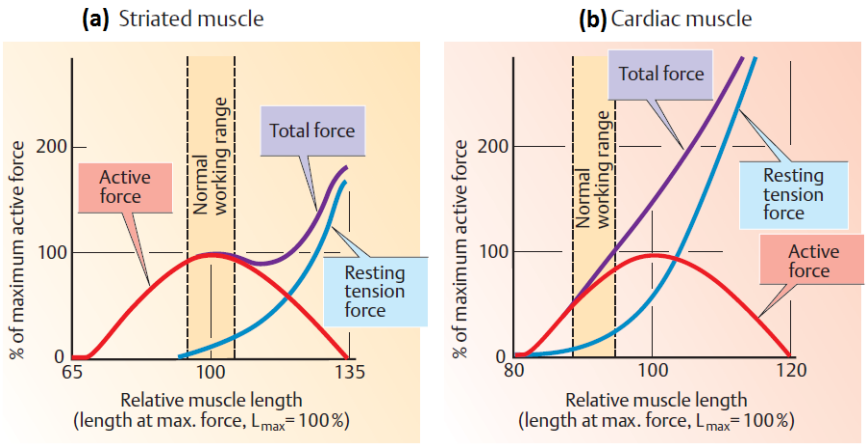

Figure 2.18 Length-force curve (a) for skeletal muscle, (b) for cardiac muscle [44]

The length (L) and force (F) or "tension" of a muscle are closely related. The relation between force and the muscle length is presented in Figure 2.18, both for striated, skeletal muscles and cardiac muscles. The total force of a muscle is the sum of its active force and its extension force at rest. Since the active force is determined by the magnitude of all potential actin-myosin interactions, it varies in accordance with the initial sarcomere length [33, 44]. In Figure 2.19 sarcomere length in µm and corresponding tension percentage is given for systole and diastole, according to the cat papillary muscle experimental studies.

Skeletal muscle can develop maximum active (isometric) force (F_0) from its resting length (L_{max}; sarcomere length ca. 2 to 2.2 µm). When the sarcomeres get shorten ($L<L_{max}$), part of the thin filaments overlap, allowing only forces smaller than F_0 to develop. When L is 70% of L_{max} (sarcomere length: 1.65 µm), the thick filaments make contact with the Z disks, and F becomes even smaller. In addition, a greatly pre-extended muscle ($L>L_{max}$) can develop only restricted force, because the number of potentially available actin–myosin bridges is reduced. When extended to 130% or more of the L_{max}, the extension force at rest becomes a major part of the total muscle force.
The length–force curve corresponds to the cardiac pressure–volume diagram in which ventricular filling volume corresponds to muscle length, and ventricular pressure corresponds to muscle force. Changes in the cytosolic Ca^{2+} concentration can modify the pressure–volume relationship by causing a change in *contractility*.

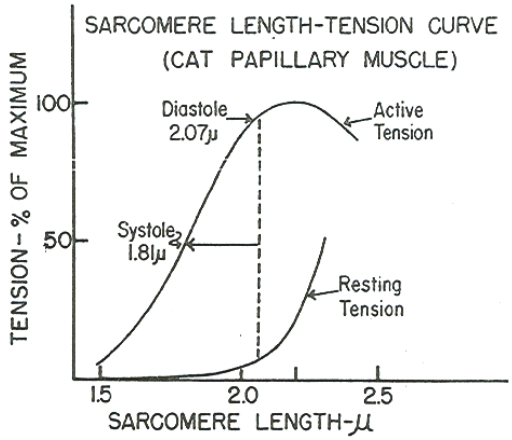

Figure 2.19 Length-Tension curve. Average sarcomere lengths in diastole and systole[33]

Since skeletal muscle is more extensible than the cardiac muscle, the passive extension force of cardiac muscle at rest is greater than that of skeletal muscle. Skeletal muscle normally functions in the plateau region of its length–force curve, whereas cardiac muscle tends to operate in the ascending limb (below L_{max}) of its length–force curve without a plateau. Hence, the ventricle responds to increased diastolic filling loads by increasing its force development, which is called: *Frank–Starling mechanism.* In cardiac muscle, extension also affects troponin's sensitivity to Ca^{2+}, resulting in a steeper curve.

Action potentials in cardiac muscle are of much longer duration than those in skeletal muscle because g_K temporarily decreases and g_{Ca} increases for 200 to 500ms after rapid inactivation of Na^+ channels. This allows the slow influx of Ca^{2+}, causing the action potential to reach a *plateau*. As a result, the refractory period does not end until a contraction has almost subsided. Therefore, tetanus cannot be evoked in cardiac muscle.

Unlike skeletal muscle, cardiac muscle has no motor units. Instead, the stimulus spreads across all myocardial fibers of the atria and subsequently of the ventricles generating an *all-or-none contraction* of both atria and, thereafter, both ventricles.

In cardiac muscle but not in skeletal muscle, the duration of an action potential can change the force of contraction, which is controlled by the variable influx of Ca^{2+} into the

cell. The greater the force (load) is, the lower the velocity of an (isotonic) contraction will be. Maximal force and a small amount of heat will develop if shortening does not occur. The maximal velocity and a lot of heat will develop in muscle without a stress load. Light loads can therefore be picked up more quickly than heavy loads. The total amount of energy consumed for work and heat is greater in isotonic contractions than in isometric ones [33, 44].

2.4. Cardiac Diseases

Cardiovascular disease affects both the heart itself and/or the blood vessel system. Research on disease show that, women who suffer cardiovascular disease usually suffer from the blood vessel diseases and men usually suffer from diseases that directly affect the heart muscle itself. In this part of, some of the most commonly seen heart diseases are presented and investigation methods are given. [53-55]

Heart failure is the inability of the heart to supply necessary blood flow and therefore oxygen delivery to peripheral tissues and organs. If the oxygen delivery of organs is not enough, this will lead to reduced exercise capacity, fatigue, and shortness of breath. It can also lead to organ dysfunction in some patients, even death in some. [54]

Heart failure causes can be listed as: myocardial infarction, coronary artery diseases, valve disease, cardiomyopathy, myocarditis, pericarditis, arrhythmias, chronic hypertension and also some other diseases which are not directly related to cardiovascular system: thyroid disease, pregnancy and/or septic shock [55]

Coronary artery disease refers to the failure of the coronary circulation of cardiac muscle itself and surrounding tissue. Coronary artery disease (CAD) causes changes in both structure and function of the blood vessels and cause an abnormal deposition of lipids in the vessel wall, vascular inflammation, plaque formation and accumulation of them within the arteries and thickening of the vessel wall may cause the clog up of the artery and therefore decrease in supply the myocardium. The disease called **atherosclerosis** is narrowing and “hardening of the arteries”, which has no known cure. The hardening and thickening of the arteries causes a decrease in the blood circulation

through the affected vessel and affects the organs it serves. When CAD restricts blood flow to the myocardium (**ischemia**) there is an imbalance between oxygen supply and oxygen demand. Furthermore, acute or chronic ischemia caused by CAD can impair cardiac electro-mechanical activities leading to heart failure and arrhythmias. **Angina pectoris** (chest pain) and **myocardial infarction** (heart attack) are the main symptoms of coronary heart disease [54].

Angina, also known as **angina pectoris**, refers to pain originating from the heart. Chest pain or pressure in the chest or in other words “tightness in the chest”, which may spread to some other organs (the neck, jaw, shoulders, both arms, hands) are the commonly seen symptoms of angina pectoris. The painful condition occurs when the heart muscle tissue does not receive enough oxygen, especially during periods of exercise or excitement [54].

Cardiomyopathy means "heart muscle disease". The tissue can either be enlarged, abnormally thick, rigid, or replaced with scar tissue. It is the deterioration of the function of the myocardium for any reason. Coronary artery disease and heart attacks cause ischemic cardiomyopathy. Scars in the heart muscle from heart attacks leave areas of the heart which are unable to contribute to the pumping. People with cardiomyopathy are often at risk of **arrhythmia** and/or **sudden cardiac death** [2, 54].

Cardiomyopathies represent the second largest group of patients who experience sudden cardiac death. Sustained ventricular **tachycardia** and **left ventricular hypertrophy** are the strongest risk factors for sudden cardiac death. The left ventricle is the largest, strongest chamber of the heart because it pumps oxygenated blood out to the body. When the body does not get enough blood, the heart muscle may respond by dilating. The inside area of this ventricle enlarges as the muscle surrounding it stretches and thins (dilates). A dilated ventricle pumps with less force than a healthy ventricle. Often, the heart muscle will continue to stretch in an effort to compensate for the reduced pumping action. Thus, the atria and right ventricle may also dilate as this disease progresses.

Arrhythmias, abnormal heart rates or rhythms, may occur as cardiomyopathy interferes with the heart's electrical signaling system. Arrhythmias may result in the loss of a heart beat (cardiac arrest).

Patients with primary **electrophysiological abnormalities** represent the disease where the mechanical function of the myocardium is normal and an electrophysiological disorder represents the primary cardiac problem, which includes patients with the diseases of the conduction system. A frequent cause of arrhythmia is coronary artery disease because this condition results in myocardial ischemia or infarction.

Cardiac arrhythmias are pathological changes in cardiac *impulse generation or conduction*. Disturbances of impulse generation change the sinus rhythm. *Sinus tachycardia* is called to the abnormal rise in the sinus rhythm up to 120 beats per minute in resting measurements while the *sinus bradycardia is the heart* rate fall below 60 beats per minute. In both cases the rhythm is regular whereas in *sinus arrhythmias* the rate varies. Ectopic pacemakers can be initiated by foci in the atrium, AV node or ventricles, even when normal stimulus generation by the SA node is taking place. The rapid discharge of impulses from an atrial focus can induce atrial tachycardia, which triggers a ventricular response rate of up to 200 beats/min. Purkinje fibers act as impulse *frequency filters*, because they transmit stimulus to the ventricles only every second or third due to their long AP durations and refractory period. [54]

Ventricular tachycardia is a rapid train of impulses originating from a ventricular (ectopic) focus, starting with an extra-systole (ES). The heart therefore fails to fill, and the stroke volume decreases. Because of failure of the ventricle to transport blood, the results can be fatal [44].

Fibrillation is a rapid, irregular twitching of the heart muscle tissue. In order to function as a pump, the muscle tissue if the heart must contract and relax in a smooth, coordinated manner [54-56].

This condition may affect either of the two sets of chambers of the heart: atria and ventricles.

- Atrial fibrillation is the extremely rapid twitching of the upper chambers (atria) of the heart. When the atria starts to contract non-rhythmically, the ventricles do not receive a regular stimulus to contract. This results in an inefficient pumping of the blood and irregular pulse. In Figure 2.20 rhythm changes due to atrial fibrillation can be seen. Representative action potentials are shown from the SA node, atrium, AV node and ventricles. The vertical line on each action potential recording corresponds to a common time reference. LA, left atrium; LV, left ventricle; RA, right atrium; RV, right ventricle.

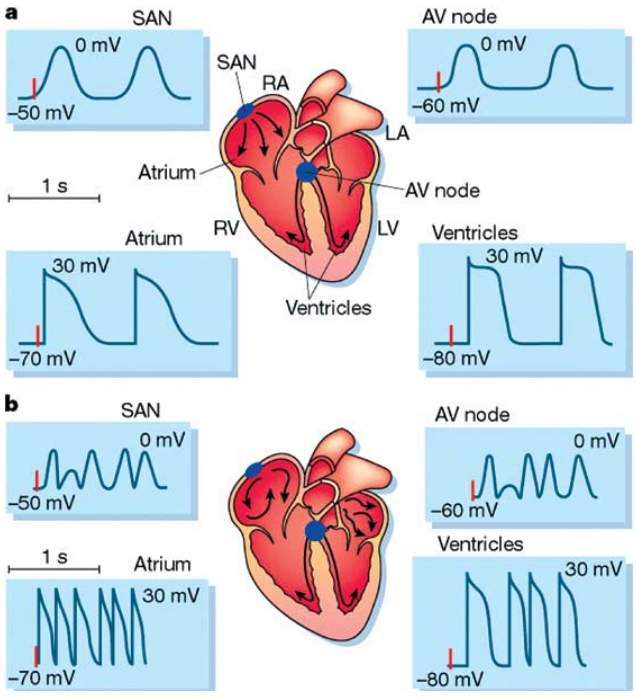

Figure 2.20 Diagram of electrical activity during atrial fibrillation. a, Normal rhythm; b, atrial fibrillation [57]

- Ventricular fibrillation is similar to atrial fibrillation; however, it affects the lower chambers of the heart. This condition may have fatal results within minutes because the rapid, “fluttering” of the ventricles pumps little or no blood through the circulatory system of the body.

Ventricular fibrillation mainly occurs when an ectopic focus fires during the relative refractory period of the previous AP. The APs generated during this period have *smaller slopes, lower propagation velocities, and shorter durations*. This leads to re-excitation of myocardial areas that have already been stimulated (***re-entry*** *cycles*). Ventricular fibrillation can be corrected by a controlled electrical shock with a *defibrillator* [53-58].

Congenital heart defects (CHD) are problems with the heart's structure that developed in the embryonic heart or early development and are present at birth or shortly thereafter. Congenital heart defects are often thought to be genetic, but they can also be caused by illness or behavioral factors in the mother such as viral infections like German measles, certain prescription drugs and over-the-counter medicines, alcohol, or illegal drugs. Some conditions like Down syndrome and Turner syndrome are associated with CHDs [54].

Valvular disease is a chronic disease process is responsible for defective valves in older individuals. Sometimes, the disease results from a triggering event many years earlier, such as rheumatic fever. Bacterial infection, viral infection and inflammation of valves can trigger changes in valve structure and function. Normally, valve leaflets are very thin and flexible, but they can become thickened and rigid in response to a disease processes. When this occurs to a valve, it may not be able to fully open or to completely close. Valve disease found in younger individuals is usually due to a congenital defect in the embryologic development of the heart. Valve dysfunction can occur secondarily to other cardiac diseases, such as coronary artery disease, cardiac hypertrophy and cardiac dilation [56].

There are two general types of cardiac valve defects: stenosis (narrowing) and insufficiency, and combination of those may also occur. The disease can have serious cardiac consequences, and produce the following clinical symptoms: shortness of breath, fatigue, reduced exercise capacity, heart failure, hypertension, edema, chest pain, arrhythmias and stroke [54].

Investigation methods of cardiac diseases can be listed as: electrocardiogram (EKG or ECG), holter monitor, implantable loop recorders, chest X-ray, echocardiogram,

transesophageal echocardiography (TEE), exercise stress tests, phonocardiography (PCG), radionuclide tests, positron emission tomography (PET) scanning, magnetic resonance imaging (MRI), blood/cardiac enzyme tests, cardiac catheterization, coronary angiography, and myocardial biopsy [56].

Each of the disease given above have some different features that is different from normal tissue and can be detected by the diagnostic techniques.

Valvular heart diseases can be detected using: PCG, ECG, echocardiogram, and chest X-rays, while atherosclerosis and heart attack can be detected using cardiac related blood tests, angiography, and ECG.

Even though each of the techniques gives different diagnostic investigations as a result, the most commonly used start point of cardiac diagnosis is ECG.

CHAPTER 3

THEORY

3.1. Modeling the Electro-Mechanical Activity of the Heart

Modeling of cardiac electromechanics provides knowledge of physiological and pathological phenomena. The model parameters are based on measurement data of protein, cell, tissue, or organ properties for the heart tissue. Detailed studies carried out for the cardiac tissue and physiological properties have been presented in the background information section. Model of the human heart provides a tool to investigate the dynamical behavior in a detailed way that cannot be achieved experimentally. On the other hand, models are always simplified descriptions of the real process and thus the results need to be validated.

The modeling of cardiac electromechanics includes several different research topics, i.e. anatomy, electrophysiology, conduction, force development and shape change. The anatomical model builds the basis to describe the individual heart. The electrophysiological model reproduces the electrical activity of macroscopic cardiac tissue. Models of the electrical current flow in tissue determine the conduction. The mechanical model describes the displacement process in the contractile unit.

The focus of this work is directed to mathematical modeling of left ventricle anatomy, electrophysiology and contraction in the human heart. A main objective is to reconstruct human electromechanical inhomogeneity in schematic anatomical models. The fiber orientation is inserted in the ventricular model with angular based placed layers.

Furthermore, several different pathological states were modeled to see the capacity of the models reconstructing cardiac dysfunction. A special focus is given on ectopic beats and reentry for pathological cases.

Models of biological tissues combine concepts of space, time, and interaction. Interest in macroscopic approaches, has lately grown due to the recent availability of measured anatomical data and has triggered the development of new mathematical models, such as *cellular automata*. Such models allow us to follow and analyze spatio-temporal dynamics at the individual nodes on tissue.

The model results should be relatively robust with respect to the chosen space-time-state framework. In specifying the interactions, namely the rules of the physiological states, one can choose several levels of description involving different resolutions of spatial detail, ranging from *microscopic* to *macroscopic* perspectives. Transitions from one level to the other involve *approximations* with regards to the spatio-temporal nature of the underlying interactions.

Table 3.1 Mathematical modeling approaches to spatio-temporal pattern formation (ODE:ordinary differential equation, PDE: partial differential equation [59]

Model approach	Space variable	Time variable	State variable
I. PDEs, integro-differential eqs.	Continuous	Continuous	Continuous
II. Spatial point process, set of rules	Continuous	Continuous	Discrete
III. Integro-difference eqn.	Continuous	Discrete	Continuous
IV. Set of rules	Continuous	Discrete	Discrete
V. Coupled ODEs	Discrete	Continuous	Continuous
VI. Interacting particle systems	Discrete	Continuous	Discrete
VII. Coupled map lattices, system of difference eqns.,	Discrete	Discrete	Continuous
VIII. Cellular automata,	Discrete	Discrete	Discrete

One way to classify approaches to modeling spatially extended dynamical systems is to distinguish between continuous and discrete state, time and space variables. A classification of different approaches is presented in Table 3.1.

3.2. Cellular Automata

A cellular automaton is the simplest model of a spatially distributed process that can be used to simulate various real-world processes. They consist of a two-dimensional array of cells that evolve step-by-step according to the state of neighboring cells and certain rules that depend on the simulation. Cellular automata (CA) are an idealization of a physical system, which takes only place in the discrete world [60]. CA can be explained in terms of discrete dynamical systems: discrete in space, time, and state. Spatial and temporal discreteness are also inherent in the numerical analysis of approximate solutions, e.g., partial differential equations. As long as a stable *discretization scheme* is applied, the exact continuum results can be approximated. The results are getting closer to original results, as the number of nodes and the number of time steps is increased, i.e. the numerical scheme is convergent.

The discreteness of cellular automata with respect to the limited number of possible states is not typical of numerical analysis, where a small number of states would correspond to an extreme *round-off* error. It is possible to devise cellular automaton rules that provide approximations to partial differential equations [61].

Cellular automata can act as good models for physical, biological and sociological phenomena. It is a commonly used method in explaining many physical systems; e.g. traffic flow [62], biology, neurobiology, population biology, predator, prey models, an activator–inhibitor circuit that corresponds to a reaction–diffusion process [63]. The reason for this is that each person, or cell, or small region of space "updates" itself independently (parallelism), basing its new state on the appearance of its immediate surroundings (locality) and on some generally shared laws of change (homogeneity). The remarkable thing about CAs is their ability to produce interesting and logically deep patterns on the basis of very simply stated preconditions. In both physics and in CAs,

i) the world is happening in many different places at once, ii) there is no action at a distance, and iii) the laws of nature are the same everywhere.

CA provides a theoretical framework on which to build a rigorous mathematical model that can be analyzed and further refined [64]. Although the physical world really is not an exact cellular automaton, CAs are rich enough to describe physiological and pathological conditions of tissues. The cell models provide an exact description of the electrophysiology of a single cardiac cell as well as of parts of the heart. Still the simulation of a depolarization and repolarization cycle for the whole heart with their means is a non-trivial task requiring a huge computational power.

In the heart modeling many research groups use CA to explain the structures of following anatomical and physiological features of the heart: beats in fibrillation phenomena, excitable and reaction-diffusion media [65, 66], excitation propagation with simplified action potentials, diffusion and speed of the electrical wave [67, 68], biventricular excitation propagation system [69], anisotropic canine heart model for electrical wave propagation, arrhythmia and fibrillation in the heart [70], approximation to cardiac pacemaker [71], and basic features in both normal and pathological cases like hypertrophy and dilatation [60].

The cellular automaton is a convenient mathematical model to describe the excitation propagation through the heart macroscopically. If the transmembrane voltage of a myocardial cell exceeds the threshold potential, the cell gets excited and triggers the excitation of the neighboring cells.

The CA based cardiac model is able to simulate various cardiac diseases. For example, decreasing the action potential amplitude and excitation propagation velocity in some regions of the myocardium represents an ischemia or an infraction.

3.2.1 Neighbors

A cellular automaton (CA) is a mechanism for modeling systems with local interactions. A CA is a regular lattice of cells with local state, which interact with their neighbors subject to a uniform rule which governs all cells. The neighborhood in a CA is the set of

nodes whose state can affect a given cell at one instant. Neighbors can be classified by the dimensionality of the automaton (most experimentation is done with one- or two-dimensional automata), and by the geometric fashion in which cells are interconnected [61-72].

In Figure 3.1, three different algorithms used in one-dimensional CA studies were shown. Periodic, reflecting and fixed end points can be used in different algorithms. In the proposed algorithm, fibers are represented in one dimensional fixed cellular automaton (Figure 3.1(c)). In one dimensional case, the propagation to both sides is at the same velocity.

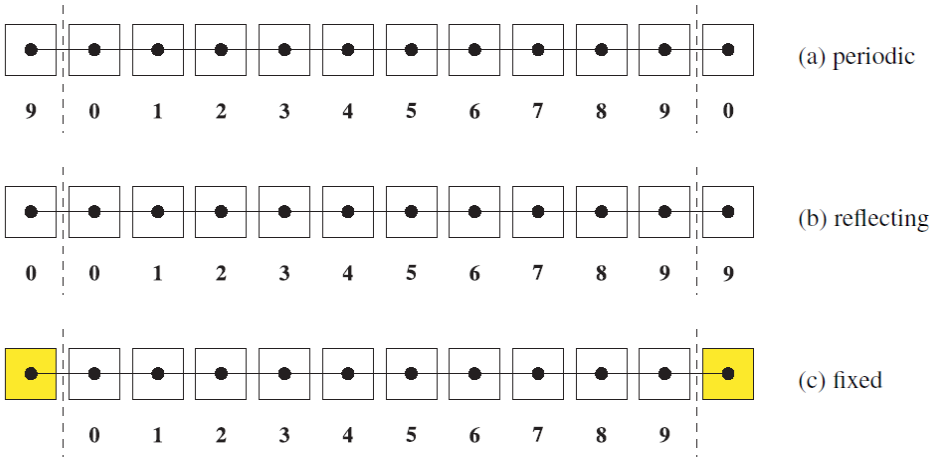

Figure 3.1 One-dimensional Cellular Automata: (a) periodic, (b) reflecting and (c) fixed [59]

The tissue and some of the disease cases were represented by two dimensional cellular automata. Also three-dimensional geometry has its basis from two dimensions; only layered based geometry was set for a realistic three-dimensional application.

Two-dimensional propagation, propagation on a sheet, also uses “fixed” (Figure 3.1(c)) cellular automata approximation, while “periodic” (Figure 3.1(a)) cellular automata neighborhood is used in implementation of the proposed algorithm in three-dimensional ventricular electrical excitation propagation.

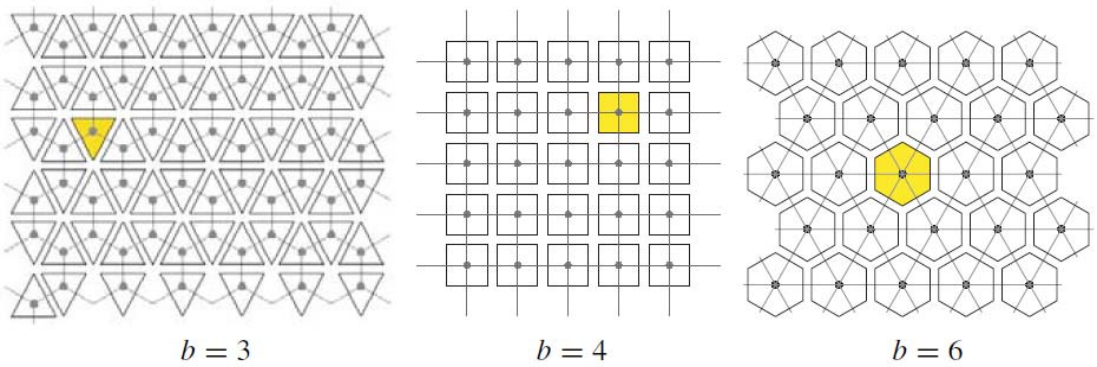

Figure 3.2 Two-dimensional Cellular Automata: (a) 3 neighbors, (b) 4 neighbors, (c) 6 neighbors [59]

Using two dimensions, many different numbers of neighbors can be taken in consideration. Figure 3.2 shows the possible neighboring techniques: b=3, 4, 6 first order neighbors are given.

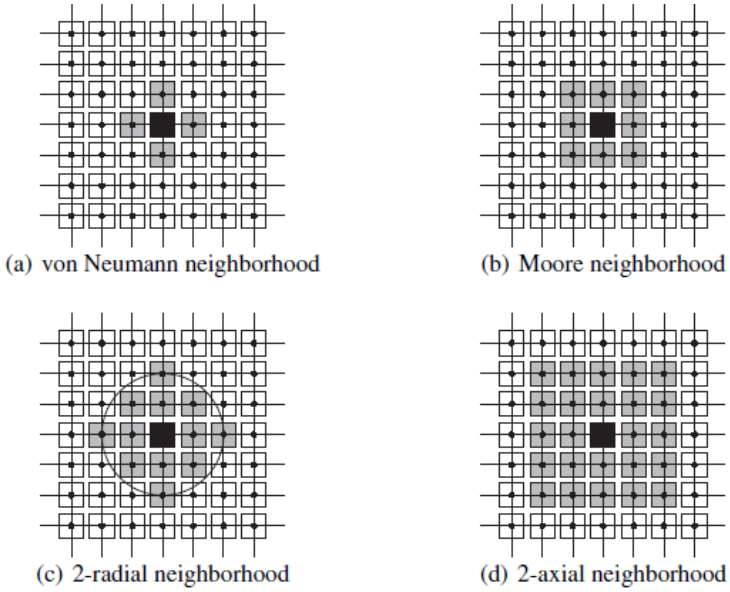

Figure 3.3 Examples of interaction neighborhoods (gray and black cells) for the black cell in a two-dimensional square lattice [59]

In the proposed algorithm two dimensional cellular automata geometries were prepared for rectangular neighborhoods. As it is seen in Figure 3.2 (b), for rectangular geometry,

each node has 8 first neighboring cells. However, in cellular automata, choosing the number of neighbor and their locations are also a part of computation [73].

Figure 3.3 represents the possible neighborhood scenarios that can be taken into consideration, as Cellular Automaton geometry is prepared. Although in proposed algorithm Moore neighborhood approximation is used (Figure 3.3 (b)), the rules of each neighbor are not the same.

Also 2- and more-axial neighborhood is used in some cases, especially for modeling the fiber angles. The CA based algorithm is highly affected by the different scale of time step of model and different number of neighborhoods and the number of nodes in the model geometry.

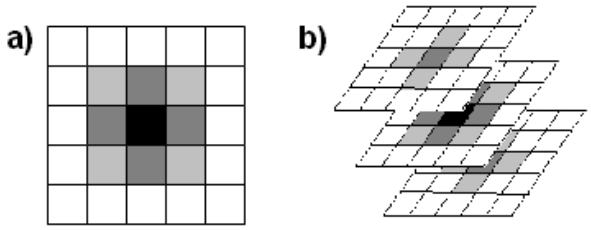

Figure 3.4 Cellular automaton-neighbors in (a) two-dimensions and (b) three-dimensions in proposed algorithm

Figure 3.4 illustrates the proposed algorithms' neighborhood pattern, in 2D and 3D. The black node represents the active node and gray ones represent the neighboring cells. According to gray level of the neighbor, the rule of propagation changes through this neighbor.

3.2.2 Rules

The rule is the "program" that governs the behavior of the system. All cells apply the rule, over and over, and it is the recursive application of the rule that leads to the remarkable behavior exhibited by many cellular automata. When experimenting with cellular automata, one is primarily engaged in defining new rules which lead to interesting or useful behavior.

Most of the programs in Cellular Automata are two-dimensional cellular automata. In these programs the computer screen is divided up into "cells" which are colored rectangles or dots. Each cell is repeatedly "updated" by changing its old color to a new color.

3.3. Implementation of the Model

3.3.1. Electrical Activity of the Heart

In the proposed algorithm, the complex ionic phenomena are represented in terms of changes of state of each model unit. Each state is assigned a physiological significance and specific rules govern the state transitions and propagation of the activation from one element to its neighbors. In different approximations, the action potential is simulated in different shapes. The membrane potential change in time presented in Figure 3.5(a), can be simulated as a single step function [68] or a ramp following a step function [67], or a function step by step decrease like a ladder [9]. It has been shown in Gharpure's PhD. thesis work [9] that an anatomically accurate cellular automaton model incorporating anisotropy of propagation based on recorded fiber orientations can be quantitatively shown to achieve the activation and propagation phenomena comparable to those in normal heart.

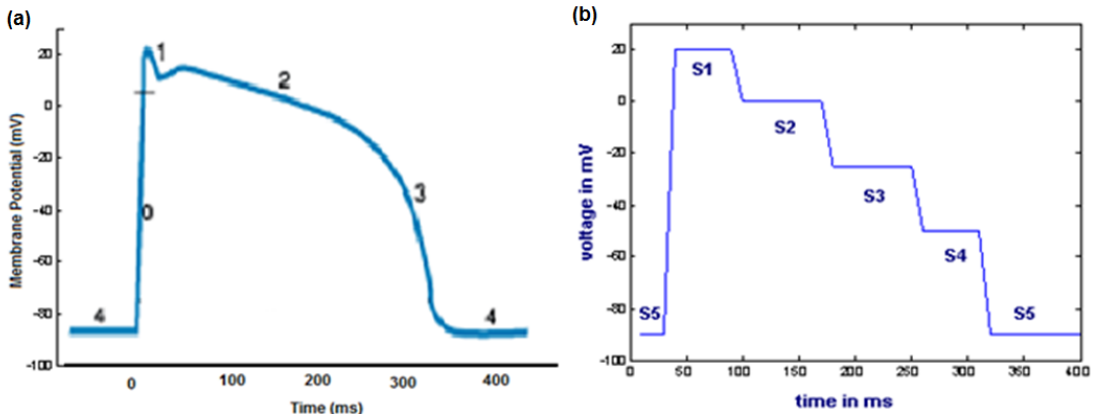

Figure 3.5 Implementation of Cellular Automata: State transitions in electrical part (a) The membrane potential change in time [52], (b) cellular automata implementation of membrane potential change

The complex electrical ionic changes can be described as state transitions in our model, as it is presented in Figure 3.5 (b). This model will be used to generate activation, recovery and propagation of the electrical behavior of the cardiac tissue.

Table 3.2 Implementation of Cellular Automata: State transitions in electrical part

STATE	**VOLTAGE (in mV)**	**DURATION (in ms)**
State1	+20	50
State2	0	80
State3	-25	80
State4	-50	50
State5	-90	- (in rest state)

A stimulated action potential, which is equivalent to the state diagram of the model, is given in Figure 3.5 and the parameters are given in Table 3.2.

The resting potential is given as -90 mV, in which state a node can be stimulated. It can either be stimulated by an external force or by an activated neighbor. External forces represent the “ectopic beats”. Normally, a ventricular muscle can only be excited by the Purkinje fibers, which trigger the simultaneous excitation of both and full ventricles.

Once a node gets excited, it changes its resting state to State 1 (S1), Figure 3.5 (b), which represents “Phase 0”, in Figure 3.5 (a), during which the quick Na+ channels open and due to depolarization, membrane potential rises up to +20 mV. Then slower K^+ channels open, “Phase 1” of Figure 3.5 (a) represented by State 2 (S2) in Figure 3.5 (b) and the outward flow of K^+ stops the rising potential due to Na^+. After a while, Na^+ channels close while K^+ channels are still open. Those sliding changes in membrane potential are represented also by State 2 (S2). “Phase 3” in Figure 3.5 (a) is represented by State 3 in Figure 3.5 (b), during which the slow Ca^{++} channels open and stay opened for approximately 20 sec causing the plateau in the membrane potential

due to the inward flow of Ca^{++}. At State 4 (S4) in Figure 3.5 (b), Ca^{++} channels close and repolarization occurs and membrane voltage returns to its resting value of -90 mV in State 5 (S5) in Figure 3.5 (b), which is the cellular automata representation of “Phase 4” in Figure 3.5 (a). As described above, each of the states represent a different physiological condition of the cell, and membrane voltage changes due to the ion movements.

Once a cell begins to develop its action potential, the procedure never stops in the middle and goes on until the cell reaches its resting potential. Unless a node is in its resting value, it cannot be re-excited under normal conditions (absolute refractory period). Only a stimulation higher in magnitude than a stimulus normally required for AP generation can excite a cell if it is in State 4 (S4) (relative refractory period). The absolute and relative refractory periods were also added to the model. Due to its refractory periods, the electrical wave has its own propagation pattern as a result of excitation from 2 or more points.

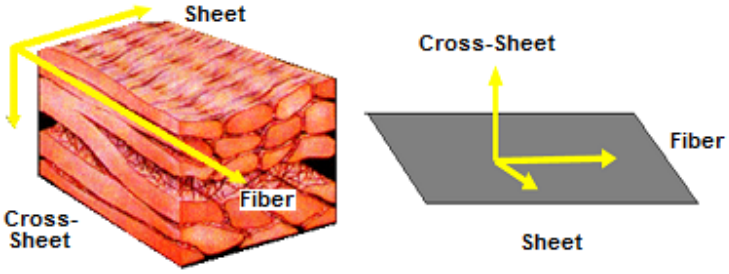

Figure 3.6 Fiber direction representations of the model: fiber, sheet, and cross-sheet directions [9]

Also the fiber orientation can be taken into account in the model via the change of velocity of the propagation. In the proposed algorithm, three main directions are taken into account: fiber, sheet and cross-sheet directions which are presented in Figure 3.6. Not only the propagation velocity but also the mechanical behavior of the tissue change through these directions. The delay of each neighbor lying on the given direction is considered and the delay values vary in those directions, which are used to determine the velocity of excitation propagation.

3.3.2. Mechanical Behavior of the Heart Muscle

The major mechanical properties of myocardium can be listed as three main terms; nonlinearity, anisotropy and viscoelasticity [7, 31-33]. To be able to analyze the mechanical properties of a material, the stress; "force per area" or “intensity of force”, and the strain; “measurement of deformation” are considered. Deformation and force relationship are studied by the stress-strain curves of materials. The stress and strain relationship for non-linearity and anisotropy properties has been illustrated in Figure 3.7. As it has been considered in electrical properties of the cardiac tissue section, the mechanical properties also vary in fiber, sheet and sheet normal axis.

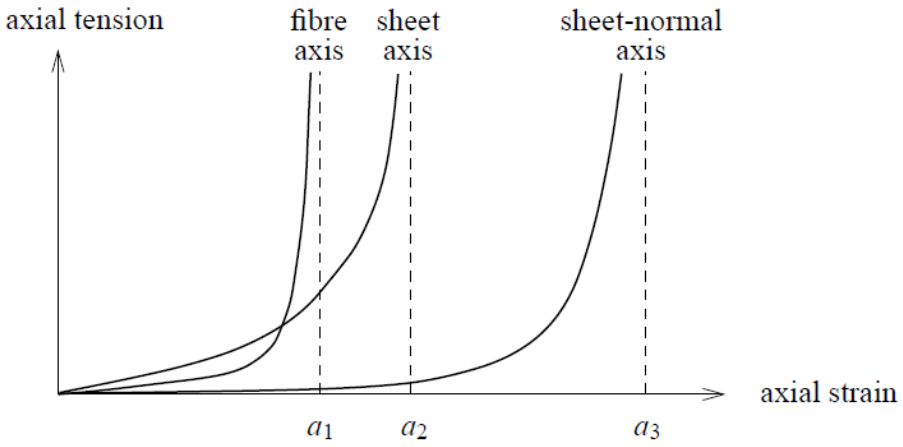

Figure 3.7 Typical nonlinear stress-strain properties of ventricular myocardium: fiber, sheet, and cross-sheet directions [32]

The main concepts of material mechanical behavior can be explained by stress, strain and relation between them. Stress and strain can be calculated using following equations;

Stress;

(3.1)

Strain;

(3.2)

Stress can be calculated by the ratio between force applied to the body and the area it has applied. And the strain can be found by the ratio between elongations of the material over initial length of the material. Since the interaction between applied force and the elongation, in other words interaction between the stress and the strain is not a straight line for smooth tissues, the cardiac tissue is said to be a non-linear material. However; it is not the only property comes out while the tissue is examined for stress and strain analysis done. Loading and unloading paths are not equal to each other, which brings the viscoelacticity of the material. Figure 3.8 represents the stress-strain curve of a non-linear viscoelastic material while loading and unloading paths are applied to the material.

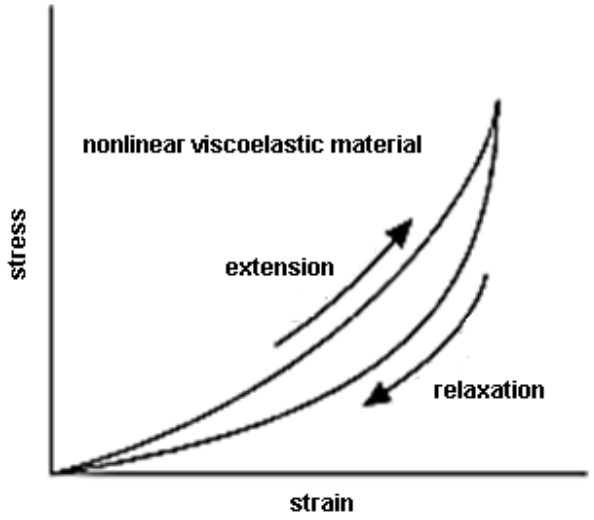

Figure 3.8 The stress-strain curve, nonlinear viscoelastic material behavior, loading and unloading paths [88]

Other analyses done to determine the viscoelasticity of a material are **creep** (Figure 3.9 (a) - (b)) and **relaxation** (Figure 3.9 (c) - (d)) tests [88]. If a constant stress is applied to the material, the strain-curve is recorded in the creep analysis, and we see the result for viscoelastic material in Figure 3.9 (b). Alternatively by subjecting the material to constant strain, stress required to maintain this length varied in viscoelastic materials, which is presented in Figure 3.9 (d). Those tests are used to determine the magnitude of the viscous response for a viscoelastic material.

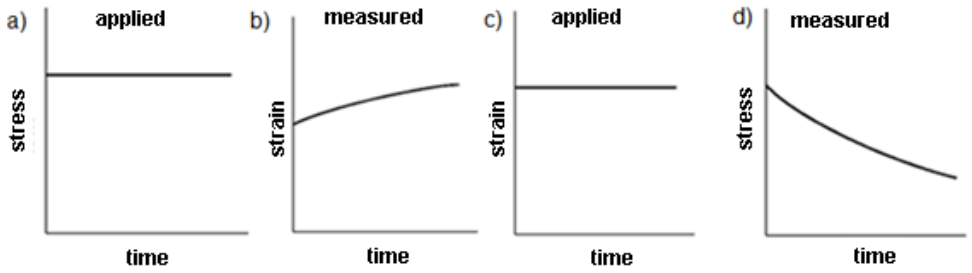

Figure 3.9 The stress and strain versus time curves of viscoelastic material, a) applied stress for creep, b) deformation in creep, c) applied strain for relaxation, d)stress value in relaxation [88]

As a simplification, in the proposed algorithm, it has been assumed that the cardiac tissue is linear, elastic and anisotropic material, instead of a non-linear, viscoelastic anisotropic tissue.

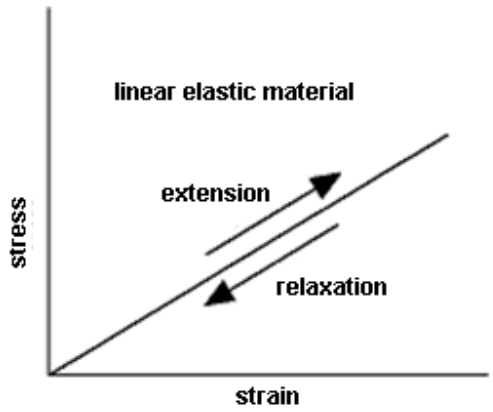

Figure 3.10 The stress-strain curve, linear elastic material behavior, loading and unloading paths [88]

The stress-strain of linear elastic material is presented in Figure 3.10. Hooke's law should be introduced to explain the approximation used for the cardiac tissue [88]. The ratio between stress and strain in linear systems is called Young's modulus and is calculated by equation (3.3):

(3.3)

And substituting the stress and strain formulas, equations (3.1) and (3.2) into this equation we obtain:

$$\frac{F}{A} = E\frac{(l - l_0)}{l_0} \tag{3.4}$$

We can simplify this formulation as follows:

$$F = a(l - l_0) \tag{3.5}$$

where;

$$a = \frac{AE}{l_0} \tag{3.6}$$

Fibers and fiber-like structures (fiber reinforcement) play an important role in the mechanical properties of biological structures. Fibers are long slender bodies that have load bearing capacities along the direction of the fiber only. The simplest approximation of the complicated mechanical behavior of muscles is to assume that they behave elastically.

For the mechanical part, contraction of the muscle has been modeled by using a relation between the force in the fiber and change in length of a fiber.

Assuming the fiber can be represented by an ideal spring that is attached to the wall from the left end and on the right end, a certain force acts (F).

If no load has been applied to the fiber, the length of the fiber is ℓ_0, initial length of the fiber. After loading the spring, the length changes to ℓ, which is called current length. It is assumed that there exists a linear relationship between the change in length and the applied force. Such relation is called *constitutive model* [74]:

$$\boldsymbol{F = a(\ell - \ell_0)} \tag{3.7}$$

The constant a reflects the stiffness properties of the spring. It depends on a material; it is specific for cardiac tissue as well.

The fibers in cardiac tissue consist of muscle fibers and myofibrils, whose interaction leads to the contraction of the muscle. In activation; the actin-myosin proteins moves towards each-other and the sarcomere shortens. Upon de-activation, the proteins move back to their original positions due to elasticity. In terms of modeling, the change of sarcomere length implies that the initial, unloaded length of the muscle changes. In this case; the state where the muscle is in a non-active state is called ℓ_0, and the contracted state is called ℓ_c. The schematic view of the spring is given in Figure 3.11.

$$F = c\left(\frac{\ell}{\ell_c} - 1\right) \tag{3.8}$$

Contraction of the spring can be explained by equation (3.8). The activated length can be expressed in terms of non-activated length using an activation/contraction stretch as follows.

$$\lambda_c = \frac{\ell_c}{\ell_o} \tag{3.3}$$

Typically λ_c <1 since it represents the contractile action. For simplicity it is assumed that λ_c is known for different degrees of activation of the muscle.

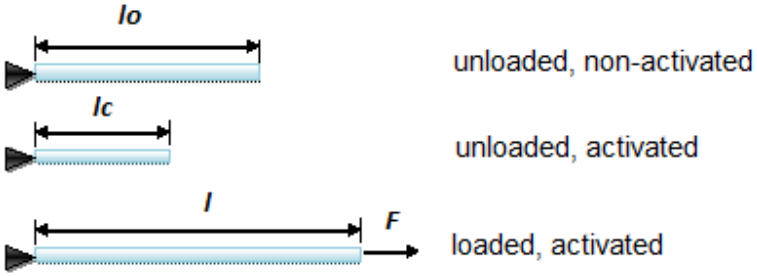

Figure 3.11 Muscle lengths for different states [74]

Force-stretch relation in equation (3.8) can be written as follows;

$$F = c\left(\frac{\lambda}{\lambda_c} - 1\right) \tag{3.9}$$

Where

$$\lambda = \frac{\ell}{\ell_o} \tag{3.10}$$

This model is the simplest model that represents the muscle contraction, represented in [74]. We used this simplified linear elastic model in our electromechanical heart tissue model.

To implement the mechanical behavior, a one-dimensional finite element model was designed. A fiber, fixed from left end gave the expected results in one-dimensional fiber behavior. However, the sarcomere behavior has a small difference than the observed result: the fiber is not fixed from one end, and the muscle contraction behavior is towards the midpoint of the contracting element. Thus, the deformation calculated through the force developed during the contraction is distributed such that the movement of the fiber after contraction will be directed into the inside of the element. Both ends will be moving due to the contraction of the fiber.

Experimental studies showed that a single sarcomere contracts almost the same in every cardiac cycle and its length changes from 2.08 μm-mean (diastole) to 1.81 μm-mean (systole) [33]. The change is approximately 12.5% for each contraction and relaxation couple. This information is used to calculate the activation stretch in this study.

In two-dimensional studies, contraction will be only in one direction, which is also called as the fiber direction. Shortening from both ends can also be monitored in 2D results of mechanical behavior, according to the fiber orientation angle of the tissue. And in normal ventricular geometry, which can be modeled like an ellipsoid, the contraction would cause the decrease in volume of the chambers. Thus, in a cardiac tissue, the deformation occurs not only due to scaling of the element but also translation (movement from one location to another) and rotation of the element.

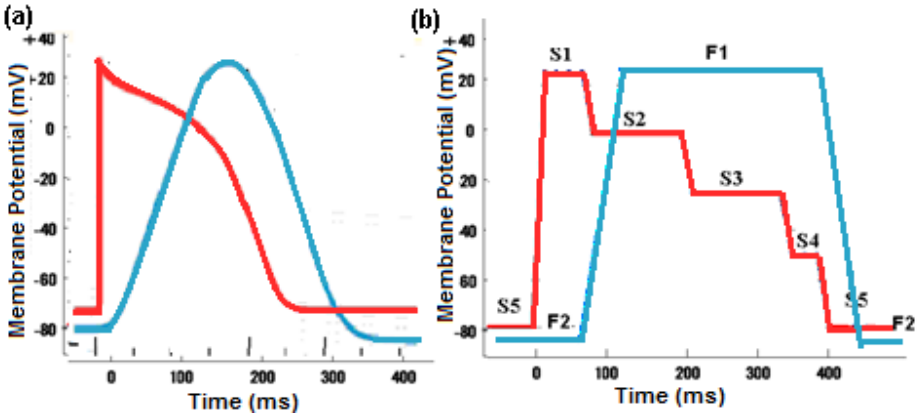

Figure 3.12 Membrane potential (red) and force (blue) curves (a) physiological values, (b) cellular automaton based states used in this work [41]

The basic contraction-relaxation is combined with the electrical activation of the muscle. Time-mechanical event coupling scheme is presented in Figure 3.12. In the proposed algorithm the mechanical behavior was not studied individually. It starts and ends with electrical excitation. As it can be seen in Figure 3.12, the force change is modeled as a step function, which begins at the second electrical step (State 2) and ends after the AP ends, which also makes the mechanical modeling part partially cellular automaton based. Mechano-electrical effects and individual stress-strain calculations are not taken into account in this thesis work.

In the proposed algorithm, for each node following information are taken into account:

- node number,
- node's coordinates
- neighbors of the node
- delays to its neighbors
- state of the node
- counter for the state change
- inner-force due to contraction and relaxation
- node's ischemic state

Initial settings are done for given node parameters, and after choosing the initial excitation points, the time and spatial loops are started in the program. Delays were set according to the distance between two nodes and the fiber direction of the tissue model.

3.3.3. Modeling the Left Ventricle Geometry

The proposed algorithm is tested in one-, two- and three- dimensional basic tissue models and also in a more realistic model of the left ventricle.

Some of the studies were done on a cylinder as a simplified geometry of the heart [81], however, a truncated ellipsoid is used as simplified left ventricle geometry in the proposed algorithm. The ventricle geometry, fiber directions and size of this ellipsoid was chosen in such a manner that it is similar to an adult left ventricle geometry and size. This ellipsoid has electrical and mechanical properties similar to the two-dimensional studies. Only the three-dimensional coordinates were set using cylinder and logarithm functions using MATLAB, is given in Figure 3.13.

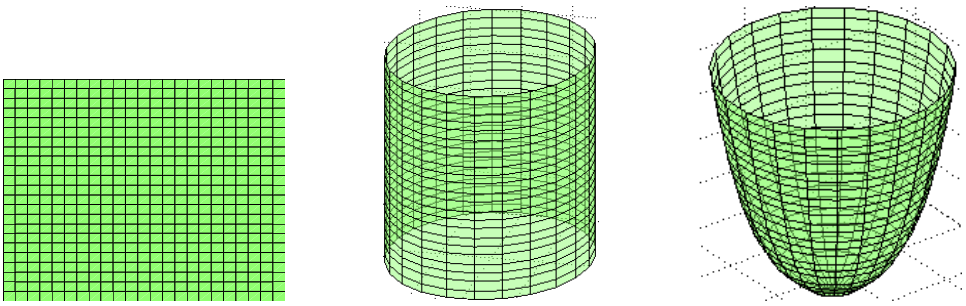

Figure 3.13 Simplified left ventricle model from 2-D to cylinder, and truncated ellipsoid

To have a more realistic tissue model, the fiber orientation change across layers was also added to the simplified left ventricle. In two different models the fiber orientations are set from epicardium to endocardium as $-70^{o}/+70^{o}$ degrees and $-45^{o}/+90^{o}$ degrees respectively, reflecting knowledge from anatomical studies, in Figure 3.14.

For the sake of simplicity the following assumptions are used:

1. The myocardial fibers of the ventricles have a layered structure, characterized by a family of nested like ellipsoids extending from endocardium to the epicardium.
2. All fiber orientations are parallel to each other within one layer.
3. The fiber orientations change about 140 degrees, from outermost layer -45 degrees (the epicardium) to the innermost layer (the endocardium) +90 degrees.
4. A second set of fiber change was chosen as from -70 degrees +70 degrees.

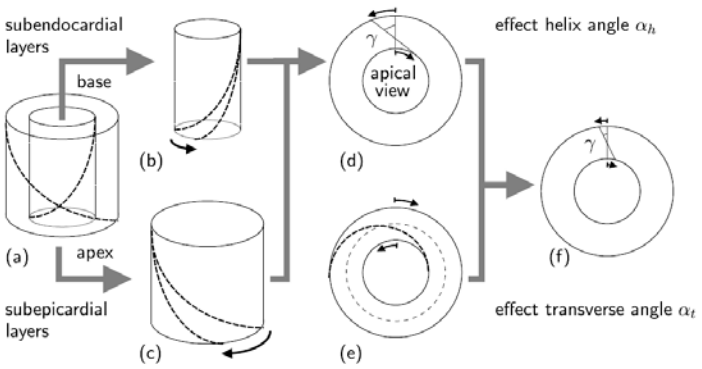

Figure 3.14 Fiber angle studies for simplified left ventricle [51]

3.3.4. Modeling the Failing Heart

To model the pathological conditions, we have assumed that both the electrical and mechanical properties and/or wave propagation characteristics have changes according to physiological knowledge.

Ectopic beats and ischemia are modeled using the proposed algorithm. Initial stimulation reactions of the ectopic beats were chosen by the user and the effects on electrical and mechanical propagation were shown in Results and Discussion section. In Figure 3.15 an action potential is given, which shows the bidirectional conductivity and the block and absolute and relative refractory period phenomena.

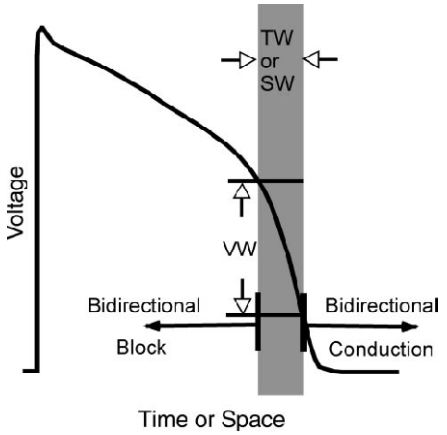

Figure 3.15 Action Potential in myocardium: bidirectional conduction and block [75]

Bidirectional block can be observed in two ectopic foci results. If a node is already excited, the action potential begins and the node cannot be excited again until it returns back to its resting state. If the node is stimulated before the normal heart beat excitation, the node will complete its AP, and it will not answer to normal excitation conductivity, since the nodes are busy. Thus the asynchrony in electrical wave propagation will be observed. In our model, absolute refractory period was taken as the whole AP duration. And for a node to reach the threshold value, the neighbors should be in their 1^{st} or 2^{nd} states. The results of failing heart due to one and more ectopic beats are analyzed in results part.

Ischemia was modeled by choosing some part of the tissue as totally or partially ischemic. In Figure 3.16, the electrical and the mechanical behaviors of the failing heart tissue are presented. According to this knowledge, we can say that the activation of a failing cardiac tissue takes longer, and the potential change in membrane voltage is shorter.

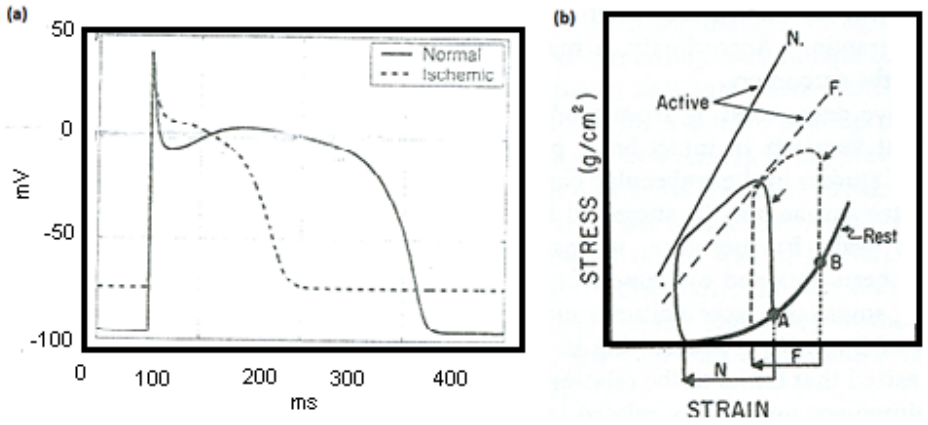

Figure 3.16 (a) Electrical behavior and (b) mechanical behavior of failing heart tissue (F) comparing to the normal tissue (N) [6, 33]

Ischemic tissue studies were done in many cardiac excitation models; ECG, ST-segment comparison for effect of conductivity changes due to ischemia [76], cardiac impulse propagation and re-entry [75], turbulence in the heart [77], cellular level ischemic conductivity changes [78, 79], and mechano-electrical feedback [80]. Each of

the studies shows that a block in normally propagating wave may cause a circular formed re-excitation electrical wave. Implementation of the failing heart parameters is done by changing the state values and durations in the model. Potential change in ischemic tissue based on proposed cellular automata model is given in Figure 3.17.

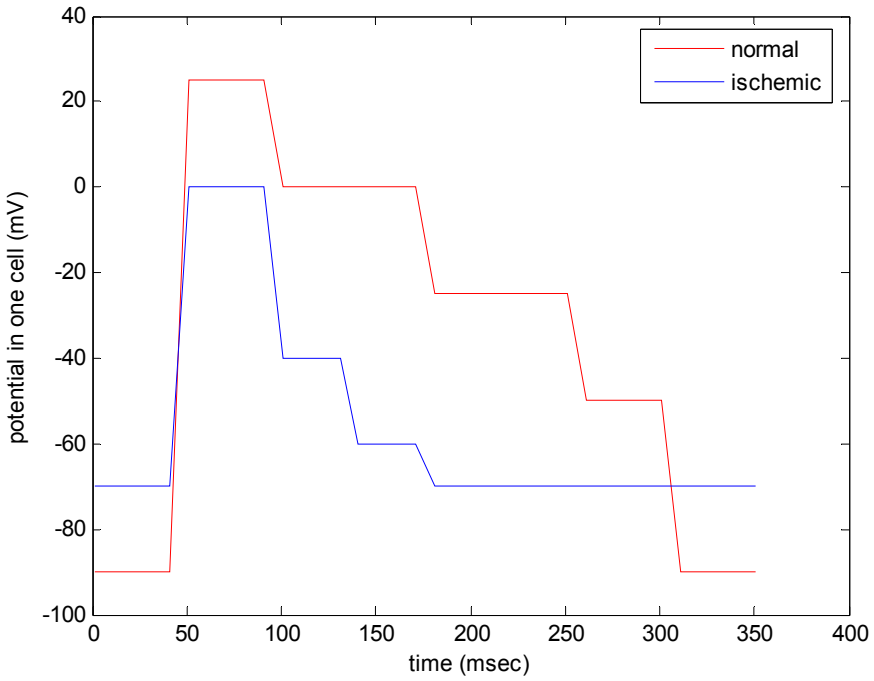

Figure 3.17 Action potential in normal and ischemic tissue

CHAPTER 4

RESULTS AND DISCUSSION

In this chapter, the results of the simulations of the cellular automaton based model are presented. The studies done can be listed as: electrical excitation in a single cell, propagation on one-dimensional (fiber long), two-dimensional (sheet) and three-dimensional (a truncated ellipsoid model which represents the simplified left ventricle muscle) model excitation results and mechanical contraction and relaxation due to the electrical excitation.

After seeing the excitation of one-dimensional and two-dimensional isotropic electrical propagation, fiber directions will be included to consider the anisotropy of the heart tissue.

Besides propagation on normal/healthy tissue, ischemic region electrical activity and propagation was also modeled using cellular automaton model.

The ventricle geometry set as simple, layered, anisotropic model is used to model ectopic focus and ischemic region electrical and mechanical effects on heart beat.

The results were presented in three main headings:

- one-dimensional studies,
- two-dimensional studies,
- three-dimensional studies,

Each of them includes studies done on electrical and electromechanical behavior, isotropic and anisotropic propagation, normal and ischemic tissue properties.

4.1. One-Dimensional Studies

4.1.1. Electrical Wave Propagation in 1D

As it is given in theory, the potential change due to excitation of a single myocardial cell is simplified as state changes. Membrane potential versus time graph is given in Figure 4.1 for a single cell.

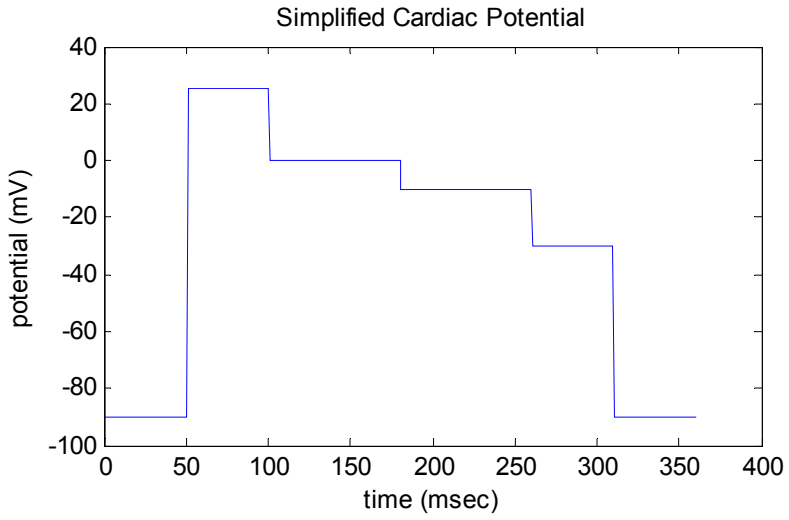

Figure 4.1 Simplified cardiac potential: state changes in cellular automaton model

Each node has this state/potential change with time presented in Figure 4.1. While the excitation occurs, it also affects the neighboring cells. Once the node is excited, the action potential generation begins and cannot seize to exist until the end.

Figure 4.2 shows the result of one dimensional propagation of electrical activity in 20 nodes. The code generates the results for 10 ms time intervals. 5^{th} node was chosen as the initial excitation point. As it is expected, the node excites its neighboring cells in both directions, after a delay of 20 ms. How long a node stays in a potential level is presented in Figure 4.1. Propagation in time is given in Figure 4.2 and Figure 4.3 (a) and (b).

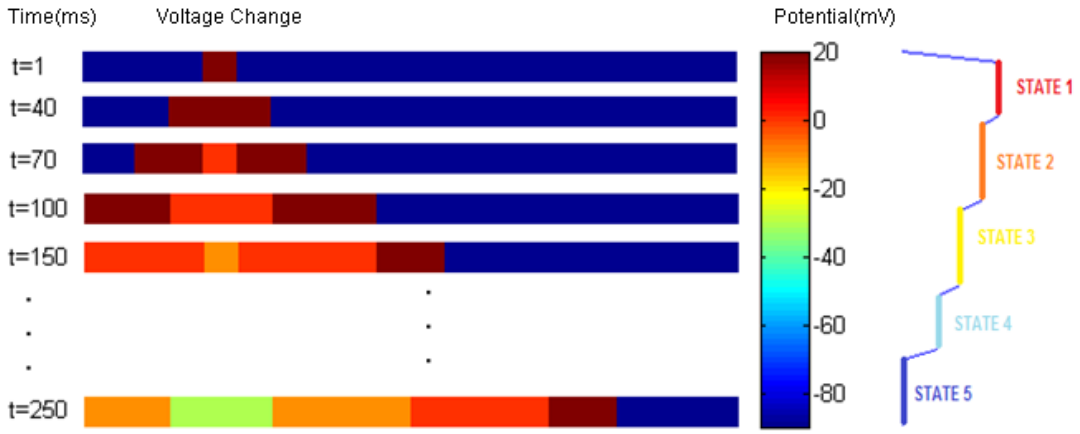

Figure 4.2 Electrical excitation propagation in 1D. Colors represent the voltage changes: Blue nodes are in resting voltage (-90mV), new excited points are dark red (+20mV). (t=ms)

Propagation for t=400 ms yields the results in Figure 4.3. The first excited point reaches its resting value in the first instance. Beginning from 5th node, from 5th to 20th node and from 5th and 1st node the propagation occurs with constant velocity. Each of the nodes has the same AP length and after their excitation, each point reaches the end of its action potential with the same delay with which it was excited.

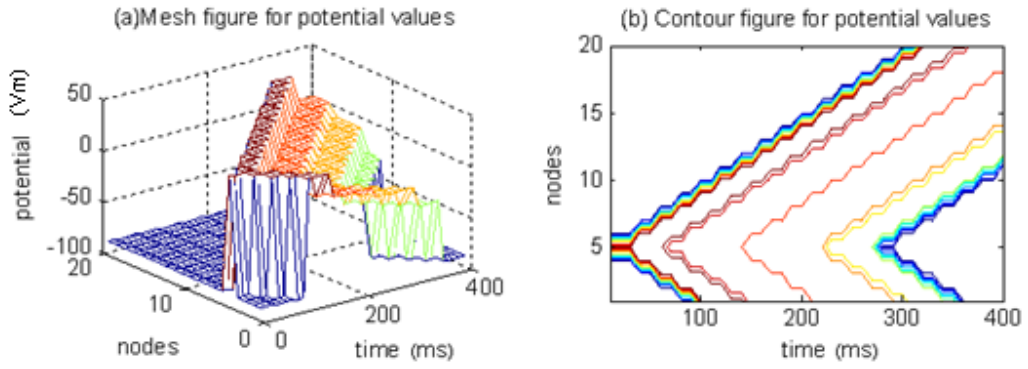

Figure 4.3 Propagation in 1D: (a) mesh (b) contour plots of potential changes (mV) of each node in time, in MATLAB.

4.1.2. Electro-Mechanical Simulation in 1D

In mechanical part, force curve of the response of Ca^{2+} changes in a single sarcomere has been modeled in steps, like the potential curve. In one-dimensional mechanical behavior studies, the curve was discretized as it is presented in Figure 4.4.

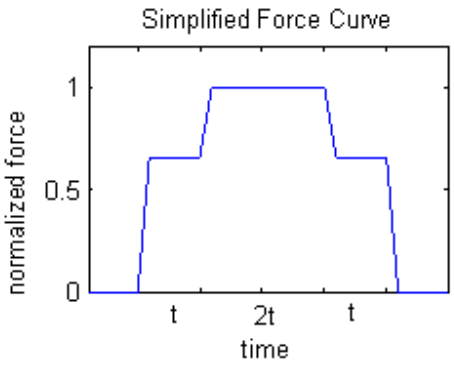

Figure 4.4 Simplified force curve: state changes in cellular automaton model

Results of the change in mechanical behavior of a single fiber in one dimensions for 6 time intervals is given in Figure 4.5. The model was generated for 9 nodes and 8 intervals. Beginning from the midpoint, (5^{th} point), mechanical response propagates as it is in the electrical wave to simulate the electro-mechanical behavior. The light gray nodes are 2/3 of the initial length and dark gray nodes are 1/3 of the initial length of the interval between two nodes. The nodes are fixed from the midpoint, which is also set as the initial excitation point.

Figure 4.5 Propagation of contraction in 1D, shortening of the fiber: Colored areas representing contraction of the interval

In the combination of the electrical wave propagation and the contraction of the fiber, the states are modeled based on the timing given in Figure 4.6 (b) graph. A simple step function describes the contraction changes in a node, which begins and the S2 state of the electrical wave and ends after the node reaches its resting state S5.

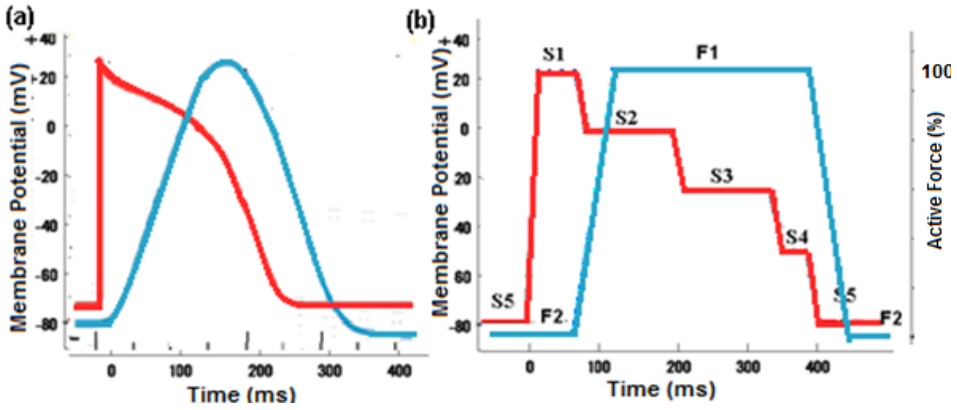

Figure 4.6 Discrete membrane potential (red) and force (blue) curves (a) physiological values, (b) cellular automaton based states [41]

The electromechanical simulation results for the excitation of a 20 node-long fiber are presented in Figure 4.7 and Figure 4.8. In Figure 4.7, excitation begins from the mid-node of the model and both electrical excitation and mechanical contraction propagates to both left and right sides. The results of propagation to both sides can be seen in Figure 4.8, where the initial excitation point has been chosen as the midpoint.

In Figure 4.7, the shortening of the fiber can be seen. Each different color represent a different time of electro-mechanical behavior of the fiber. For 50 different time instances, and for 20 nodes, change in both the length of each element and action potentials can be seen in “ribbon” figures using MATLAB.

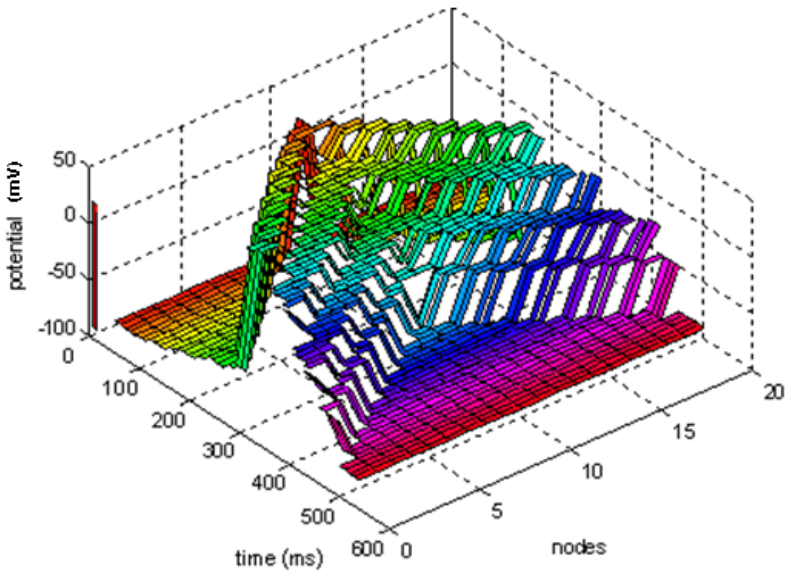

Figure 4.7 Electromechanical propagation of contraction, in 1D for 20 nodes, 500 ms (50 time steps), excited from mid-node. Each color represent different time instance

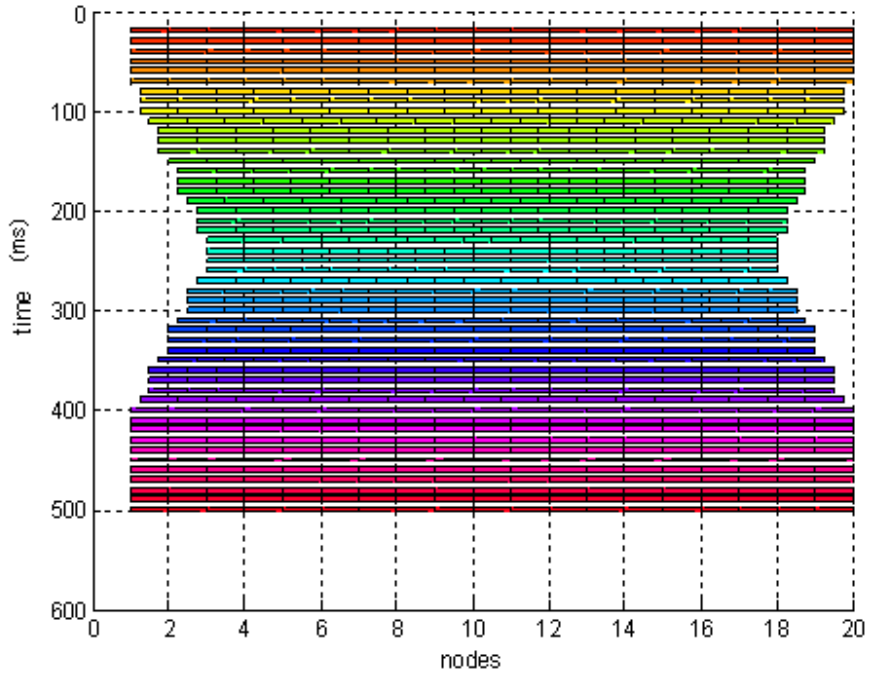

Figure 4.8 Electromechanical propagation of contraction in 1D for 20 nodes, 500 ms (50 time steps), excited from mid-node. Each color represent different time instance

4.2. Two-Dimensional Studies

4.2.1. Electrical Wave Propagation in 2D

The states and the simplified electrical activity of a single cell in two dimensions is the same as those used in the one dimensional studies. The changing factors in 2D modeling are the geometry, neighbors of each node and the propagation delay in normal tissue simulations.

If the anisotropy is neglected for the tissue as a first step, the propagation velocity from one node to any direction should be the same. Thus, the resulting view of propagation we are expecting to see is in a circular form.

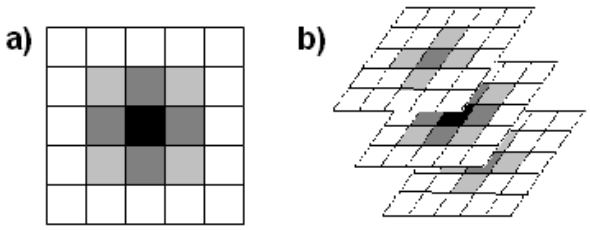

Figure 4.9 Cellular automaton-neighbors in (a) two-dimensions and (b) three-dimensions

Even in isotropic case, the propagation delays of the neighbors are not the same. Figure 4.9 shows the neighbors of a node in 2D and 3D. The midpoint (black), is the node itself, dark gray ones are its 4-adjacency neighbors, and light gray ones are the 8-adjacency neighbors. In the proposed algorithm, both the 4- and 8-adjacency neighbors were used (that is also called m-adjacency); however, propagation reaches to the 4- and 8-adjacency neighbors with a delay, which is proportional to the distance between two nodes.

Isotropic wave propagation results are presented in Figure 4.10. Similar to excitation propagation in 1D resting potential is shown in blue color and early excited points are in dark red. 24x24 points were used as 2D model and midpoint has been chosen as the initial excitation point.

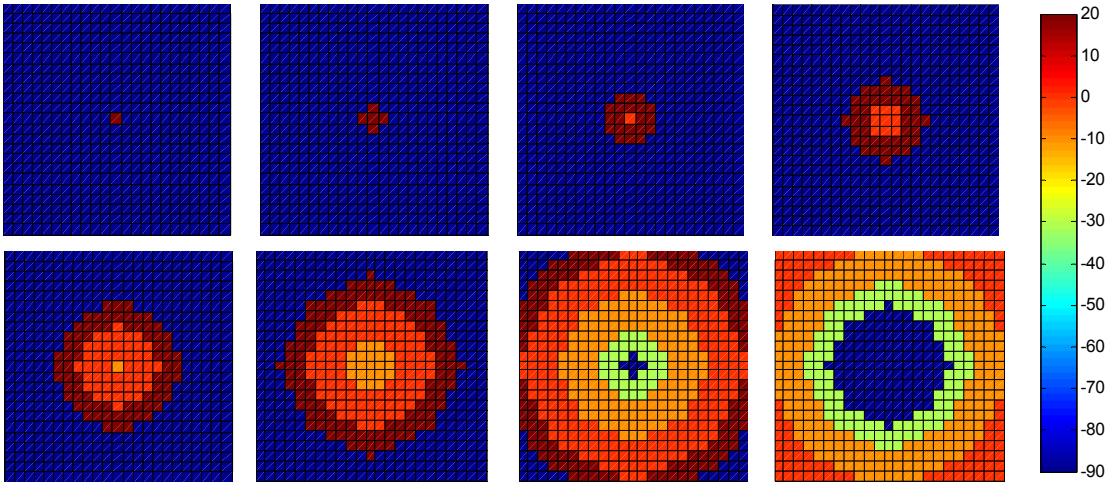

Figure 4.10 Electrical excitation propagation in 2D. Colors represent the voltage changes: Blue nodes are in resting voltage (-90mV), new excited points are dark red (+20mV). (propagation at t=1, 20, 70,100, 150, 200, 300, 400 msec)

However, in the heart tissue the propagation is not uniformly distributed in all directions. As it has been mentioned in Chapter 2, anatomy of the heart, the heart muscle is striated and conducts the electrical activity faster in one direction than the other directions.

a. Anisotropy

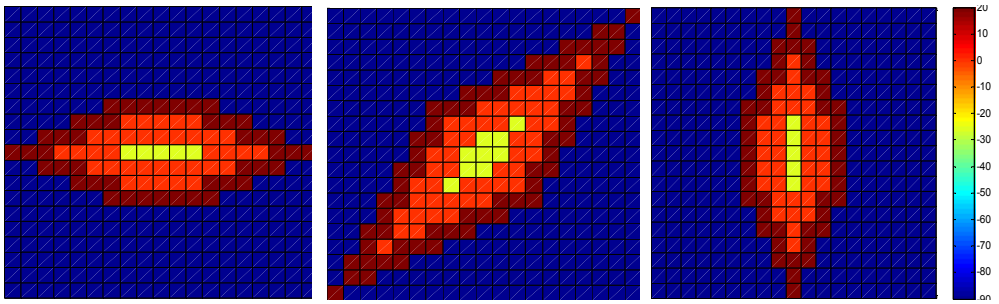

Figure 4.11 Electrical propagation in 0^o, 45^o, and 90^o fiber directions

Anisotropy of the tissue has been modeled using fiber directions at 0^o, 45^o, and 90^o degrees, represented in Figure 4.11. Those three directions (and negative values of them) can be modeled just by delays calculated using only the first neighbors of the node.

To have simulation of anisotropic propagation of arbitrary angle, except 0^o, 45^o, and 90^o degrees, degree of neighborhood must be greater than one. In the proposed algorithm, for the propagation trough the arbitrary angle chosen as fiber direction, we need to find the neighbors which stays in this direction. Since 0^o, 45^o, and 90^o fiber directions can be found in 1^{st} neighborhood, they are the easiest angles. For other degrees we need to check the neighbors in 2^{nd}, 3^{rd} and other orders of neighborhoods. And if the exact angle does not exist in the neighborhood, we need to find the closest approximation angle to be able to perform the algorithm in the approximated fiber direction.

For a given angle, the closest angle for chosen number of neighbor rank has been calculated as follows:

1. The fiber direction chosen is converted into equivalent fiber angle between ±90 degrees.
2. Number of neighbors that will be used for the neighborhood of each node is chosen.
3. Closest fiber angle will be calculated according to the closest value that can be calculated from number of chosen neighbors,
4. Delay values will be calculated for neighbors

3 different fiber directions have been chosen to demonstrate the fiber orientation application: 20, 55 and -30 degrees were analyzed for 2 different orders of neighborhood results.

20 degrees

Closest angle values found using maximum 5 neighbors and 10 neighbors' results were given in Figure 4.12 and 4.13.

In Figure 4.12 the chosen, calculated and perpendicular to calculated fiber angle plots are presented. Although in these graphs both of the calculated angles seem quite close to initially chosen angle (20 degrees), one of them uses 3^{rd} order neighbors and the other one uses 8^{th} order neighbors to set the delays for propagation. The propagation

pattern shown in Figure 4.13, has great differences, when only the neighbors lying on the line passes through the initially excited point in the fiber direction are excited.

To compare the angles calculated using 3 and 8 order neighborhood, relative error calculations are used.

$$E = \frac{x - x_a}{x} \tag{4.1}$$

Where x is the exact degree chosen as the fiber angle, x_a is the approximation of this angle. The relative error percentages will be used to compare the results.

In the first example, to simulate the 20 degrees fiber orientation, 3 closest neighbors were used, and the line passing from x=3, y=1 with 18.4349 degrees gives the result in Figure 4.14 (a) with 7.83% angle error and with a more spread propagation pattern. On the other hand, using 8 closest neighbors, the line passes through x=8, y=3, gives 20.5560 degrees with 2.78% error.

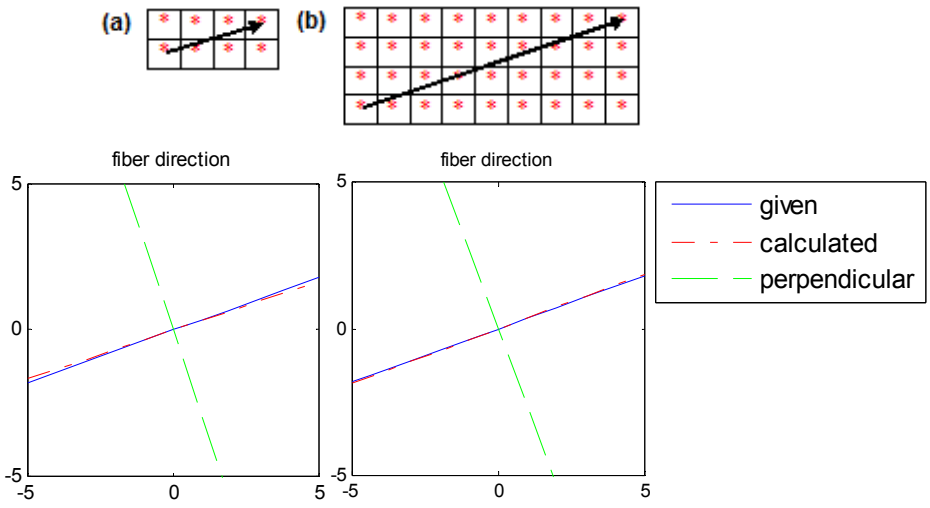

Figure 4.12 (a) Fiber angle using 3 neighbors, (b) 8 neighbors, for 20 degrees (given-blue), 18.44 degrees and 20.56 degrees calculated (red) and perpendicular directions for calculated values(green)

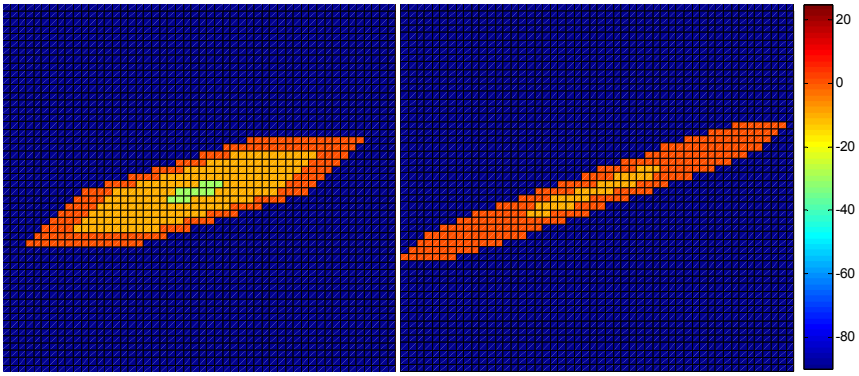

Figure 4.13 Propagation in 20 degrees, using (a) 3 neighbors, (b) using 8 neighbors for each node

55 degrees

Another example is given for the closest angle values found using maximum 3 neighbors and 7 neighbors' results for 55 degrees were given in Figure 4.14 and 4.15. In Figure 4.14, we see the 3 and 7 neighbor used angles for 55 degrees. Comparing to previous example, this time the error difference is smaller down to 1.40%.

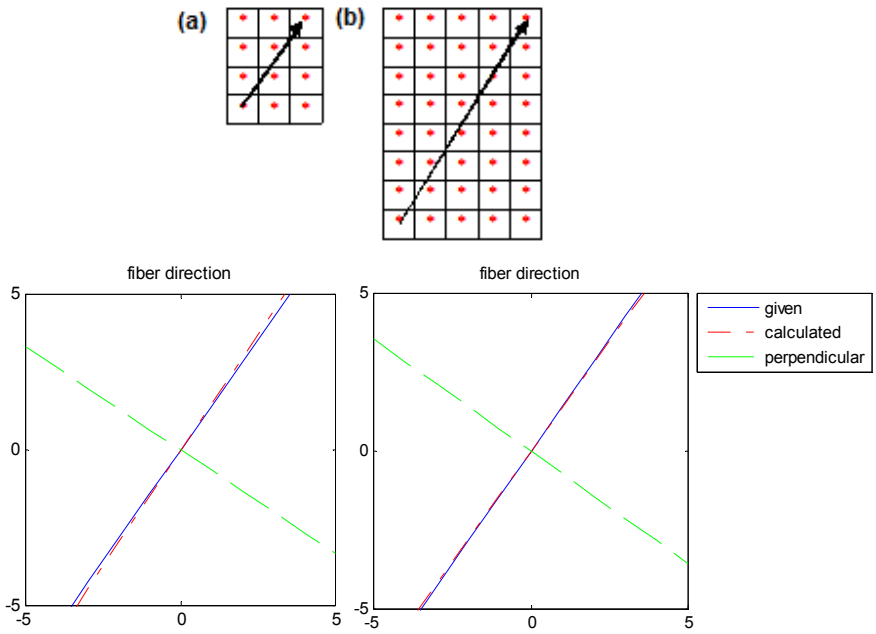

Figure 4.14 (a) fiber angle using 3 neighbors, (b) 7 neighbors, for 55 degrees (given-blue), 56.31 degrees and 54.46 degrees calculated (red) and perpendicular degrees for calculated values(green)

Using 3 neighbors, the line passes through x=2, y=3 only with 2.38% errors, and the calculated angle is 56.3099 degrees. Using up to 7 neighbors, error decreases to 0.97% for 54.4623 degrees, according to line x=5 and y=7.

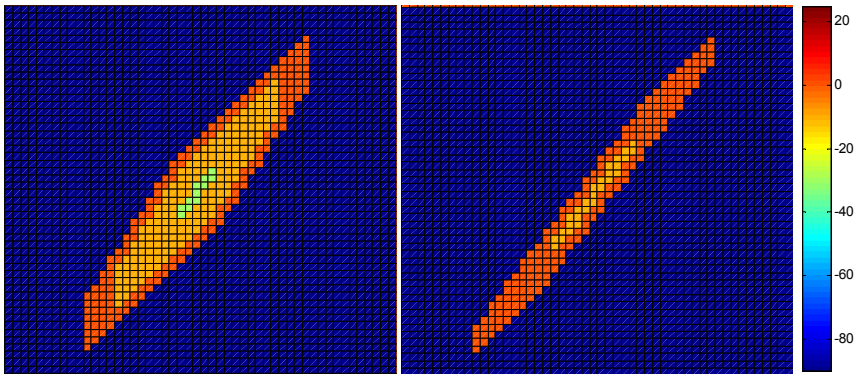

Figure 4.15 Propagation in 55 degrees, using (a) 3 neighbors, (b) using 7 neighbors for each node

As we see in Figure 4.15, although the difference is almost 1% the change is quite important, which can be seen from outputs. The difference between two outputs is due to the neighborhood information used for excitation propagation. Only the neighbors in the fiber direction and 1st order neighbors were used for each node to reduce the complexity.

-30 Degrees

The angular change is valid also for negative angles. Results for -30 degrees, using 2 neighbors give -26,5651 degrees, using the line that passes through x=2, y=-1 point. And using 7 nearest neighbors that passes through x=7, y=-4 point gives -29.7449 degrees.

The highest error value is seen in this example between 2 neighbors used example and 7 neighbors used example. The first example gives 11.45% error, while 7 neighbors used one gives only 0.85% error, thus the difference error in is 10.6%. The results of propagation are shown in Figure 4.17.

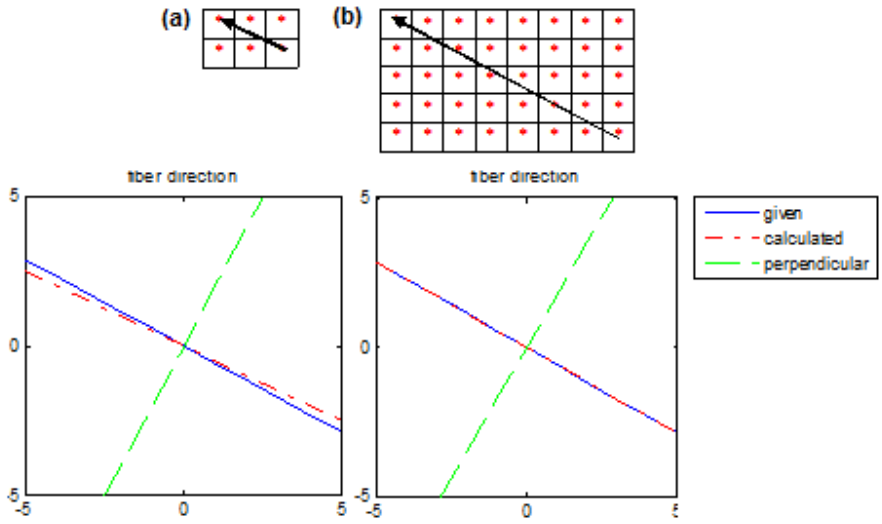

Figure 4.16 (a) fiber angle using 2 neighbors, (b) 7 neighbors, for -30 degrees (given-blue), -26.57 degrees and -29.75 degrees calculated (red) and perpendicular degrees for calculated values(green)

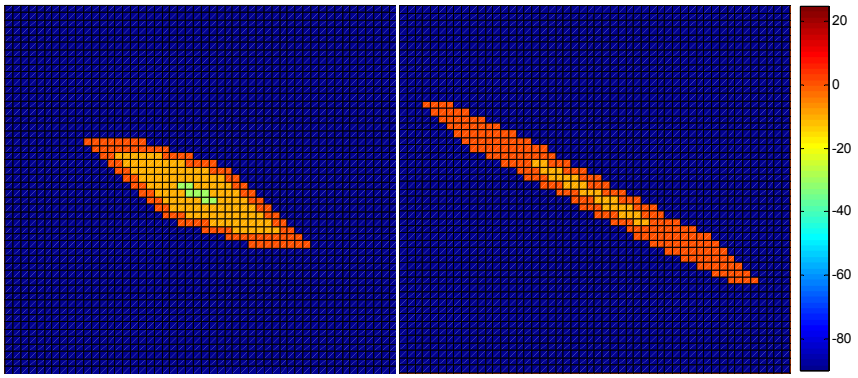

Figure 4.17 Propagation in -30 degrees, using (a) 2 neighbors, (b) using 7 neighbors for each node.

Only the neighbors in the fiber direction and 1st order neighbors were used for each node to reduce the complexity. For 7th order neighborhood, if all the 15x15 neighbors of each node would be excited, since the algorithm includes many loops go over the neighborhood and check, the computational time would increase dramatically. To be able to have an automatic and fast algorithm only the neighbors lying through the fiber angles are used to do all calculations for each node. Comparing the error in angle

calculated versus computational complexity due to the number of neighbors used for excitation propagation, the propagation using smaller than 5th order neighbors is preferred in the proposed algorithm.

b. Two ectopic beats

Once excitation begins, the node cannot be stimulated until it returns to its resting value. Following examples show results of both the absolute refractory phenomena and propagation of more than one ectopic beats.

If the anisotropy is neglected, the propagation for two ectopic beats will be as it is illustrated in Figure 4.18. As it is seen in these plots, first two beats begin to excite its neighboring nodes and when the propagating waves reaches to each other the waves cannot cross to the other side, and two waves appeared like merged.

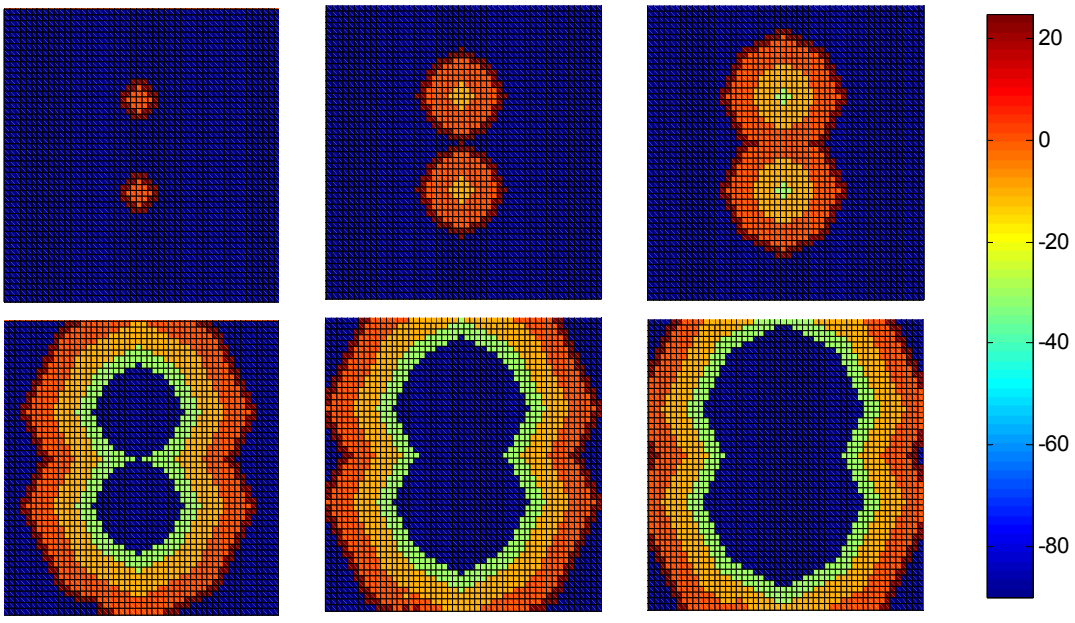

Figure 4.18 Two ectopic beats, located in y direction, propagation of the electrical activity in t=90, 180, 250, 450, 530 and 580 msec

For a closer point chosen in x direction, two excitations will merge earlier in time than in Figure 4.18. The wave would propagate as in Figure 4.19. Since we neglect the

anisotropy, points chosen in x and y directions have no major differences in terms of wave shape. Only the time it takes for the two waves to meet each other decreases if we chose closer points.

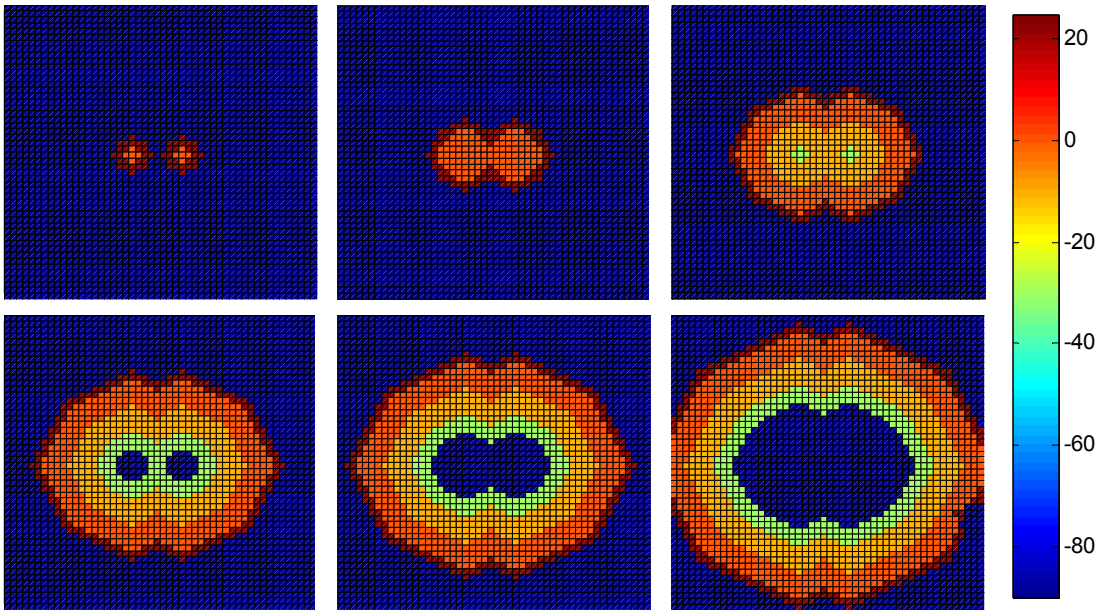

Figure 4.19 Two ectopic beats, located in x direction, propagation of the electrical activity in t=80, 140, 250, 340, 400 and 500 msec

If we reconsider the anisotropy, more than one ectopic beat will be propagated as it is given in Figure 4.20. In the figure, four different foci were chosen to stimulate and results for four different fiber angles were shown.

As it is expected, if two points are closer, the ectopic beats will combine and appears as a single ectopic beat, centered from the midpoint of two ectopic foci. Waves resulting from ectopic foci always merge however merge time and the propagation pattern changes due to the spatial positions of foci and the fiber orientation of the tissue.

For 90 degrees – two points chosen in y direction seems like one
For 0 degrees – two points in x direction seems like one
For 45 degrees - except points chosen on its direction, we always see two beats

For arbitrary angle – like in 45 degrees, if the points are in its fiber direction, the waves will seem like one as they get together.

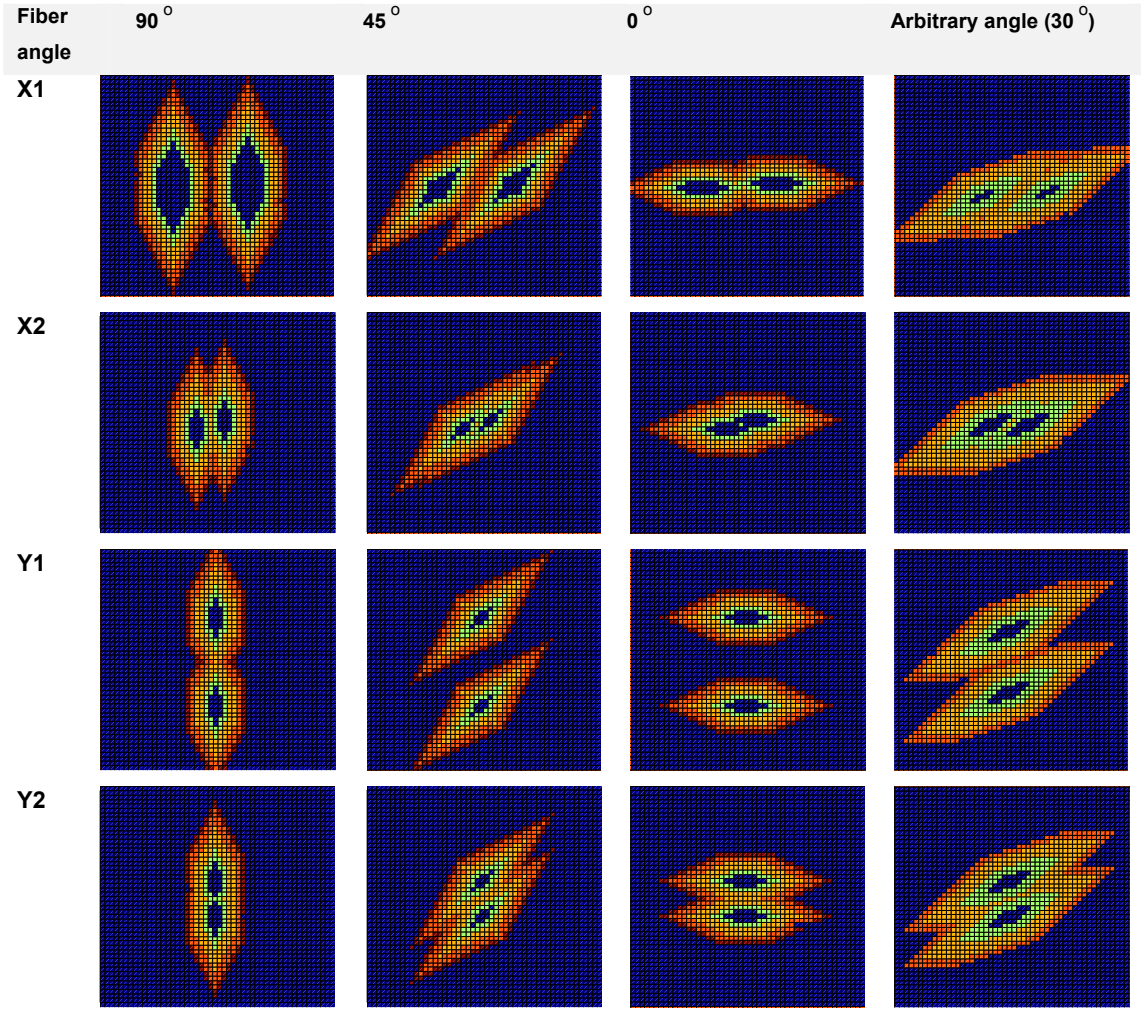

Figure 4.20 Two ectopic beats for different fiber directions, 0 °, 45 °, 90 ° and arbitrary(30°) angle, electrical wave propagation results for X1- two points in x direction, X2 - two closer points in x direction, Y1 - two points in y direction, Y2 - two closer points in y direction is given

Due to the difference between merging time and position, the propagation may lead an ectopic beat of the ventricle. If the foci merge earlier in time, it may seem like only one ectopic focus, which may also cause a pathological situation since it blocks the normal pattern of the excitation propagation. And if it reaches the conduction system it may even cause an ectopic beat of the ventricle as well.

c. Reentry

Ischemia is one of the cardiomyopathy diseases, which is caused by coronary artery disease. It affects the cardiac electro-mechanical activities and APs generated in these tissues have smaller slopes, lower propagation velocities, and shorter durations, which may lead to re-excitation of the tissue.

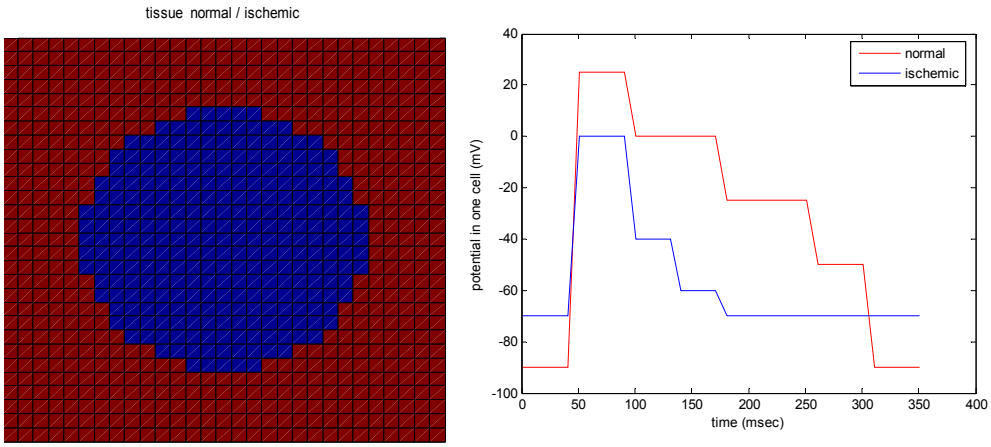

Figure 4.21 Ischemic tissue model: geometry, rules and action potential approximation for normal and ischemic tissue.

Only by choosing a region as ischemic tissue, and applying the given properties of the tissue to the CA rules, following results are gained.

If the tissue is totally ischemic, the tissue does not respond to electrical excitation, and it will not transfer the electrical activity to its neighboring cells. If the tissue is only partially ischemic, the tissue is not dead, it respond to excitation; however, it has an AP unlike the normal one, as it is shown in Figure 4.21 (b).

If a normal excitation is applied to a totally ischemic tissue; the propagation will be seen as if in Figure 4.22. When the wave reaches to ischemic region, this part of the tissue will not be excited and also it will not conduct the wave to its neighbors. Thus, the electrical propagating wave will be blocked in this region, and the wave will propagate around this part.

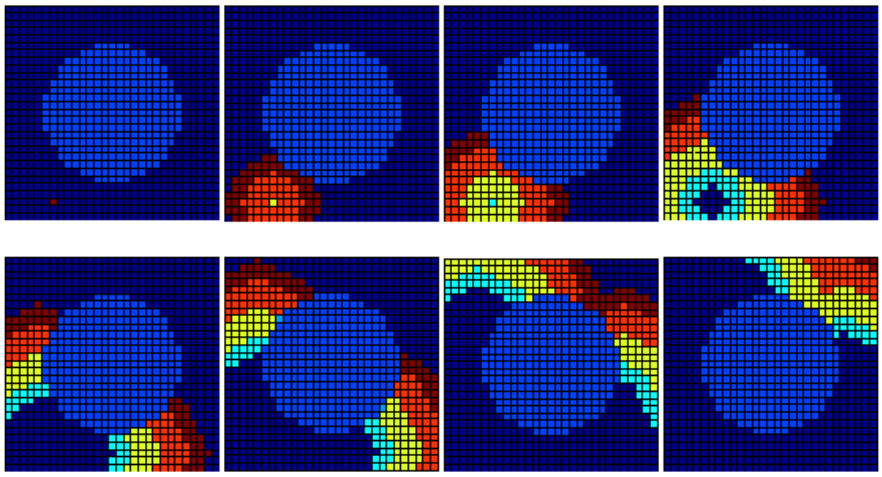

Figure 4.22 Totally ischemic tissue, electrical wave propagation, isotropic tissue model

also excites its neighbors that are in their resting states, ischemic tissue is re-excited before the normal wave passes through this section. Even if only a single node gets excited in this manner, all its neighbors and their neighbors are triggered by this excitation, and the circling waves begin due to the unhealthy tissue (Figure 4.23).

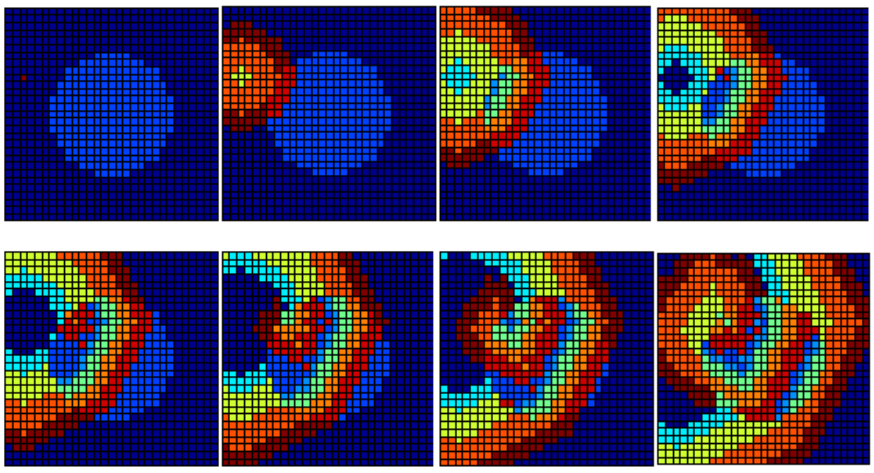

Figure 4.23 Ischemic tissue electrical wave propagation, isotropic tissue model

Ischemic tissue also has a property that causes reentry; which is called electric accumulation. An electrical activation originates in ischemic tissue and begins to

propagate (Figure 4.24). Because of the difference in action potential of normal and ischemic tissue, excitation of the nodes in resting states again forms re-entrant electrical waves.

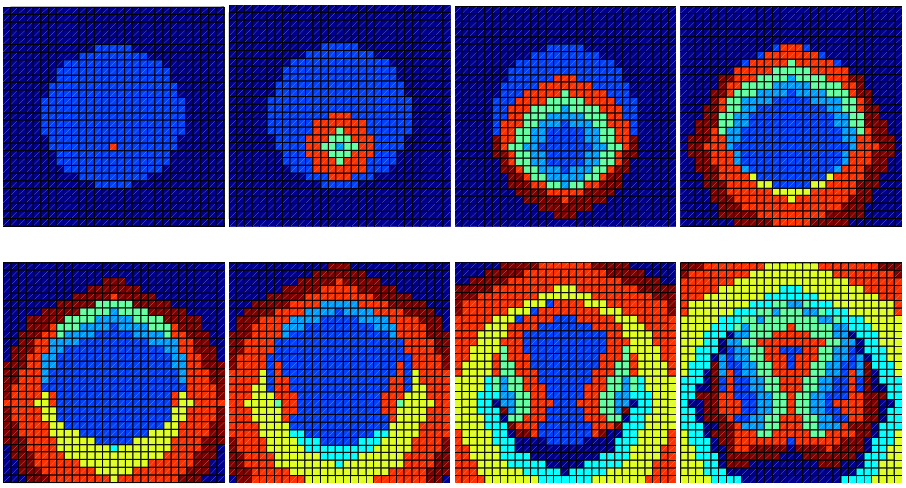

Figure 4.24 Self-initiated ischemic electrical wave propagation, isotropic tissue model

Reentry can cause fibrillation that can even lead to death. As we see the totally ischemic tissue causes no such diseases, thus less dangerous. That's why patients with ischemic tissue disease are treated by the ablation of the ischemic tissue.

The results for ischemic tissue model when we add the anisotropy has some differences compared to the homogeneous tissue model results. The totally ischemic tissue, in other words the dead tissue, has no effect on electrical propagation in homogeneous wave propagation; however, it results as it is given in Figure 4.25 and 4.26, if we add the fiber orientation to the model.

Stimulus coming from any direction propagates faster in fiber direction and slower in other directions. Thus, the infracted tissue blocks the fast propagating wave, the wave wraps around the totally ischemic tissue, thus the wave is separated into two parts because of this block.

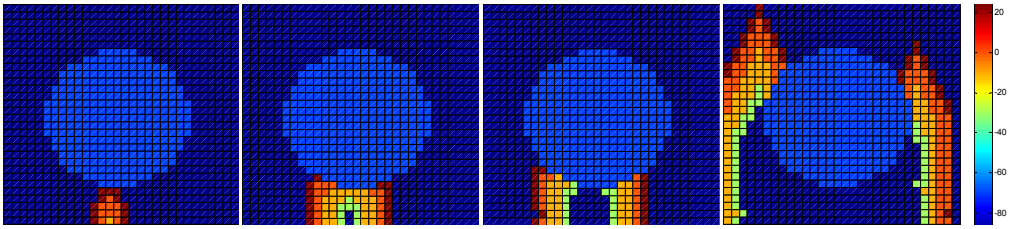

Figure 4.25 Totally ischemic tissue, electrical wave propagation, the 90^{o} fiber direction

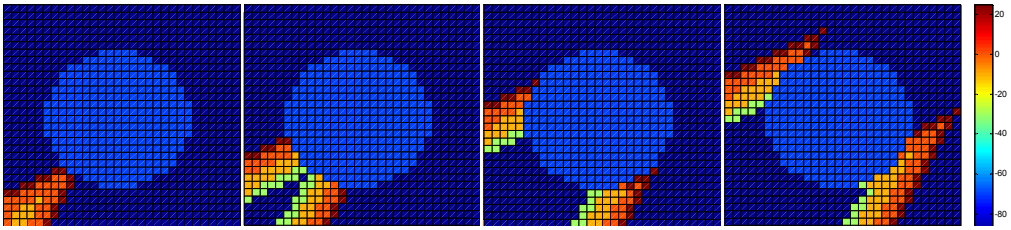

Figure 4.26 Totally ischemic tissue, electrical wave propagation, the 45^{o} fiber direction

If the tissue is not totally ischemic, the wave also propagates in this tissue and the following results are obtained if the angular change of fibers is added to the ischemic tissue results.

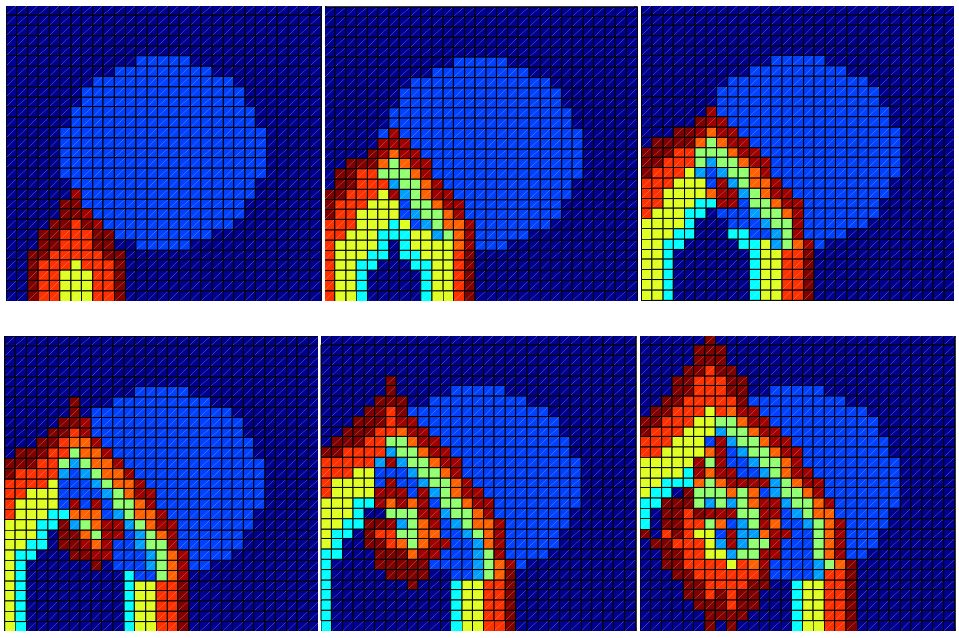

Figure 4.27 Ischemic tissue electrical wave propagation, for 90^{o} fiber angle

In Figure 4.27 we see the ischemic electrical wave propagation and reentry caused by ischemic tissue for 90^{o} fiber angle and in Figure 4.28 the 45 ^{o} fiber angle results. We observe that the wave propagates in ischemic tissue slower than in normal. And at the boundary of ischemic-normal tissue, reentry can be seen in both angles due to the fast recovery of the ischemic tissue.

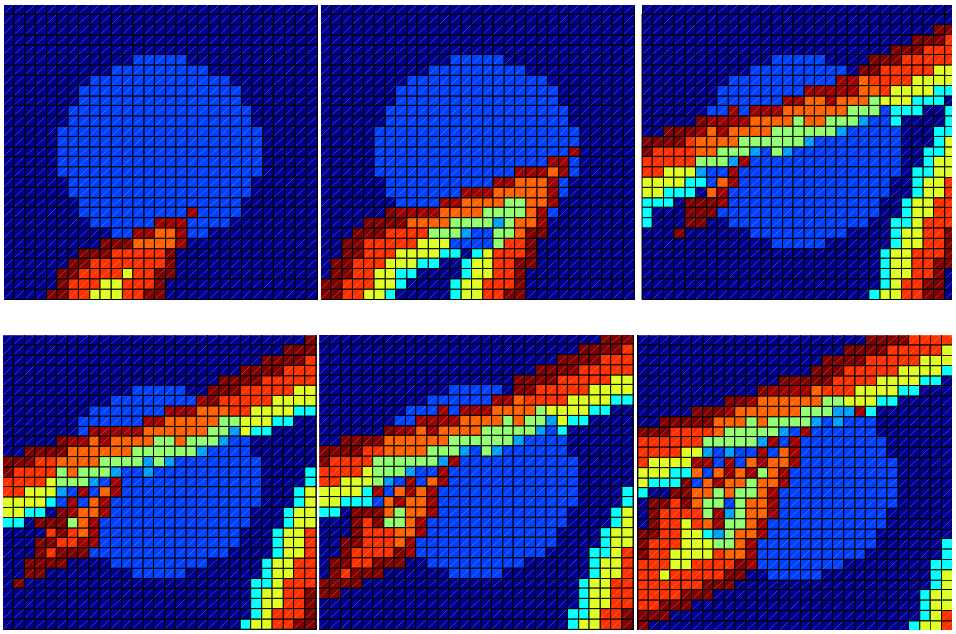

Figure 4.28 Ischemic tissue electrical wave propagation, for 45^{o} fiber angle

For the same angles, 90^{o} and 45 ^{o}, self-produced ectopic beats due to ischemic tissue are also modeled. Results can be seen in Figure 4.28 and 4.29.

Each reentry model result shows that the abnormalities in cardiac tissue cause remarkable changes in electrical wave propagation. Even though the electrical wave propagates slower in ischemic tissue, the recovery after excitation is much faster than in normal tissue. After an electrical activation begins in the failing heart tissue node, due to its potential curve length, it becomes a potentially active node again. The propagation pattern changes because of the following parameters: the fiber orientation of the tissue, initial excited point and ischemic tissue distance, and the degree of the ischemia.

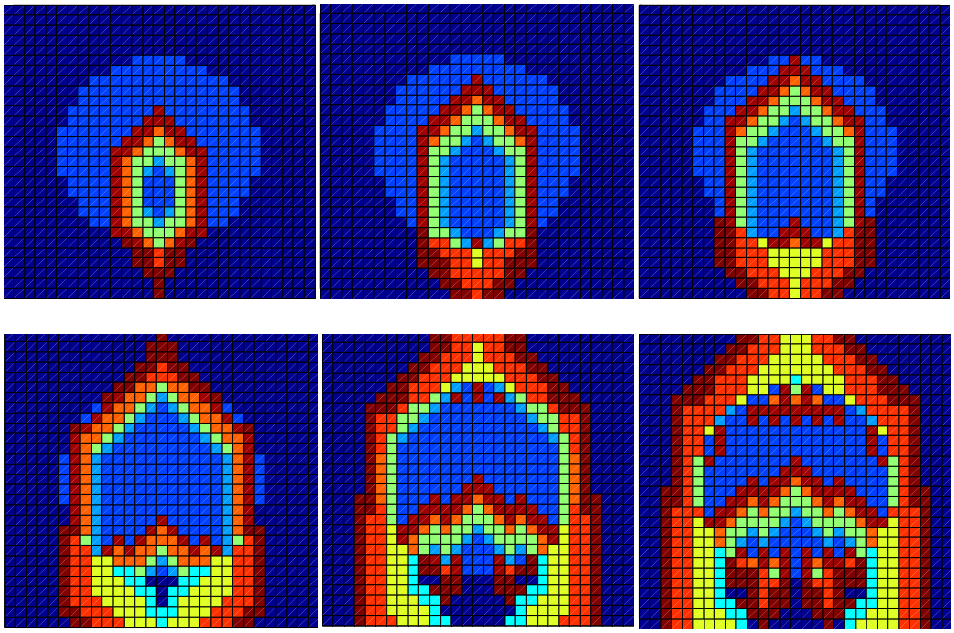

Figure 4.29 Self-initiated ischemic tissue, 90^{o} fiber angle electrical wave propagation

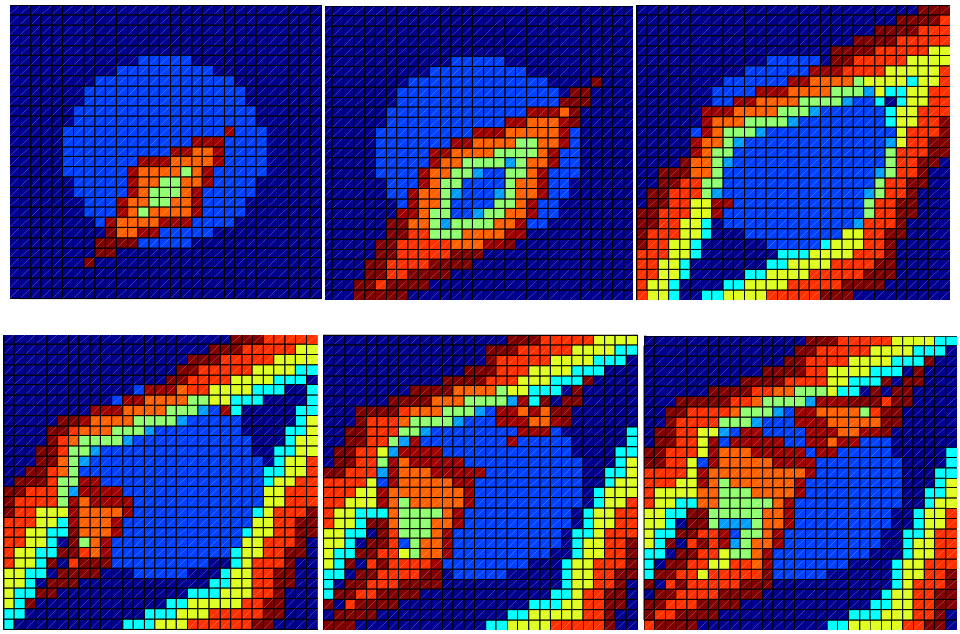

Figure 4.30 Self-initiated ischemic electrical wave propagation, 45^{o} fiber angle

4.2.2. Electro-Mechanical Simulation in 2D

The simplest electrical propagation model was established by neglecting the fiber directions and assuming spread of the electrical activity to be homogeneous in each direction. Mechanical behavior is applied to homogeneous tissue model as a first step of electromechanical behavior model.

The contraction of each element, consisting from 4 nodes, causes shortening of the tissue from every direction. Contraction begins from the mid point of the tissue model, and we see the step by step contraction in Figure 4.31.

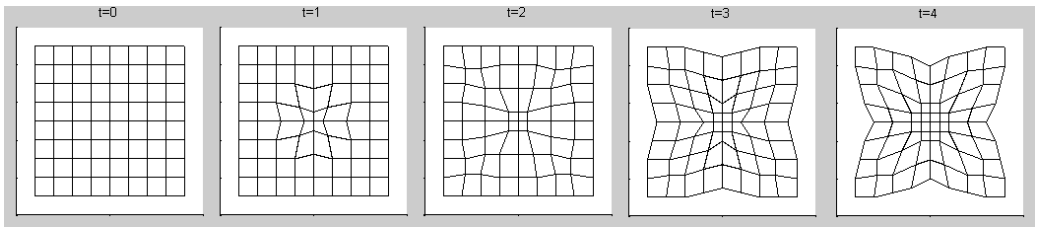

Figure 4.31 Mechanical behavior of the isotropic tissue model

If we combine the electrical wave propagation and the mechanical contraction and relaxation we have the following results. As it is given in one-dimensional studies, the mechanical activation begins after electrical excitation and also ends after the repolarization. After the electrical activity begins to propagate, the two nodes at state 2 should contract, and after state 4, each element should get back to its initial length.

For the isotropic case illustrated in Figure 4.32, the electrical wave propagation is in circular form and the resulting mechanical contraction begins in state 2, and ends in state 4. The colors in this figure represent the electrical activation, while the mechanical response can be seen as deformation, i.e. changes in coordinates.

As it is used in one-dimensional case, the model was fixed from excitation point, mainly used as the mid-point of the region.

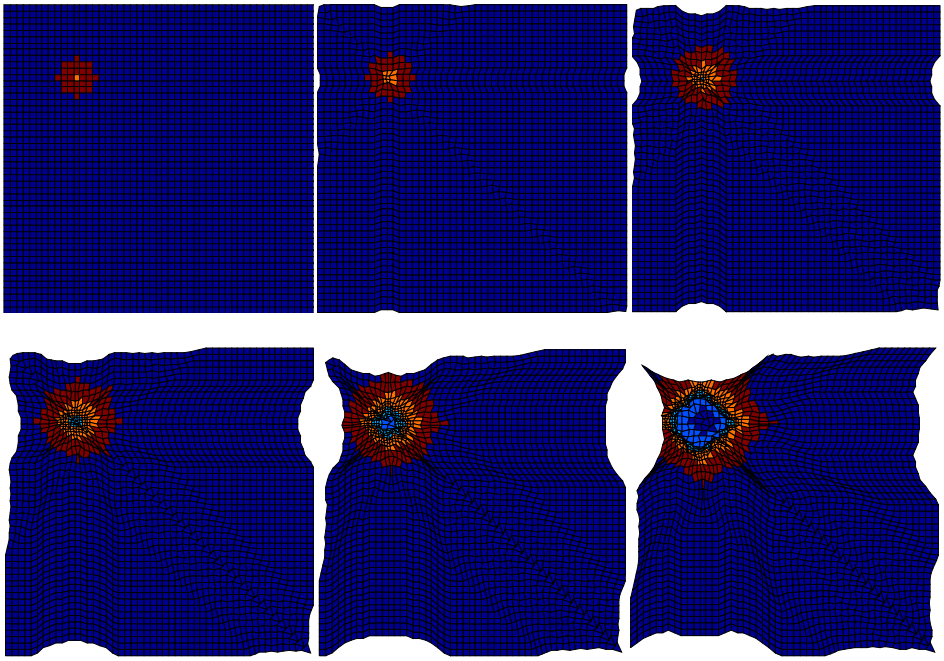

Figure 4.32 Electromechanical behavior of the isotropic tissue model

Although the simplest electrical model is the isotropic one, it is not the realistic case in the actual mechanical behavior of the heart. The contraction and relaxation should be calculated in every direction the neighboring cell lie. As the element achieves the second electrical state (S2), according to the neighborhood direction, it will cause deformation in this direction. Each node has neighbors lying in 0, 45, 90 and -45 degrees, and for each contraction the direction and other effected nodes should be taken into account.

Since the contraction occurs due to filament slides in each sarcomere, taking the contraction and relaxation in only one direction is not a simplification but a correction for the model. However, as a simplification, the angular fiber direction change is assumed to be the same in one layer, and the fibers are taken parallel to each-other. Figure 4.33 shows the one directional contraction of the sheet.

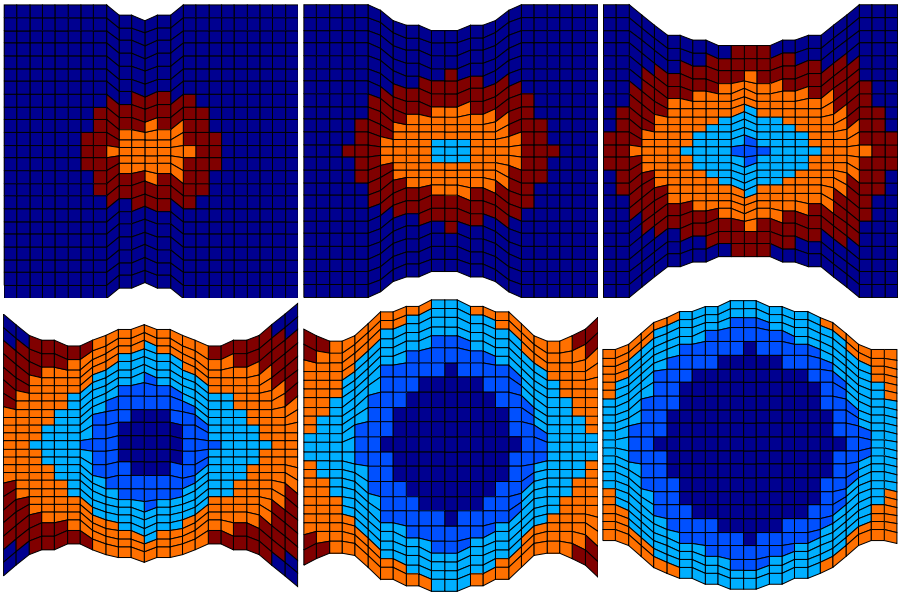

Figure 4.33 Electromechanical behavior of the anisotropic tissue model

It has been considered that, the electrical propagation in the heart tissue is not uniformly distributed in each direction, the electrical activity faster to one direction than the other directions, because of the fibers. If we add the anisotropy both for *electrical* and *mechanical* properties, the results will be as it is illustrated in Figure 4.34.

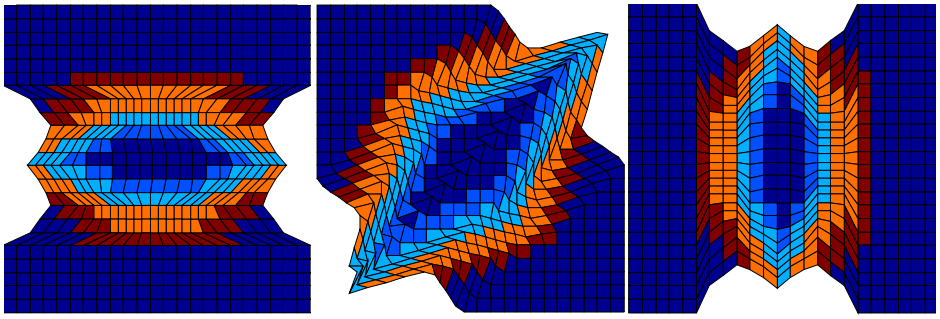

Figure 4.34 Electro-mechanical propagation in fiber directions, 0^{o} ,45^{o} ,90^{o} degrees

For arbitrary fiber direction, if two nodes, lying along the fiber direction is in the same activation state, (S2), contraction occurs for all the nodes lying along this fiber direction, as it was shown in one-dimensional studies. Couples of fiber directions, which are used in electromechanical wave propagation directions, were presented in Figure 4. 35.

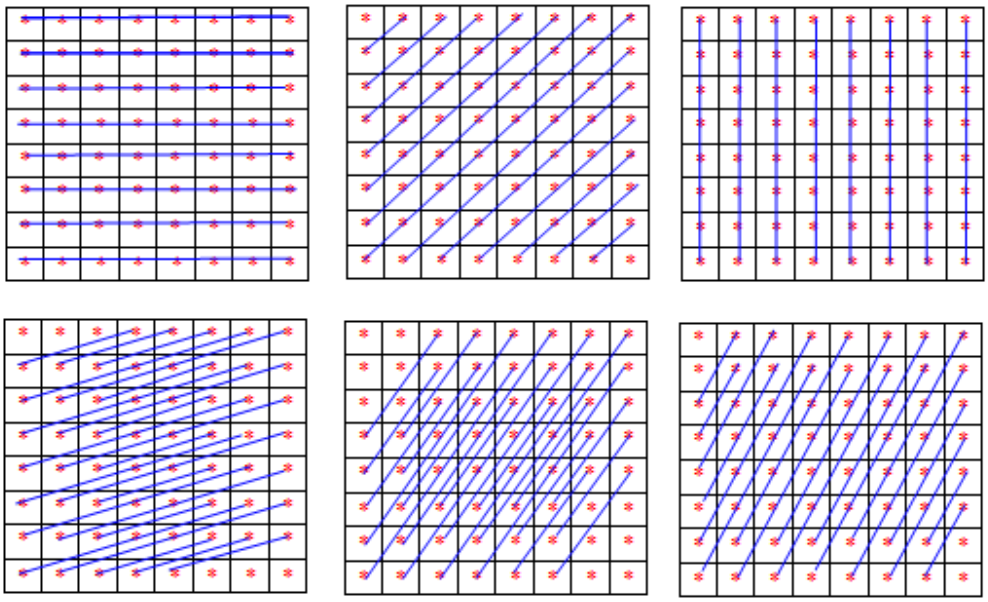

Figure 4.35 Electro-mechanical propagation in fiber directions in 2D matrices, 0°, 45°, 90°, 20°, 55°, 60° degrees fiber orientated neighborhood

a. Two ectopic beats

The effects of electrical behavior resulting from two ectopic beats applied to the two-dimensional sheet were given in Figure 4.18. Adding the mechanical response to that gives following results. In Figure 4.36 and 4.37, the homogeneous case was illustrated. Only the initial stimulus points and distances between two foci have changed and the propagation was monitored. The direction of the two points does not matter because of the isotropy of the sheet.

As it has been considered in electrical part, if two points are closer, the ectopic beats will combine and look like as it is in one ectopic beat, centered from one point, midpoint of two ectopic foci.

When the propagating electrical waves reach each other both the electrical wave and the contraction will be added to each other and summation of the waves seems like merged.

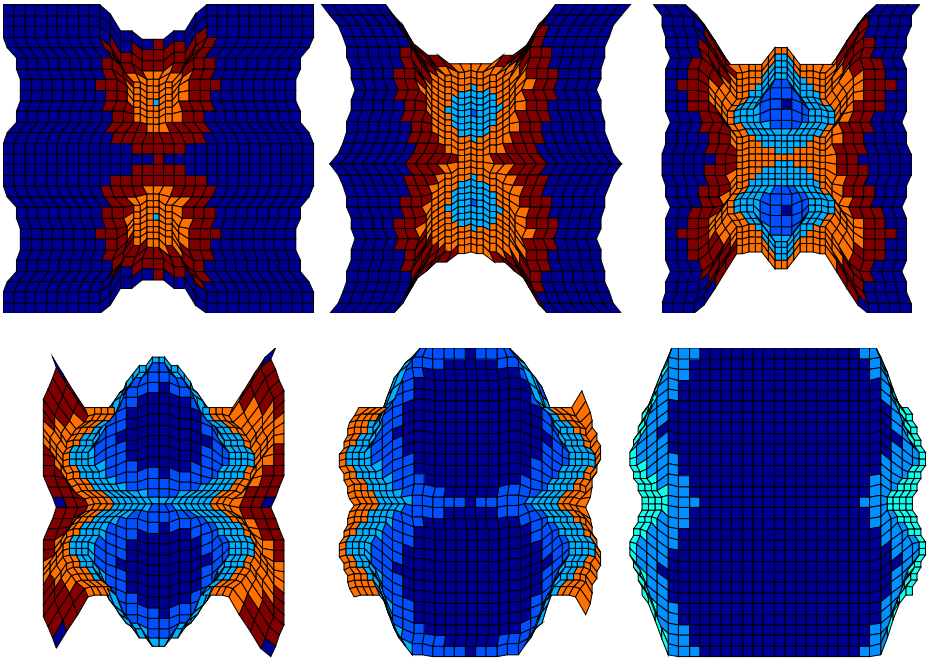

Figure 4.36 Two ectopic beats, located in y direction, propagation of the electromechanical activity in time

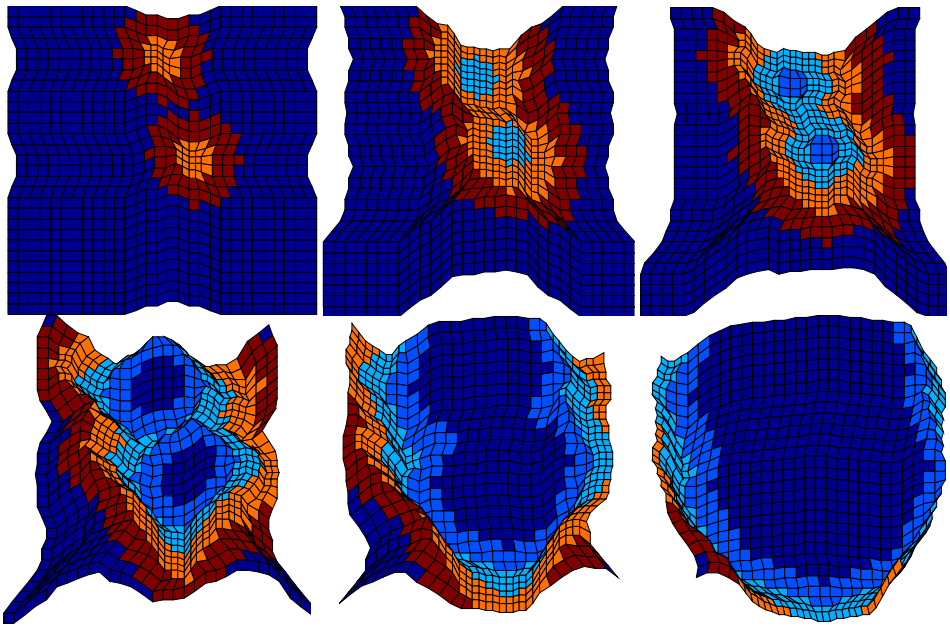

Figure 4.37 Two ectopic beats, located closer in y direction, propagation of the electromechanical activity in time

If two foci are not exactly along a single line along the x or y axes, the propagation and the contraction patterns can be seen for two different foci separately. Abnormal shrivels can be seen in Figure 4.37. One can also say that adding the mechanical response, the pathological behavior of two ectopic beats is more visible than only electrical wave results.

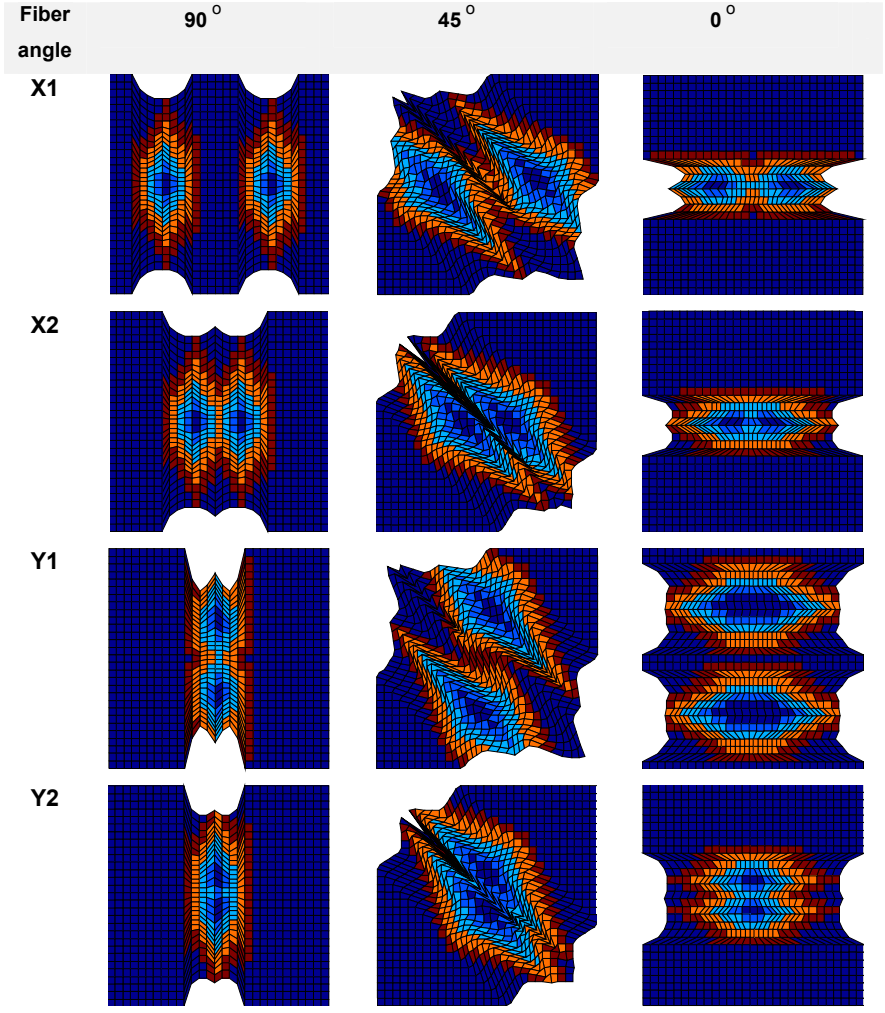

Figure 4.38 Two ectopic beats for different fiber directions, 0 °, -45 °, and 90 ° fiber angle, electromechanical wave propagation results for X1- two points in x direction, X2 - two closer points in x direction, Y1 - two points in y direction, Y2 - two closer points in y direction is given

In Figure 4.38, results of four different fiber angles and four different locations for ectopic foci were given. After each sheet is stimulated from the same focal points, the

results for four different fiber angles are different as expected. According to fiber direction of the tissue, waves resulting from ectopic foci merge earlier with respect to each other. Also according to their fiber direction and the line passes from two focus points the result changes.

For 90 degrees – two points chosen in y direction appear as one

For 0 degrees – two points in x direction appear as one

For 45 degrees - except points chosen along the fiber direction, we always see two beats

It is obvious that the contraction caused by more than one focus results in a larger deformation than the deformation of one stimulation point. Larger area is affected and if the area is the same, the contraction is added to each other.

b. Reentry

In this section, mechanical response to re-excitation of the tissue due to a partially or totally ischemic tissue is given.

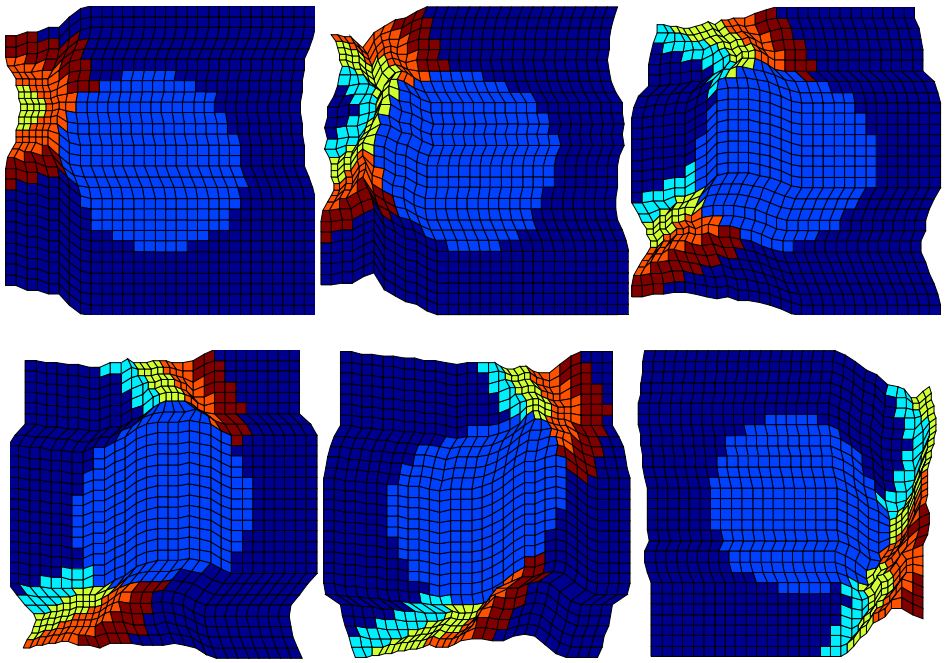

Figure 4.39 Totally ischemic tissue, electromechanical wave propagation, isotropic tissue model

Only by choosing a region as ischemic tissue, and applying the given properties of the tissue to the CA rules, following results are obtained. If the tissue is totally ischemic the tissue does not respond to electrical excitation, and it will not transfer the electrical activity to its neighboring cells. This unhealthy tissue will also not give any mechanical response.

For isotropic case, the totally ischemic tissue is excited from one node and the response is monitored as presented in Figure 4.39.

The electrically blocks are changes both electrical propagation and mechanical contraction pattern.

If the tissue is only partially deformed due to a cardiomyopathic disease, it will not block the electrical activity or contraction: however the response will not be the same with the normal tissue. We saw the electrical behavior of the sheet in electrical part, now we see the mechanical response of reentry in Figure 4.40.

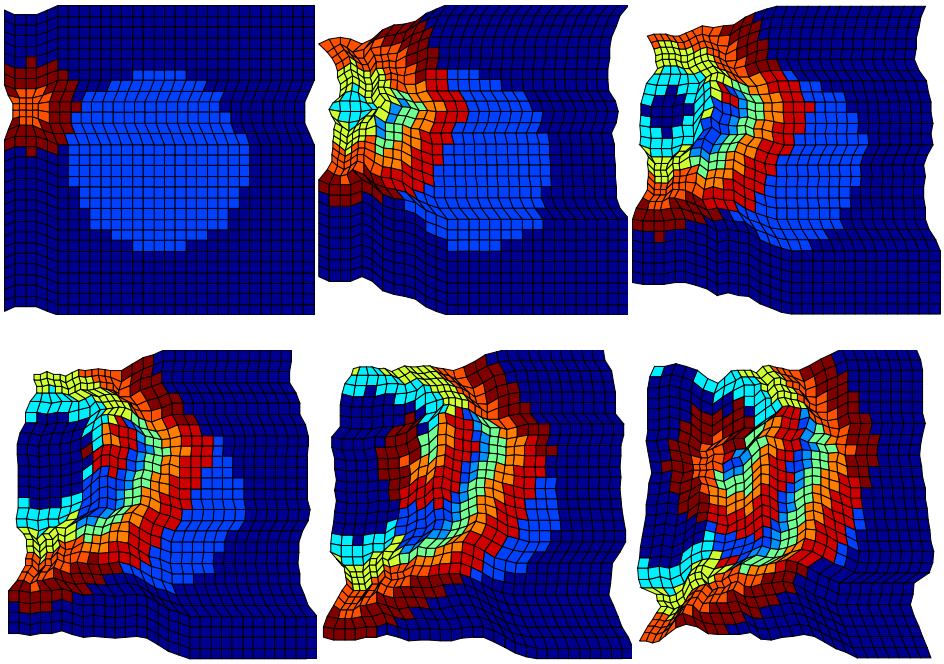

Figure 4.40 Ischemic tissue electromechanical wave propagation, isotropic tissue model

It was also mentioned that the ischemic tissue may also initiate an ectopic beat, because of its electrical accumulation property.

We can say that the reentry is seen on the edge of normal and ischemic tissue. The ectopic wave propagates in both normal and ischemic tissue, and each time, the ischemic tissue recovers earlier than normal tissue. Thus, once a reentry begins it will never end. Each excitation triggers the next excitation because of the propagation pattern.

The self initiated electrical wave propagation and the mechanical response to the electrical excitation for isotropic tissue is given in Figure 4.41.

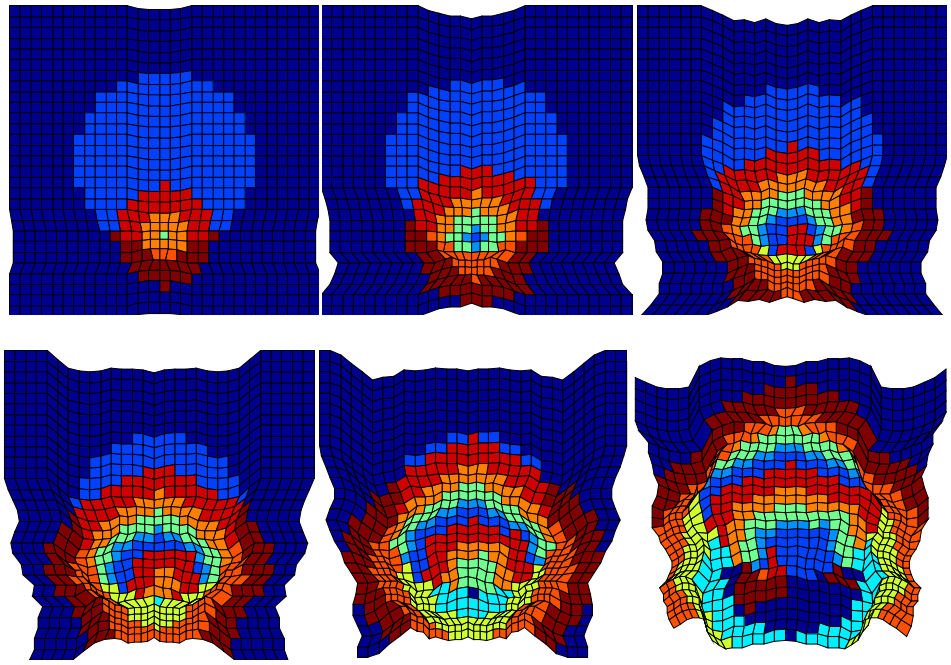

Figure 4.41 Self-initiated ischemic electromechanical wave propagation, isotropic tissue model

Adding the fiber directions to the model, the totally ischemic tissue block effects are shown in Figure 4. 42 for 90 degrees fiber direction and in Figure 4.43 for -45 degrees.

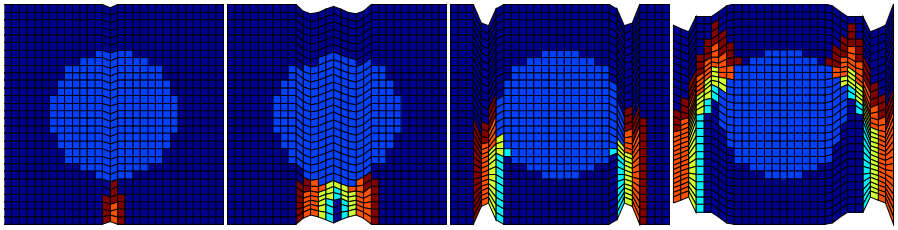

Figure 4.42 Totally ischemic tissue, electromechanical wave propagation, the 90^{o} fiber direction

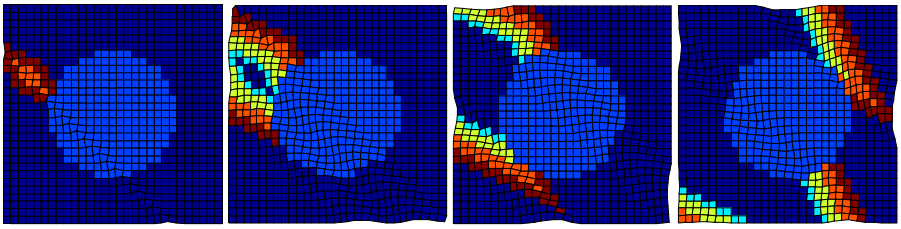

Figure 4.43 Totally ischemic tissue, electromechanical wave propagation, the -45^{o} fiber direction

If the cardiomyopathic tissue is totally dead, it will cause the separation of the electrical wave. Pathological circumstances not only are caused by non-contractile profile of the tissue, but also change in propagation pattern.

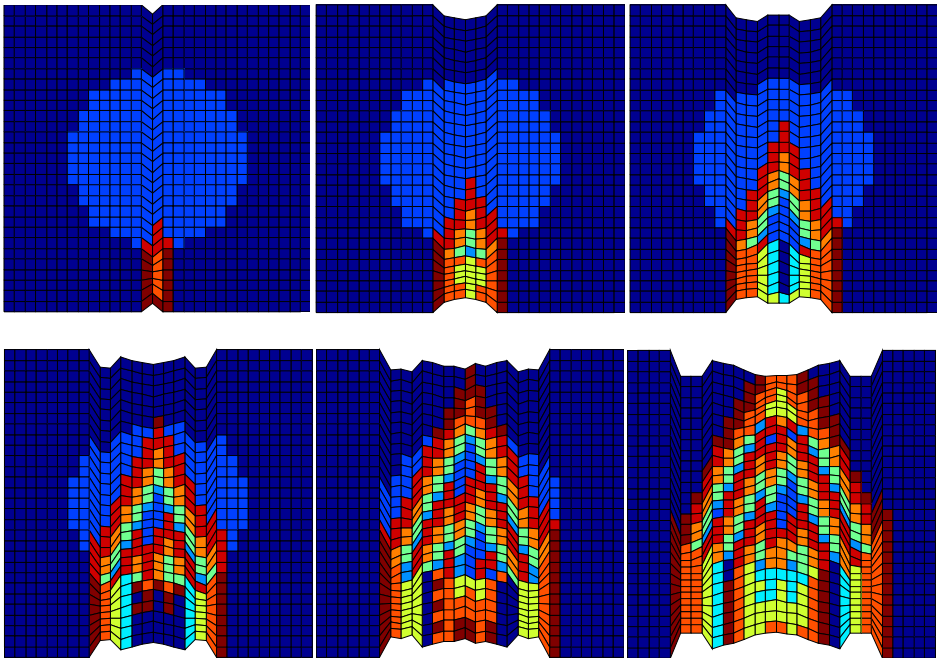

Figure 4.44 Ischemic tissue electromechanical wave propagation, for 90^{o} fiber angle.

If the tissue is only partially affected from cardiomyopathic diseases, the electrical propagation and mechanical response is as it is given in Figure 4.44 for 90 degrees fiber direction. Changes occur both in electrical and mechanical properties; the electrical wave recovers earlier; and contraction force is less than normal and it is slower, so the deformation also gets smaller in this region.

For a different angle (-45 degrees) we see a similar response to reentry, Figure 4.45. The point chosen to apply the stimulation also changes the reentry pattern.

Although the electrical propagation in ischemic tissue is slower than normal, we can still see the fiber direction effect in the figures.

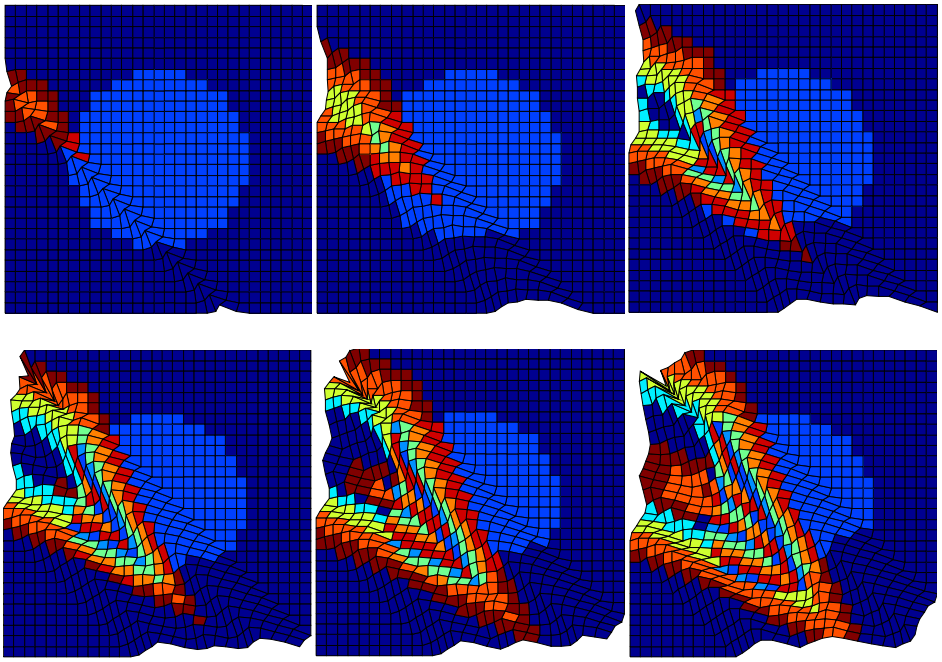

Figure 4.45 Ischemic tissue electromechanical wave propagation, for 45^{o} fiber angle

For these two different fiber angle examples, the self-initiated ectopic beats are also modeled by choosing the first excited point in the damaged tissue.

The fiber direction effect to self-initiated electrical wave propagation in ischemic tissue is given in Figure 4.46 and Figure 4.47.

As it is expected, after the depolarization of the ischemic tissue, surrounding normal tissue is still in high repolarization potential that can re-excite the ischemic tissue. And unstoppable circulation of the electrical wave begins. Due to state changes, mechanical response to electrical behavior also seems like “unstoppable”. One can say that the ischemic tissue is a potentially active node for fibrillation. By adding the mechanical response of the tissue, the pathological effects of the reentry became more visible. The asymmetric propagation pattern can be explained by changes in following parameters: the fiber orientation of the tissue, initial excited point and ischemic tissue distance, and the degree of the ischemia.

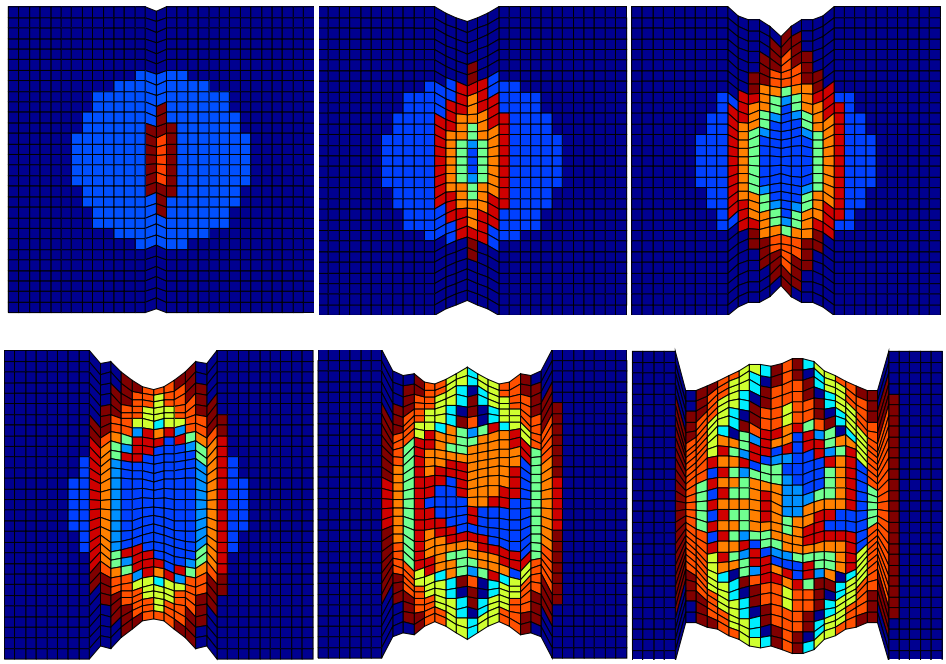

Figure 4.46 Self-initiated ischemic tissue, 90^{o} fiber angle electromechanical wave propagation.

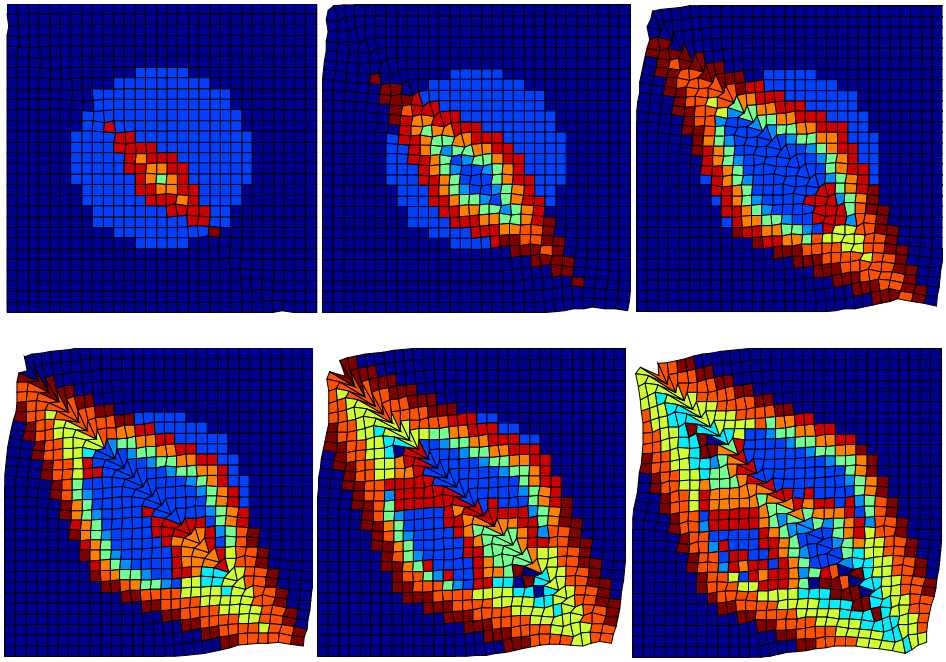

Figure 4.47 Self-initiated ischemic electromechanical wave propagation, 45° fiber angle

4.3. Three-Dimensional Studies

4.3.1. Electrical Wave Propagation in 3D

First studies done in three dimensions are generated using a simple cube. Stimulating from midpoint of mid-layer of the cube, the electrical wave propagation can be monitored as it is given in Figure 4.48. In the figure, expected results for isotropic condition, and anisotropic conditions were given. In the anisotropic propagation, fiber directional propagation in only one angle and changing angular fiber directional propagation results are considered.

According to the physiological knowledge about the cardiac muscle, the geometry of the ventricular myocardium can be modeled in layered manner. If we neglect anisotropy due to the fiber orientation, the propagation of the electrical wave should be at the same velocity in every direction on the tissue.

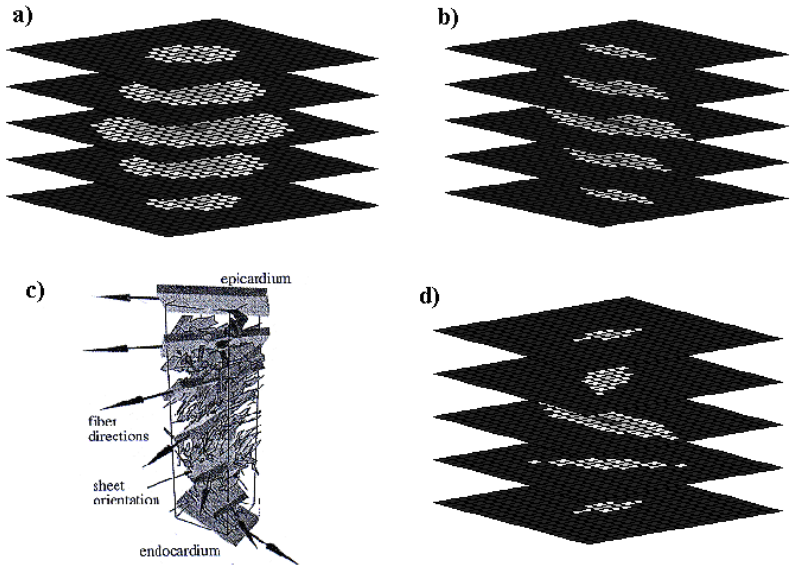

Figure 4.48 Isotropic electrical wave propagation in 3D layers; (a) isotropic tissue model, (b) model of one fiber direction for each layer, (c) changing fiber directions from epicardium to endocardium [13], (d) model of different fiber directions

In Chapter 2, it was considered that fiber orientation is the most important factor that should be taken into account in modeling the electromechanical properties of the tissue. The ratio of the velocity changes were given as (1:3:5); if the velocity is 1 along the fiber direction in one sheet, along the direction perpendicular to the fiber direction the velocity is 1/3rd of normal fiber directional velocity and the velocity of propagation across other sheets decreases even more; it becomes 1/5th of normal fiber directional velocity [9].

The studies done in 3D, multilayered cube-like geometry, show that the delays are main parameters in simulating the electrical wave propagation. Effects of fiber direction and the wave propagation across different sheets are all related to neighborhood and wave propagation velocity, which is defined in terms of delays in the proposed algorithm.

In Figure 4.49 (a) and (b), layers from 1 to 4 are tissue simulation geometry layers, while 0th and 5th layers are the total electrical wave distribution of the layers measured from uppermost and lowermost layers. Summation from upper layer is performed as follows; the layers were multiplied by a scalar which presents the distance between the

layer and uppermost layer. The closest layer was multiplied by the highest value and the scalar decreases as the distance between uppermost layer and current layer increases. Than each layer was added to each other and divided by the number of layers. Using the same approach, summation from the lower layer was also calculated.

If we neglect the anisotropy, no matter how many layers are taken into consideration, the total electrical activity distribution will be in circular form. In Figure 4.49 (b), the fiber direction is also taken in consideration; however, the layers not only are affected by the delays in its own sheet direction but also the delays coming from the upper and lower sheets may also trigger the action potential generation in a node.

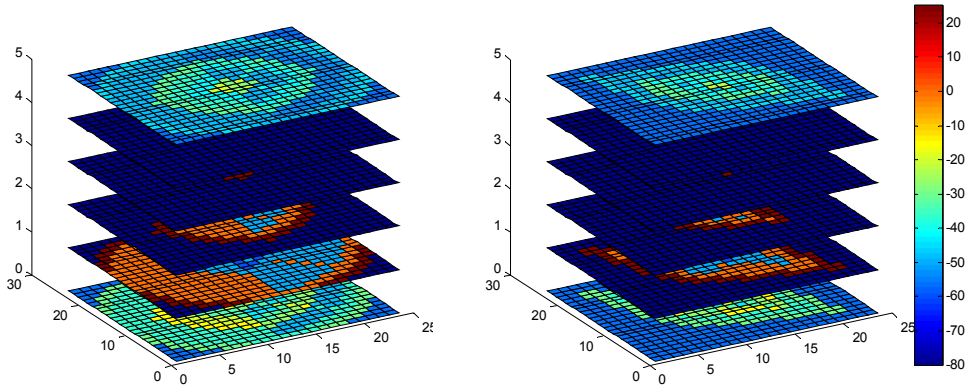

Figure 4.49 Isotropic and anisotropic electrical wave propagation in cube, sheets are 24x24 node 2D layers, summation of electrical waves are given as 0^{th} and 5^{th} layer, from lowermost and uppermost electrical distribution respectively.

In Figure 4.50 and 4.51, separate layers of electrical wave distributions and summation of the layers were given. In Figure 4.50 the fiber angles chosen are more spread; the fiber angles are -45, 0 and 90 degrees, while the example in Figure 4.51 shows the summation of the electrical activation waves for fiber orientations at 45, 30 and 0 degrees in a three-layer model.

Calculated summation in Figure 4.50 is more scattered than the summation in Figure 4.51, because the chosen fiber directions' difference is greater than that of the letter.

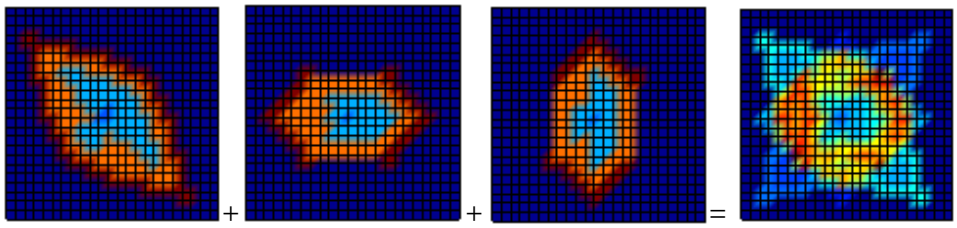

Figure 4.50 Three layer electrical activation propagation, summation of -45°, 0°, 90° fiber angles propagation wave

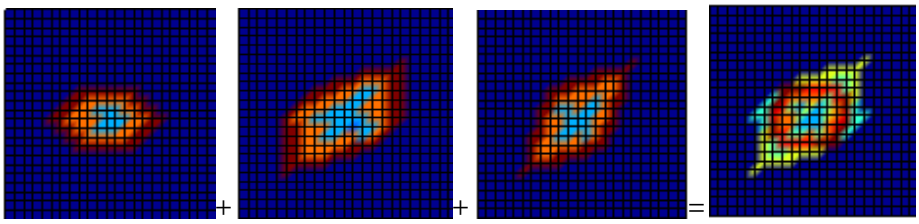

Figure 4.51 Three layer electrical activation propagation, summation of 0°, 30°, 45° fiber angles propagation wave

When the epicardial and endocardial fiber directions are fixed, according to the number of layers, chosen fiber directions will vary. The more layers are used in the model, the well-organized electrical wave propagation will be observed.

4.3.2. Mechanical Contraction Model in 3D

In multi-layered 3D tissue model, we have analyzed the mechanical contraction response of the tissue as well. The one directional contraction phenomena is used to model the mechanical activity in 3D studies.

In Figure 4.52 we see the fiber directional propagation in only one angle, 0 degrees. Each of the layers only contract due to its own sheets electrical wave propagation; however, it should also contain the interactions between layers which are also affected by the deformation of upper and lower sheer neighbors.

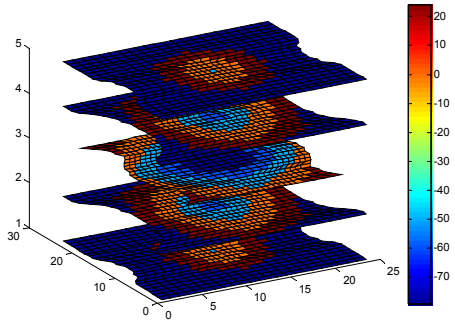

Figure 4.52 Five layer electromechanical activation and contraction in 0° fiber angle isotropic electrical propagation model

As it has been considered in electrical activation propagation studies the fiber angle changes for each layer. Effect of fiber change is shown in Figures 4.52 and 4.53. However, it is assumed that the contraction and deformation occurs only in one layer and it does not affect the nodes in other layers in multi layered model studies. We can see total deformation in the cube like figure, and the deformation in each layer is given in Figure 4.53.

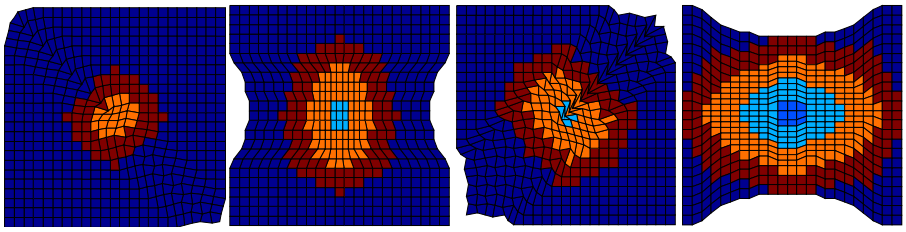

Figure 4.53 Electromechanical activation and contraction in each layer due to its fiber direction, each layer contracts separately

4.3.3. 3D Studies with a Simple Left Ventricle Model

a. Electromechanical Studies with Single Layer Simple LV Model

Single layer simple left ventricle model is generated by cylinder and logarithm functions and the neighborhoods were set as it is in the two dimensional studies, but one edge is set as the wave propagates through to the other edge, by changing the neighboring algorithm from “fixed” to “periodic”, which was explained in Chapter 3, in Figure 3.1.

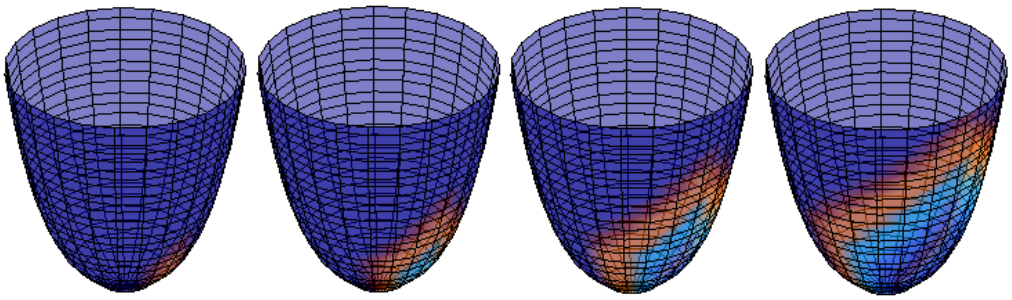

Figure 4.54 Electrical wave propagation in one layer simple LV

In Figure 4.54 the electrical wave propagation in single layer simple LV can be seen for an ectopic excitation point. Normally the wave runs through the Purkinje fibers and excites the whole ventricle synchronously.

To model the normal contraction behavior of the ventricle, initial excitation point has been chosen as the apex of the ventricle. When the cells reach 'State-2' the contraction begins. As the electrical excitation wave propagates from apex to base, the contraction can also be observed in those excited regions. The contraction of the ventricle model is presented in Figure 4.55.

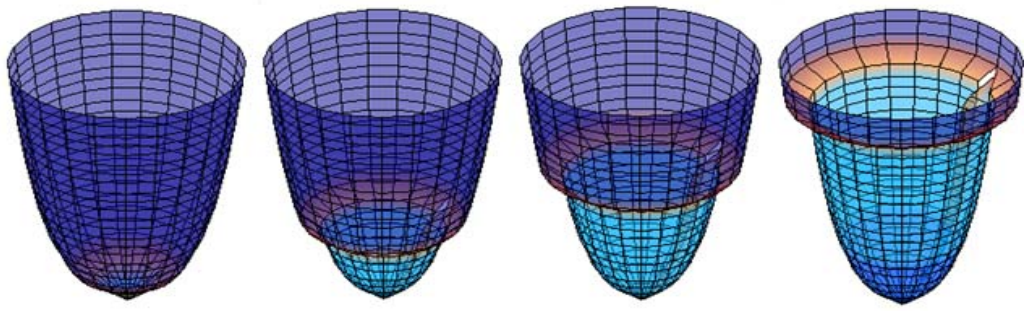

Figure 4.55 Electromechanical wave propagation in one layer simple LV: normal heart beat, from apex to base

If two or more ectopic foci initiate electrical excitation waves in the ventricle, according to the location of ectopic foci, the merging of the waves can be observed. In Figure 4.56 waves are chosen from two different points close to the base and close to each other,

and in Figure 4.57, points chosen from left and right parts of the base to initiate the ectopic action potential. As the waves merge in Figure 4.56, we can see the waves in Figure 4.57 separately, surrounding the entire ventricle model.

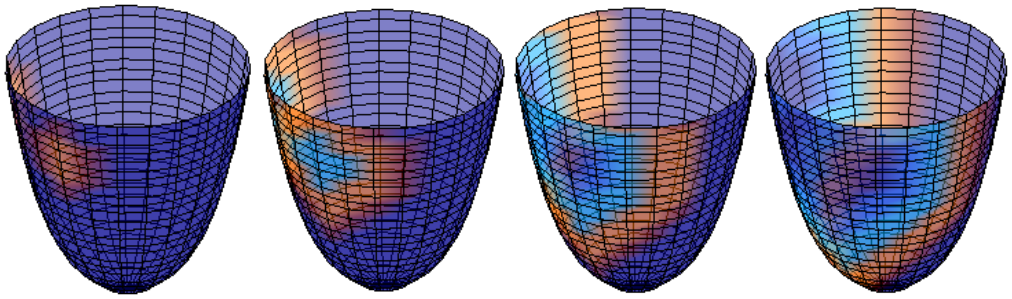

Figure 4.56 Electrical wave propagation in one layer simple LV, two ectopic foci, closer points

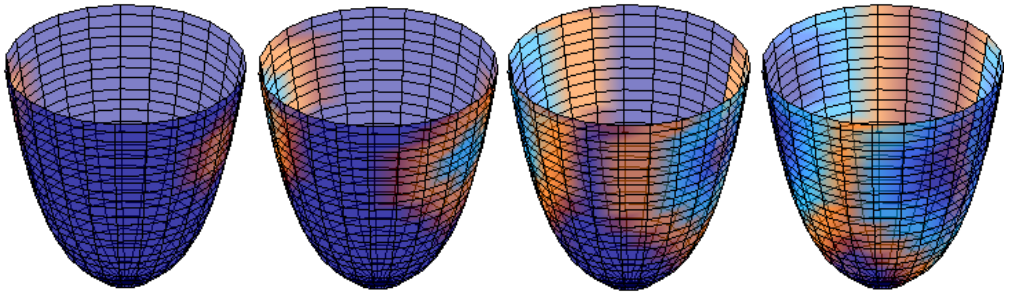

Figure 4.57 Electrical wave propagation in one layer simple LV, two ectopic foci, two separate foci chosen

The mechanical response to ectopic beat is shown in Figure 4.48. Whole ventricle does not contract, only effected region responds to the ectopic electrical activation. And these excited regions will not be able to respond to the normal heart excitation wave, because they will be in the refractory period at the time the normal wave reaches to those nodes.

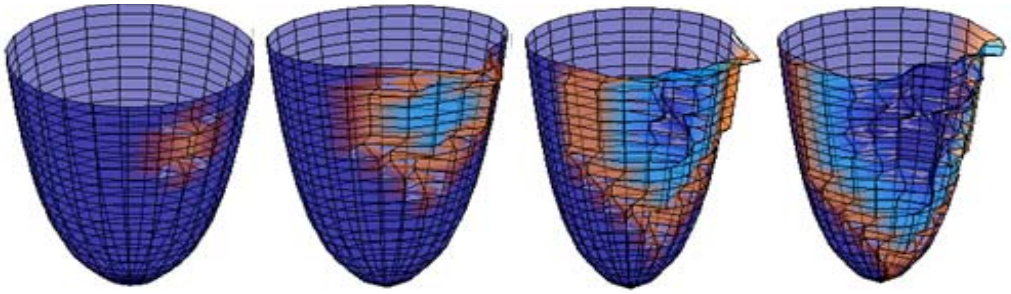

Figure 4.58 Electromechanical wave propagation in one layer simple LV, ectopic focus

As it has been shown in 2D studies, cardiomyopathy may cause reentry of electrical excitation. 3D distribution of the reentry is shown in the following examples.

In single layered simplified LV, chosen ischemic region is shown in Figure 4.59. And the electrical wave states for normal and ischemic tissue are same as the ones we used for 2D studies. The same three cases were realized in 3D studies: totally ischemic tissue, partially ischemic tissue and self-initiated ectopic beat caused by the ischemic tissue.

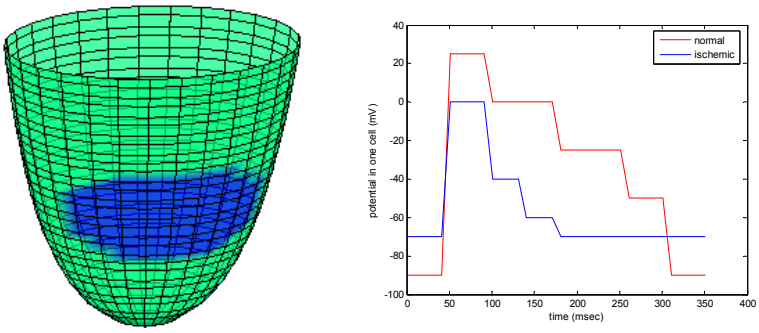

Figure 4.59 Ischemic tissue model: geometry, rules and action potential approximation for normal and ischemic tissue

In totally ischemic tissue, the wave will propagate around the ischemic region and the dead region would not respond to electrical excitation, as it has presented in Figure 4.60.

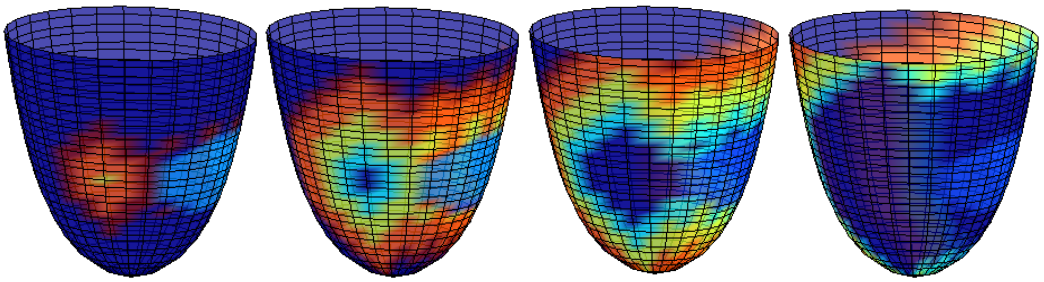

Figure 4.60 Ischemic tissue model: electrical wave propagation in totally ischemic tissue

In totally ischemic tissue re-entry does not observed, on the other hand, partial ischemic tissue causes re-entry. Results of re-entry model are presented in Figure 4.60 and Figure 4.61. the partially ischemic tissue will respond to the excitation, but in a different way compared to the normal tissue, and the shortened action potential cycle will cause the re-excitation of the tissue, whenever it gets back to its resting state, in Figure 4.61.

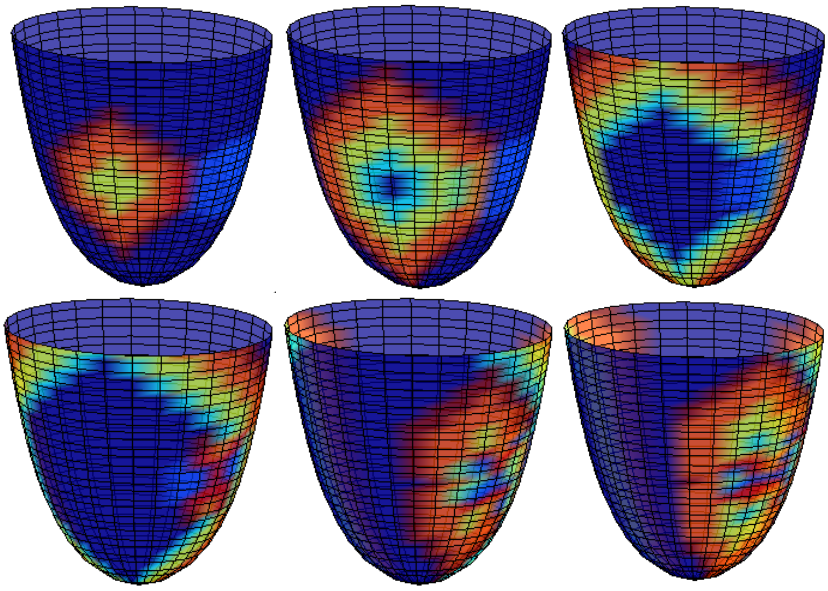

Figure 4.61 Electrical wave propagation in one layer simple LV, ischemic tissue, reentry model

As it has been presented in the 2D studies, the tissue may also create self-initiated ectopic beats. Reentry wave is also observed in this phenomenon. Three dimensional distribution of the wave propagation is given on single layered simplified LV model, in Figure 4.61.

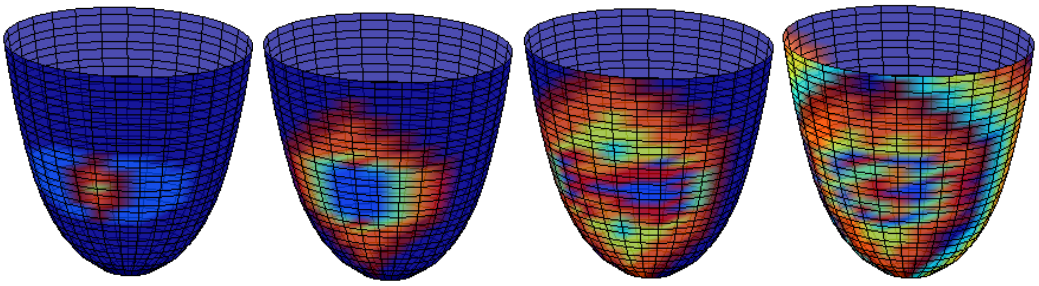

Figure 4.62 Electrical wave propagation in one layer simple LV, self-initiated, ectopic wave propagation in ischemic tissue, reentry model

b. Electrical Studies with Multiple Layer Simple LV Model

It has been mentioned that the left ventricle can be modeled as a multi-layered structure and the electrical wave propagates through these layers with a low velocity compared to the activation along the fiber direction in one layer.

The multi-layer model is given in Figure 4.63. Four layered simple model is used to observe the fiber direction, electrical wave propagation and mechanical contraction simulation studies.

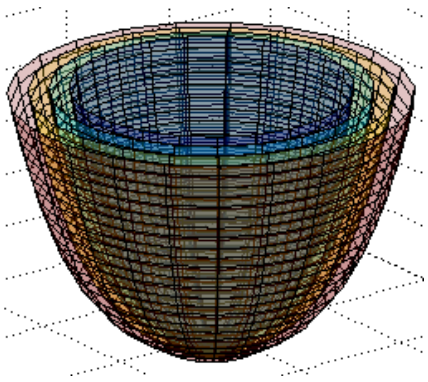

Figure 4.63 Multi-layered simplified LV model

As the excitation begins from a single point, the electrical wave propagation in multi-layer model is given in Figure 4.64. Four layered simple model has different fiber rotations in each layer. And the electrical wave distribution in the outermost layer can be seen in the figure with -45 degrees fiber angle.

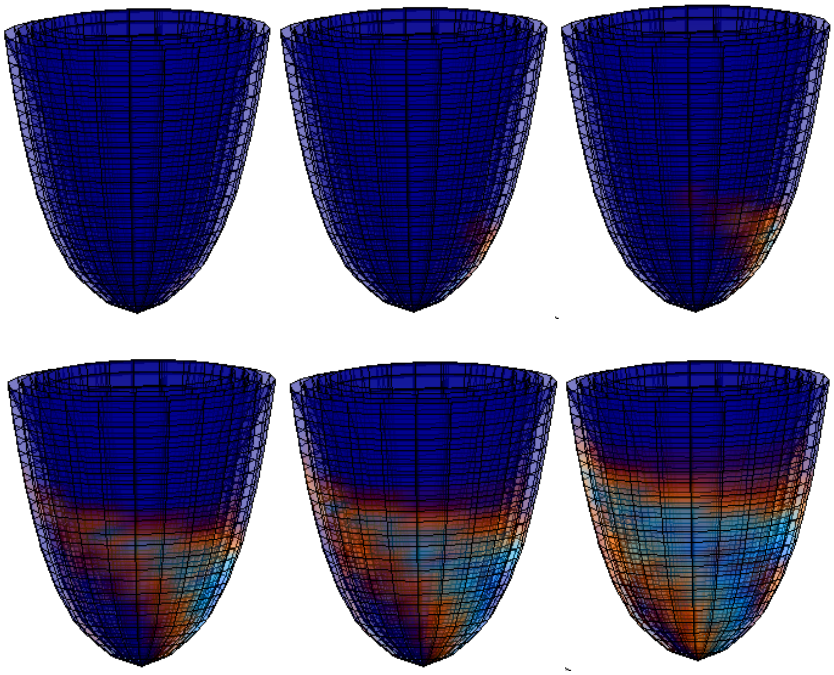

Figure 4.64 Electrical wave propagation in multi-layer simple LV model

Electrical excitation propagation in each layer and summation of the potential of the multi-layer model is presented in Figure 4.65.

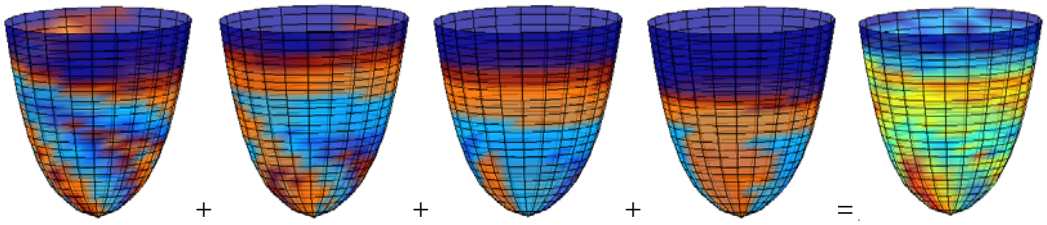

Figure 4.65 Electrical wave propagation in each layer: summation of total electrical distribution

In Figure 4.65, we can see that the total electrical activity has no direct fiber oriented distribution, but as the wave reaches the base of the ventricle in one layer (-45 degree fiber oriented outermost layer), almost whole left ventricle is affected by the excitation of a single node. And we cannot define the fiber directions of each layer, since each of the layer also affected by its neighboring layers.

CHAPTER 5

CONCLUSION

The design of computational models of human organs is a new research field, which opens new possibilities for medical analysis, therapy, and understanding of the biological phenomena. In heart modeling studies, many researchers limit their study either the mechanical or electrical aspects. This thesis work is the combination of those alternations, and is the first step to understand the electrical and mechanical properties of cardiac tissue in normal and cardiomyopathic conditions in macroscopic scale. The goal of this study was to develop an anisotropic electromechanical model of the heart left ventricle. The model we presented was designed at a macroscopic level with a limited number of nodes and rule based interactions of the parameters. Left ventricular excitation and motion is modeled by an easy to use, simple model that explains the ventricular electrical activity, excitation and propagation, and the mechanical respond of the tissue to this excitation. The simulations represent a single cardiac cycle including electrical depolarization and repolarization as well as mechanical contraction and relaxation, in a fiber, on a sheet and finally on a truncated ellipsoid, which represents simplified left ventricle geometry.

Cellular automaton model was chosen to study electrical propagation, which can be used to better understand physiology and pathophysiology of the heart without using complex differential equations. The thesis work does not include complex ionic differential equations from the electrical point of view or the non-linear, viscoelastic properties of the tissue from a mechanical point of view. However, the conduction of electrical wave and the deformation can still be seen by using rule based cellular automaton model, which is accepted as the easiest and fastest approach in modeling the heart functions.

In mechanical simulation part, electrical excitation and force development are related to each other by the anatomical knowledge of ionic changes, and timing. The simplest approximation of the complicated mechanical behavior of muscles is to assume that they behave elastically. For the mechanical part, contraction of the muscle has been modeled by using an elastic relation between the force in the fiber and change in length of a fiber. We assumed that the contraction happens only along the fiber direction and the developed source is always the same if the node is excited. And relaxation occurs after the electrical wave is attenuated.

The results were given in three main titles: one-dimensional, two-dimensional and three-dimensional studies. In each part and for each different geometry, following major problems were focused on: (1) electrical propagation in anisotropic normal tissue, (2) effect of fiber directions to electrical excitation, the anisotropy, (3) electromechanical interactions, contraction due to electrical excitation in isotropic and anisotropic normal tissue, (4) electrical excitation disorders, effects of two ectopic excitation foci, (5) mechanical respond of the tissue to two ectopic beats, (6) electrical propagation in ischemic tissue models: totally and partially cardiomyopathic tissue models, (7) mechanical respond of the tissue to ischemia.

The results obtained in the current study are summarized as follows:

In one dimensional study results, one cannot talk about the isotropy; what is observed in electrical excitation and propagation is that the wave spreads in both directions with the same velocity, and early excited node gets back to its resting value first and the others are following it with a delay. In two dimensional studies, the effect of homogeneity and heterogeneity of the tissue can be observed directly. While the propagating wave is in circular form in isotropic model, the fiber directional wave propagation is faster along the fiber direction. Results were shown for many different angles. For 0, 45, 90, -45, and -90 degrees, the propagation can be modeled by using

the first order neighbors, while the remaining angles should include at least second order neighbors to yield the appropriate fiber direction.

Delays for directions were chosen such that the propagation velocity in the fiber direction is V, and perpendicular to the fiber direction is 0.3V, according to the studies done in biological studies. It is also considered that the propagation velocity also decreases across different sheets, and the velocity across sheets is chosen as 0.2V in multilayered models.

Electromechanical interactions are best explained in one-dimensional studies, which can be assumed as a single fiber. Fiber orientation has an important role both in electrical and in the mechanical properties of biological structures. The contraction and relaxation of each element is modeled as a consequence of electrical state changes. After two nodes in the given fiber direction gets excited contraction happens, and after the electrical wave gets to resting state the relaxation happens. In two and three-dimensional studies, the fiber long contraction and relaxation could still be observed. In truncated ellipsoid the deformation due to electrical excitation causes the ejection of the blood. The decrease of ventricular volume and contraction of the simple model has observed in the results.

Two ectopic excitation foci have different effects in isotropic and anisotropic tissue models. Due to the propagation velocity differences models that took fiber orientation into account, the locations of foci have different effects on electrical and mechanical responses of the myocardial models. By modeling two ectopic beats, the absolute refractory period phenomenon has also been explained. Once a node begins to generate its own action potential, it cannot be excited by its neighboring cells. Thus, an unwanted, early ectopic beat may cause asynchrony in cardiac excitation and contraction. The studies done in simplified ventricle obviously show this result, especially in mechanical studies.

The ultimate aim of our modeling method is to explain the functions of the damaged tissue which produces pathological conditions. Beside the electrical excitation disorders, we have also considered the effects of cardiomyopathic disorders, diseases

in myocardial tissue, in this thesis work. Electrical propagation in ischemic tissue models were considered using totally and partially ischemic tissue models. In the literature, the re-entry phenomena was explained in only two-dimensional studies and mostly in isotropic tissue models. In our study, the ischemia results both in electrical and electro-mechanical simulations were given in two and three dimensional studies. The unstoppable electrical wave re-excitation is observed in partially damaged tissue. Totally dead region also causes disorders in contraction, which is caused by separation of the electrical wave. The reentry results for homogeneous tissue model and fiber orientation added tissue model are observed both in normally initiated excitation propagation, and ectopic beat formed within this damaged region.

The ventricle geometry is modeled in a layered structure to analyze the 3D distributions of the results. The fiber orientation is set using knowledge from anatomical studies with a 140 degrees change from epicardium to endocardium. As the number of fiber oriented layers increase, the approximated electrical wave distribution in model become well-organized.

This thesis work includes the studies carried out to model the coupling of electrical and mechanical properties in normal and some pathological conditions, which can be considered as a simple “Beating Heart Model”. The validation of this study has only been done with the cardiac anatomy and physiology basis. Comparing to the knowledge of the anatomy and physiology of the real tissue, the complex electromechanical phenomenon has been modeled by using a simple, but an efficient model.

5.1. Future Work

As a further research, it is needed to quantify the results illustrated in this study. More realistic geometries should be used to see the effectiveness and to validate the proposed algorithm. To be able to compare our results with that form the literature, the geometry used should be the same. Many studies in the literature were performed on the geometry obtained from the “visible human data”. The algorithm can be compared with existing studies by a more realistic geometry. The first study as a future work

should be to change the geometry. Anatomically detailed models of the ventricles, including fiber orientations and sheet structure, will be used to analyze the electrical and mechanical behavior of the whole organ. Also real/original electrical propagation and mechanical response should be compared with biological studies.

Although the straightforward, time efficient model explains many properties of the tissue we know that many important simplifications were done in modeling. In the mechanical part, we used the simplest model to analyze the contraction. We neglected the non-linearity and also viscoelasticity. A more realistic mechanical model can be applied and combined with the electrical excitation of the tissue. Stress and strain relationship can be calculated for each node, which is assumed constant in the proposed algorithm, as the tissue gets excited.

Also the electrical model accepted here is the simplest model to study the electrical excitation in the literature. Another macroscopic, tissue based model can be used to simulate the electrical activation.

The clinical motivation of this work is the quantitative measurement of important ventricular function parameters from cardiac images, like the ejection fraction, the myocardium thickness and the local strain and stress. Those parameters are useful to detect ischemic zones, measure the pathology extent and control the therapy effectiveness. The long-term objective is to build a procedure that automatically adjusts all those electrical and mechanical parameters to the dataset of the patient.

Another long term goal is to use this model to extract quantitative parameters of the ventricular function from cardiac images. We believe that this beating heart model could help understand the consequences of local electrical or mechanical failures on the global motion.

The required electrical propagation can be related to ECG simulation. This would also be the step for body surface potential simulation studies.

The model can be used to better understand physiology and pathophysiology of the heart, to improve diagnostics of infarction and arrhythmia and to enable quantitative therapy planning. It can also be used as a regularization tool to gain better solutions of the ill-posed inverse problem of ECG.

REFERENCES

[1] World Health Organization Organisation Mondiale de la Sante Department of Measurement and Health Information December 2004, http://www.who.int/entity/ healthinfo/statistics/bodgbddeathdalyestimates.xls, last visited on 23.08.2010.

[2] Zipes, DP, Wellens, HJ. "Sudden cardiac death", *Circulation,* 98:2334-2351, 1998.

[3] Gilmour R. F., "The anatomy of an arrhythmia" *Journal of Clinical Investigation*; 113(5):662 doi:10.1172/JCI21223, 2004.

[4] Rangayyan R.M., *Biomedical Signal Analysis: A Case-Study Approach*, IEEE Press and Wiley, New York, NY. 2002.

[5] Waller A.D., "A demonstration on man of electromotive changes accompanying the heart's beat*", J. Physiol*. 8. 229-34, 1887

[6] Sundnes, J., Lines, G.T., Cai, X., Nielsen, B.F**.,** Mardal, K.A., Tveito**,** A., *Computing the Electrical Activity in the Heart,* Monographs in Computational Science and Engineering, Vol. 1, Springer, The Netherlands, 2006.

[7] Sachse F. B., *Computational Cardiology: Modeling of Anatomy, Electro-physiology, and Mechanics*, Springer, 2004.

[8] Hunter P.J., Pullan A.J., Smaill B.H.,"Modeling Total Heart Function", *Annu. Rev. Biomed*. Eng.5:147–77, 2003.

[9] Gharpure P.B.,"A cellular automaton model of electrical wave propagation in cardiac muscle", PhD Thesis, Department of Bioengineering, The University of Utah, August 1996.

[10] Xia L., Dou J.H., Gong Y.L., Zhang Y., Deng D.D., "Simulation Analysis of Mechanical Properties of the Canine Heart with Bundle Branch Block Based on a 3-D Electromechanical Model", *Computers in Cardiology*;34:673−676, 2007.

[11] Clayton R.H., "Computational models of normal and abnormal action potential propagation in cardiac tissue: linking experimental and clinical cardiology", Physiol. Meas. 22 R15–R34, 8 February 2001.

[12] Hunter P.J., Pullan A.J., Smaill B.H.,"Modeling Total Heart Function", *Annu. Rev. Biomed*. Eng.5:147–77, 2003.

[13] Pullan A. J., Cheng L. K., Buist M. L., *Mathematically Modelling the Electrical Activity of the Heart, From Cell to Body Surface and Back Again*, World Scientific, 2005.

[14] Noble D.," Modeling the Heart",Review, *Physiology* 19: 191–197, 2004.

[15] DiFrancesco D., and Noble D., “A model of cardiac electrical activity incorporating ionic pumpsand concentration changes”, *Philos. Trans. R. Soc. London. Ser. B* 307, 353, 1985

[16] Belik M.E., Usyk T.P., McCulloch A.D., “Computational methods for cardiac electrophysiology”. In (Ayache N, Guest Ed) *Computational Models for the Human Body,* Special Volume of (Ciarlet PG, Ed) Handbook of Numerical Analysis, Volume XII. *Elsevier B.V.,* pp. 129-188, 2004

[17] Sermesant M., Coudière Y., Delingette H., Ayache N., “Progress towards an electromechanical model of the heart for cardiac image analysis*”, INRIA Sophia-Antipolis Projet Epidaure, route des Lucioles 06902 Sophia-Antipolis,* France, 2004.

[18] Kerckhoffs R.C.P, Healy S.N., Usyk T.P., and Mcculloch A.D.,“Computational Methods for Cardiac Electromechanics”, Proceedings of the IEEE, Vol. 94, No. 4, April 2006

[19] Sermesant M., Delingette H., Ayache N.,,”An Electromechanical Model of the Heart for Image Analysis and Simulation”, *IEEE Transactions On Medical Imaging,* VOL. 25, NO. 5, May 2006.

[20] Nash M.P., Panfilov A.V., “Electromechanical model of excitable tissue to study reentrant cardiac arrhythmias”, *Prog Biophys Mol Biol*;85(2-3):501-22, Jun-Jul, 2004

[21] Hurmusiadis V., “Virtual Heart: Cardiac Simulation for Surgical Training & Education”, Primal Pictures Ltd, 159-163 Great Portland Street, London W1W 5PA, UK, 2007

[22] Dössel O., Farina D., Mohr M., Reumann M., Seemann G. and Weiss D.L., Modelling and Imaging Electrophysiology and Contraction of the Heart, Advances in Medical Engineering, 2007

[23] Appleton B., Wei Q., Liu N., Xia L., Crozier S., Liu F., Wilson S., “An Electrical Heart Model Incorporating Real Geometry and Motion”, Proceedings of the 2005 IEEE Engineering in Medicine and Biology 27th Annual Conference Shanghai, China, September 1-4, 2005

[24] Hunter PJ, McCulloch AD, and Keurs HE., “Modelling the mechanical properties of cardiac muscle”, *Prog Biophys Mol Biol*.;69(2-3):289-331., 1998

[25] Hu Z., Metaxas D.N., Axel L., “Computational modeling and simulation of heart ventricular mechanics from tagged MRI", *Functional Imaging and Modeling of the Heart Conference*. 369-383, January , 2005

[26] Xia L., Huo M., Wei Q., Liu F. and Crozier S.,”Analysis of cardiac ventricular wall motion based on a three-dimensional electromechanical biventricular model, institute of physics publishing, physics in medicine and biology”, *Phys. Med. Biol*. 50, 1901–1917, 2005.

[27] Guccione J.M., McCulloch A.D., “Mechanics of active contraction in cardiac muscle: Part I--Constitutive relations for fiber stress that describe deactivation”, *J Biomech Eng*.; 115(1):72-81., February 1993

[28] Guccione J.M, Waldman L.K, McCulloch A.D.,” Mechanics of active contraction in cardiac muscle: Part II--Cylindrical models of the systolic left ventricle.”, *J Biomech Eng.;*115(1):82-90. February 1993

[29] Nickerson D., Niederer S., Stevens C., Nash M., and Hunter P., “A Computational Model of Cardiac Electromechanics” Proceedings of the 28th IEEE EMBS Annual International Conference New York City, USA, Aug 30-Sept 3, 2006

[30] Usyk T.P., LeGrice I.J., McCulloch A.D., “Computational model of three-dimensional cardiac electromechanics”, *Comput Visual Sci* 4: 249–257, 2002

[31] Taber L.A., Nonlinear *Theory of Elasticity Applications in Biomechanics*, World Scientific, 2004.

[32] Nash M.P., Hunter P.J., “Computational Mechanics of the Heart:From Tissue Structure to Ventricular Function*” Journal of Elasticity* 61: 113–141, 2000

[33] Mirsky I., Ghista D.N., Sandler H.,*Cardiac Mechanics: Physiology, clinical, and mathematical considerations*, *Eds.* New York, NY*:*Wiley, 1974.

[34] Kojic M., Mijailovic S., Zdravkovic N. , “Modelling of muscle behaviour by the finite element method using Hill's three-element model”, *Int. J. Numer. Meth. Engng*. 43, 941{953, 1998

[35] Nash M.,”Mechanics and material properties of the heart using an anatomically accurate mathematical model”, Thesis (PhD--Engineering Science)--University of Auckland, 1998

[36] Brandy A.J., “The Three Element Model of Muscle Mechanics: Its applicability to Cardiac Muscle”, *The Physiologist* 75-86, 1967

[37] Holmes J.W. , “Teaching from classic papers: Hill’s model of muscle contraction”, *Adv Physiol Educ* 30: 67–72, 2006

[38] Costa K.D., Hunter P.J., Rogers J.M., Guccione J.M., Waldman L.K., McCulloch A.D., “A three-dimensional finite element method for large elastic deformations of ventricular myocardium: I--Cylindrical and spherical polar coordinates.”, *J Biomech Eng.* Nov;118(4):452-63., 1996

[39] Costa K.D., Takayama Y., McCulloch A. D., and Covell J. W., “Laminar fiber architecture and three-dimensional systolic mechanics in canine ventricular myocardium”, *Am J Physiol Heart Circ Physiol* Vol. 276, Issue 2, H595-H607, February 1999

[40] Costa K.D., Holmes J.W., McCulloch A.D.,“Modelling cardiac mechanical properties in three dimensions”, *The Royal Society, Phil. Trans. R. Soc. Lond. A*, 2001

[41] Fox S. I., *Human Physiology*, 10th Edition,McGraw Hill International Edition, New York, 2008.

[42] The geology of the human heart, http://planetearth.nerc.ac.uk/ news/story.aspx?id=369, last visited 24.08.2010.

[43] Siem K.V.L., "Modelling fibre orientation of the left ventricular human heart wall", Master of Science thesis, Department of Computer and Information Science, Norwegian University of Science and Technology, June 2007.

[44] Despopoulos A., Silbernagl S., *Color Atlas of Physiology*, 5th Edition, Thieme, New York, 2003.

[45] Katz A.M., "Physiology of the Heart", New York: Raven Press (1977)

[46] Karp G., *Cell and Molecular Biology: Concepts and Experiments*, Third Edition, John Wiley & Sons, Inc., New York, 2002.

[47] Ganong W. F., *Review of Medical Physiology*, 13th Ed., Appleton and Lange, Norwalk, CT, 1987.

[48] Interactive Physiology - adam.com® and Benjamin Cummings 2003 http://www.interactivephysiology.com/login/index.html, last visited 24.08.2010

[49] Buckberg G.D., Mahajan A., Jung B., Markl M., Hennig J., Ballester-Rodes M.,"MRI myocardial motion and fiber tracking: a confirmation of knowledge from different imaging modalities", *European Journal of Cardio-thoracic Surgery* 29S, S165—S177, 2006

[50] Wua E.X., Wua Y., Tang H., Wang J., Yanga J., Ng M.C., Yangd E.S., Chane C.W., Zhue S., Laue C.P., Tsee H.F.,"Study of myocardial fiber pathway using magnetic resonance diffusion tensor imaging", *Magnetic Resonance Imaging* 25,1048–1057, 2007

[51] Ubbink S.W.J., Bovendeerd P.H.M., Delhaas T., Arts T., Van de Vosse F.N.,"Towards model-based analysis of cardiac MR tagging data: Relation between left ventricular shear strain and myofiber orientation", *Medical Image Analysis* 10,632–641, 2006.

[52] Dr. LAM Tat Chung Paul, Psychotropic drugs and the risk of sudden cardiac death, http://www.hkma.org/english/cme/onlinecme/cme201006set.htm, last visited on 06.09.2010

[53] Wynne, J., and Braunwald, E., *Cardiomyopathies and myocarditides. In Heart Diseases, a Textbook of Cardiovascular Medicine*, Ed., 3rd ed., Chap. 42. Saunders, Philadelphia,1988.

[54] Healing Hearts For Healthy Lives- 2006 Cardiovascular Consultants, http://www.cardioconsult.com/CommonConditions, last visited on 26.08.2010

[55] Cardiovascular Physiology Concepts, Richard E. Klabunde, Ph.D., http://www.cvphysiology.com/, last visited on 26.08.2010

[56] Keynes M., *Understanding cardiovascular diseases*, Open University Worldwide, 2007.

[57] Diagram of electrical activity during atrial fibrillation http://www.nature.com/nature/journal/v415/n6868/fig_tab/415219a_F1.html, last visited on 27.08.2010

[58] Yang H., El-sherif N., and Restivo, M., "A logical state model of circus movement atrial flutter, role of anatomic obstacles, anisotropic conduction, and slow conduction zones on induction, sustenance, and overdrive paced modulation of reentrant circuits." *IEEE Trans. Biomed. Eng.* BME-41, 537, 1994

[59] Deutsch A., Dormann S., *Cellular Automaton Modeling of Biological Pattern Formation Characterization, Applications, and Analysis*, Birkhäuser Boston,2005

[60] Siregar P., Sinteff J. P., Julen N., and Le Beux P., "An Interactive 3D Anisotropic Cellular Automata Model of the Heart", *Computers and Biomedical Research* 31, 323–347, 1998

[61] Wolfram S., "Statistical mechanics of cellular automata", The American Physical Society *Rev. Mod. Phys.* 55, 601–644, 1983

[62] Emmerich H., Rank E., "An improved cellular automaton model for traffic flow simulation", *Physica* A 234: 676-586, 1997

[63] Kiskowski M.A., Alber M.S., Thomas G.L., Glazier J.A, Bronstein N.B., Pu J. and Newmand S.A., "Interplay between activator–inhibitor coupling and cell-matrix adhesion in a cellular automaton model for chondrogenic patterning", *Developmental Biology* 271:372–387, 2004

[64] Ermentrout G.B., Edelstein-Keshet L., "Cellular Automata Approaches to Biolojical Modelling" *J. theor. Biol.,* 160, 97-133, 1993

[65] Adamatzky A., Holland O., "Phenomenology of Excitation in 2-D Cellular Automata and Swarm Systems", *Chaos, Solitons & Fractals* Vol. 9, No.7, pp. 1233 1265, 1998

[66] Jun K.R., Seong Y.R., Kim T.G., "A cellular automata model of activation Process in Ventricular Muscle",SCSC'94, 769 - 774,July 1994.

[67] Freudenberg J., Schiemann T., Tiede U., HoÈ hne H.K.,"Simulation of cardiac excitation patterns in a three-dimensional anatomical heart atlas", *Computers in Biology and Medicine* 30:191-205, 2000

[68] Adam D.R.," Propagation of Depolarization and Repolarization Processes in the Myocardium- An Anisotropic Model", IEEE Transactions on Biomedical Engineering, Vol. 38. No: 2, February 1991

[69] Dössel O., Bauer W.R., Farina D., Kaltwasser C., Skipa O., “Imaging of Bioelectric Sources in the Heart Using a Cellular Automaton Model”, *Proceedings of the 2005 IEEE Engineering in Medicine and Biology 27th Annual ConferenceShanghai*, China, September 1-4, 2005

[70] Gharpure P.B. and Johnson C.R., “A Cellular Automaton Model of Electrical Activation in Canine Ventricles: A Validation Study technical report” , UUSCI-1995-002, Scientific Computing and Imaging Institute, University of Utah, 1995

[71] Makowiec D., Umeo H. et al”The Heart Pacemaker by Cellular Automata on Complex Networks. (Eds): ACRI 2008, LNCS 5191, pp. 291–298, 2008

[72] Chou H-H, Huang W., Reggia J.A., “The Trend Cellular Automata Programming Environment” *Simulation,* Vol. 78, Issue 2, 59-75, February 2002

[73] Zhu H., Pang P.Y.H., Sun Y. and Dhar P., “Asynchronous adaptive time step in quantitative cellular automata Modeling” *BMC Bioinformatics,* 5:85 doi:10.1186/1471-2105-5-85, 2004

[74] Oomens C., Brekelmans M., Baaijens F., *Biomechanics; Concepts and Computation*, Cambridge University Press, Cambridge, UK, 2009

[75] Kleber E.G. and Rudy Y., “Basic Mechanisms of Cardiac Impulse Propagation and Associated Arrhythmias” *Physiol Rev* 84: 431–488, 2004

[76] Hopenfeld B., Stinstra J.G. and MacLeod R.S., “The Effect of Conductivity on ST-Segment Epicardial Potentials Arising from Subendocardial Ischemia”, *Annals of Biomedical Engineering*, Vol. 33, No. 6, pp. 751–763, June 2005

[77] Panfilov A.V., “Three-dimensional organization of electrical turbulence in the heart”, *Physical Review*, E Volume:59, Number:6, June 1999

[78] Stinstra J.G., Shome S., Hopenfeld B., MacLeod R.S., “Modelling passive cardiac conductivity during ischaemia”, *Med. Biol. Eng. Comput*., 43, 776-782, 2005

[79] Stinstra J.G., Hopenfeld B., and MacLeod R.B., “Using models of the passive cardiac conductivity and full heart anisotropic bidomain to study the epicardial potentials in ischemia” Conf Proc IEEE Eng Med Biol Soc;5:3555-8, 2004

[80] Keldermanna R.H., Nash M.P., Panfilov A.V., “Modeling cardiac mechano-electrical feedback using reaction-diffusion-mechanics systems”, Physica D 238, 1000_1007, 2009

[81] Clancy E.A., Smith J.M., and Cohen R.J., “A Simple Electrical-Mechanical Model of the Heart Applied to the Study of Electrical-Mechanical Altemans”, *IEEE Transactions on Biomedical Engineering* Vol:38, No:6, June 1991

[82] Maurel W., Wu Y., Thalmann N. M., Thalmann D., *Biomechanical Models for Soft Tissue Simulation*, Springer, Verlag, 1998.

[83] Janssens K., Raabe D., Nestler B., Kozeschnik E. and Miodownik M., “Cellular Automata”, *Computational Materials Engineering: An Introduction to Microstructure Evolution*, Chapter 4:109-150, Academic Press, Aug, 2007

[84] Pollard A.E., Burgess M.J., and Spitzer K.W., “Computer Simulations of Three-Dimensional Propagation in Ventricular Myocardium Effects of Intramural Fiber Rotation and Inhomogeneous Conductivity on Epicardial Activation”, *Circ. Res.*;72;744-756, 1993

[85] Clayton R.H.,“Computational models of normal and abnormal action potential propagation in cardiac tissue: linking experimental and clinical cardiology”, Topical Review, *Physiol. Meas*. 22: R15–R34, 2001

[86] Hodgkin, A.L. and Huxley, A.F. “A quantitative description of membrane current and itsapplication to conduction and excitation in nevre”. *In:* Journal of Physiology. Vol. 177,pp. 500-544., 1952

[87] McCulloch A.D., Sung D., Thomas M.E., and Michailova A., Katila T. et al., “Experimental and Computational Modeling of Cardiac Electromechanical Coupling”, (Eds.): FIMH 2001, LNCS 2230, pp. 113-119, 2001.

[88] Biomechanics – Constitutive Law, http://www.e-sunbear.com/biomech_05.html, Last visited on 27.08.2010